Monitoring regression models for lifetimes

Carlos Arturo Panza Ospino

Universidad Nacional de Colombia
Faculty of Sciences
Department of Statistics
Bogotá, D.C.
November, 2016

Monitoring regression models for lifetimes

Carlos Arturo Panza Ospino

Dissertation submitted for the degree of
Ph.D. in Sciences-Statistics

Advisor
José Alberto Vargas Navas, Ph.D.

Research line
Statistical Process Control

Research group
Industrial Statistics

Universidad Nacional de Colombia
Faculty of Sciences
Department of Statistics
Bogotá, D.C.
November, 2016

Acceptation Note

Thesis Work
Accepted

Jury
Philippe Castagliola
Université de Nantes
France

Jury
Nelcy González Gutiérrez
Universidad Nacional de Colombia
Colombia

Jury
Stefan Steiner
University of Waterloo
Canada

Bogotá, D.C., July 18th, 2017

Abstract

Monitoring regression models for lifetimes

The current study addresses the monitoring of regression models with response variable having a distribution for lifetimes. Certain aspects of this research have relevant importance. First of all, in most of the existing literature, monitoring regression models is treated as a special case of profile monitoring. However, especially in some industrial and healthcare applications, regression models can adequately represent process quality but cannot always be qualified as profiles. This is the case of regression models for lifetimes. The fact is that lifetimes can be measured just once at most in the same experimental unit. Consequently, the nature of responses while monitoring regression models is not multivariate necessarily.

However, the main goal of monitoring regression models for lifetimes aims to check the stability of the distributions of n response variables $Y_i, i = 1, \cdots, n$. As all these distributions are linked by the same parameter vector, the stability of the formers depends on the one of the latter. Thus, it is clear that profile monitoring and regression monitoring share the same purpose. Techniques from profile monitoring can be used for successfully monitoring regression models for lifetimes as well.

Some methodologies for monitoring Weibull regression models for lifetimes with common shape parameter and in phase II processes will be addressed depending on the composition of available regression data structures. The monitoring of the parameter vector characterizing the Weibull regression model allows us to make conclusions about the mean value of the response variable.

It will be shown that the monitoring of regression models for lifetimes can be carried out by redesigning existing methods from monitoring continuous quality variables and profile monitoring. In the presence of uncensored lifetimes, it was found out that it is possible to adapt conventional control charts for single observations to the monitoring of the common shape parameter. It is also possible to adapt control techniques and methodologies from profile monitoring to the case of monitoring the entire parameter vector characterizing the basic model. In both cases, chart designing depends on the asymptotic normality of the maximum likelihood estimator of the parameter vector. Thus,

it is necessary to implement some existing corrections to the monitoring statistics so that existing control charts work acceptably well when non-large enough data sets are available.

When a type I right-censored mechanism is operating on lifetimes, the monitoring can be carried out with the help of one-sided likelihood ratio based cumulative sum control charts. Theese procedures can be used for monitoring one or more of the parameters in the parameter vector and has practically no restrictions respect to the dataset dimension needed for monitoring. Conducted simulations suggest that this chart is more effective than the multivariate exponentially weighted moving average method when detecting the deterioration of the process is wanted.

Key words: Censorship, extreme value distribution, lifetimes, likelihood ratio, profile monitoring, regression model, Weibull distribution.

Resumen

Monitoreo de modelos de regresión para tiempos de vida

El presente estudio se aborda el monitoreo de modelos de regresión para tiempos de vida. Ciertos aspectos de este trabajo son de crucial importancia. Como primera medida, en gran parte de la literatura especializada, el monitoreo de modelos de regresión se trata como un caso particular del monitoreo de perfiles. Sin embargo, existen muchas aplicaciones, especialmente en ingeniería y en cuidados en salud, en las cuales los modelos de regresión pueden caracterizar adecuadamente la calidad de los procesos pero no siempre pueden considerarse como perfiles. Es el caso de los modelos de regresión para tiempos de vida. El hecho es que, en general, un tiempo de vida puede medirse a lo sumo una vez en la misma unidad experimental. Consecuentemente, la naturaleza de las respuestas en el monitoreo de modelos de regresión no necesariamente es multivariada.

Sin embargo, el objetivo principal del montireo de modelos regresión apunta a verificar la estabilidad de las distribuciones n variables respuesta $Y_i, i = 1, \cdots, n$. Como todas estas distribuciones están relacionadas entre sí por un único vector de parámetros, la estabilidad de las primeras depende de la estabilidad de este último. De este modo, es claro que tanto el monitoreo de modelos de regresión como el de perfiles comparten el mismo propósito. Es así como las técnicas usadas para monitorear perfiles pueden también usarse par monitorear acertadamente los modelos de regresión para tiempos de vida.

Se presentan algunas metodologías para monitorear modelos de regresión para tiempos de vida con respuesta Weibull, dependiendo de cómo están conformadas los conjuntos de datos disponibles. El monitoreo del vector de parámetros de modelos de regresión Weibull permite hacer conclusiones acerca del valor medio de la variable respuesta.

Se mostrará además que se puede encarar el monitoreo de modelos de regresión para tiempos de vida mediante el rediseño de las metodologías de control que comúnmente se usan para monitorear variables de calidad continuas o para monitorear perfiles. Cuando la respuesta no es censurada, se encontró que es posible adaptar las cartas de control convencionales para observaciones individuales de la característica de calidad, al monitoreo del parámtero de forma de un modelo de regresión Weibull. Es posible

también adaptar las metodologÃas de control usadas en el monitoreo de perfiles para monitorear todo el vector de parámetros que caracterizan los modelos de regresión Weibull. En ambos casos, el diseño de las cartas se basa en la normalidad asintótica del estimador máximo verosímil del vector de parámetros. Por consiguiente, se hace necesario implementar correcciones existentes a las estadísticas de monitoreo para que las cartas de control trabajen aceptablemente aún cuando no se disponga de conjuntos de datos lo suficientemente grandes.

Cuando un mecanismo de censura a derecha de tipo I opera sobre los tiempos de vida, se puede realizar el monitoreo con la ayuda de cartas de control unilaterales de sumas acumuladas basadas en la estadística de razón de verosimilitudes. Estos esquemas se pueden utilizar para monitorear uno o varios parámetros que conforman el vector de parámetros y prácticamente no tienen restricciones respecto a la cantidad de observaciones necesarias para realizar el monitoreo. Los estudios de simulación sugieren que estos esquemas son más efectivos que los métodos multivariados de promedios móviles ponderados exponencialmente cuando se desea detectar el deterioro de los procesos de calidad.

Palabras clave: Censuramiento, distribución de valor extremo, distribución Weibull, modelo de regresión, monitoreo de perfiles, razón de verosimilitudes, tiempos de vida.

Abbreviations and conventions

In the following table, there are listed some abbreviations and conventions used throughout this document.

Short expression	Extended expression
ARL	Average run length
ARL_0	In-control average run length
ARL_1	Out-of-control average run length
CL	Central line
$CUSUM$	Cumulative sum
$EVRM$	Extreme value regression model (or models)
$EWMA$	Exponentially weighted moving average
GLM	Generalized linear model
LRT	Likelihood ratio test
LCL	Lower control limit
$MEWMA$	Multivariate exponentially weighted moving average
MLE	Maximum likelihood estimator
pdf	Probability density function
SPC	Statistical process control
UCL	Upper control limit
WRM	Weibull regression model (or models)
$EV(\mathbf{a};\mathbf{b})$	The extreme value distribution with parameter vector $(\mathbf{a};\mathbf{b})$
$EV(0;1)$	The standardized extreme value distribution
$N(\mathbf{a};\mathbf{b})$	The normal distribution with parameter vector $(\mathbf{a};\mathbf{b})$
$N(0;1)$	The standard normal distribution
$W(\mathbf{a};\mathbf{b})$	The Weibull distribution with parameter vector $(\mathbf{a};\mathbf{b})$
χ^2_p	The chi-square distributions with p degrees of freedom
$X \sim \mathcal{D}(\mathbf{A})$	The random variable X follows a known distribution $\mathcal{D}$ with parameter vector $\mathbf{A}$

Aknowledgements

The author expresses his gratitude to all those who have contributed to the development and successful completion of this work. The author would especially like to thank:

- Professor J.A.Vargas, advisor of the thesis, for giving the opportunity to work in Staistical Quality Control,
- The members of the jury evaluating this work for their comments and contributions that greatly enriched the final version of the thesis manuscript,
- The reviewers of the articles and communications in specialized events that are products of this research work,
- The executive staff of the Department of Statistics, professors in charge of doctoral courses and activities, coworkers and classmates for the support provided,
- Mother and sisters.

Contents

List of Tables

List of Figures

CHAPTER 1

Introduction

1.1 Statistical quality control

The use of statistical methods in quality improvement is increasingly common. Years ago, the concept of quality was exclusively associated to manufacturing processes. Nowadays, methods for quality improvement are applied not only in manufacturing processes but in service operations as well. Success or fail of companies depend on the quality of goods or services they produce. Companies are aware that quality improvement leads to an increasing productivity and consequently to a reduction in the cost per produced unit.

Several definitions of quality can be found in specialized literature. Duncan [17], Ryan [53] and Montgomery [36] present a wide discussion on this topic. All of them agree that process quality is closely related to the satisfaction of consumer's needs. They insist that quality of products can be measured in terms of the number of defects in them.

1.2 Charting procedures

In 1924, Walter A. Shewhart first implemented control charts as an essential statistical tool for quality improvement. In Shewhart [60], theoretical basis for statistical quality control are established. Conceptually, a control chart is a statistical plot for analysing and monitoring repetitive processes. The theoretical framework of charting procedures states that the variability in the quality of a product is mainly due to the joint action of both random and assignable causes. If the observations of a process satisfy certain desirable properties and their variability is only due to random causes, the process is said to be in control. Otherwise, if assignable causes are identified, the process is said to be out-of-control. Thus, a control chart is a monitoring procedure for verifying the state of a process. The main objective of charting is to detect the occurrence of shifts in the process as soon as possible, so that corrective actions can be undertaken in order to bring the out-of-control process back to previously established working conditions.

The basic design of a control chart is explained in the following. Suppose that the quality of a process is defined in terms of a random variable. For monitoring one or more of the parameters characterizing the distribution of the quality variable, a control chart is designed by using a statistic T that is related to the parameters we are interested in. The statistic T is evaluated each time a new sample is taken from the process. It is clear that all the T values are subjected to sampling fluctuations that are distributed according to a certain random pattern. The central line CL and the control limits of the chart corresponds respectively to the mean and some extreme values of the distribution of the plotting statistic T.

For instance, if the vertical axis of a coordinate system is calibrated in terms of the units of the plotting statistic T and the horizontal axis represent the sampling sequence $j = 1, 2, \cdots$, then the horizontal lines drawn through the estimated mean and the extreme quantiles of the distribution of T represent a control chart for monitoring the process mean. The horizontal line for the estimated mean is often referred to as the central line CL and the ones for the extremes of the distribution, the upper control limit UCL and the lower control limit LCL. The chart is said to signal if $T_j > UCL$ or $T_j < LCL$ indicating a possible out-of-control state. The basic sketch of a control chart for monitoring the process mean is shown in Figure 1.1.

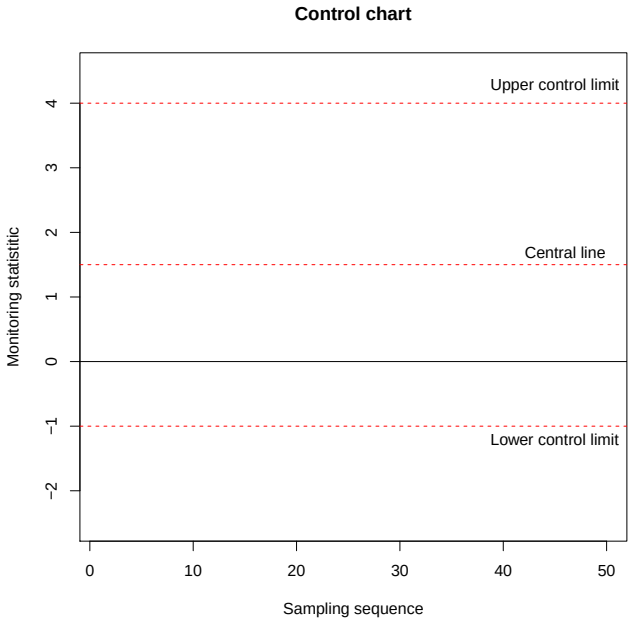

FIGURE 1.1. Sketch of a control chart

The use of control charts often requires data analysis in two phases. In Phase I, the in-control values of the process parameters are estimated after removing unusual observations with assignable causes from available historical data sets. Chart performance in Phase I studies is usually measured in terms of the probability of obtaining at least one charted point beyond the control limits. This is called the *probability of a signal*.

In Phase II, the main purpose is to monitor on-line data in order to quickly detect shifts in the process from the in-control state determined by a Phase I analysis. Chart performance

in Phase II studies is often measured in terms of the run length distribution. The average run length (ARL) is defined as the mean of the total samples inspected until the control scheme first signals.

1.3 Monitoring continuous variables

In the following, it will be addressed the design of a control chart for monitoring the mean level of a process whose quality characteristic follows a normal distribution. However, the basic idea of the design can be extended for monitoring any parameter, rather than a location one, of any distribution, rather than the normal one. For more details about control charts for monitoring single quality variables, the reader is referred to Vargas [66] or Montgomery [36].

1.3.1 The $\bar{X}$ chart

The $\bar{X}$ chart shows the variation pattern of the sample mean. Let $X \sim N(\mu; \sigma^2)$ be a quality variable characterizing a process. In phase II analysis, the distribution parameters are known, so the chart is set to be

$$\mu \pm z_{\alpha/2} \frac{\sigma}{\sqrt{n}} \tag{1.1}$$

where α is the false alarm rate, that is chosen to reach a desirable ARL_0, and n is the size of the subgroup of observations at every monitoring moment. In expression 1.1, there are presented the control limits in phase II of a conventional control chart whose central line is $CL = \mu$.

However, in the first stages of monitoring, in phase I analysis, the normal parameters are usually unknown. Historical data sets collected from the process are used to estimate the normal parameters along with the debugging of the information until the process is considered to be stable. By assuming equal subgroup sizes n, on-line monitoring is continued with the help of the chart

$$\bar{\bar{X}} \pm A_2 \bar{R} \tag{1.2}$$

where $A_2 = \frac{3}{d_2\sqrt{n}}$ and the constants d_2 are tabulated. The quantities $\bar{\bar{X}}$ and $\bar{R}$ are estimations of μ and σ based on the sample means and the sample ranges, respectively, of the in-control historical subgroups.

Both charts given by (1.1) and (1.2) are classic Shewhart charts. Charts with control limits defined by the $\alpha \times 100\%$ percentile of the plotting statistic T are often referred to as probability limit schemes. These are Shewhart-type charts and are especially useful when the distribution of the plotting statistics is different from the normal distribution and/or in the case of monitoring subgroups with varying in time sample sizes. Shewhart-type charts are proved to be effective in detecting large sustained shifts in the mean of the quality characteristic. The sketch in Figure 1.1 is a classic Shewhart-type chart.

1.3.2 Enhanced control charts

Basically a control chart indicates a possible out of control situation when one or more points are located outside the control limits while monitoring is being carrying out. Additional criteria are sometimes used to increase the sensitivity of control charts to a small process shift in order to respond more quickly to assignable causes. The Western Electric Handbook [69] suggests a set of sensitivity rules for detecting non-random patterns in control charts. Champ and Woodall [9] investigated the performance of the average run length for the Shewhart control chart with several sensitivity rules. They found out that using these rules improves control chart ability to detect smaller shifts in the process mean. However, they also found out that the in control average run length can be substantially degraded.

In order to avoid an excessive number of false alarms due to the use of sensitivity rules, Reynolds *et al.* [49] proposed to vary the time interval between successive sampling moments during process monitoring. The $\bar{X}$ chart with variable sampling interval (VSI) uses a short interval if the sample mean is close but not outside the control limits and a longer one if the sample mean is close to the target value. Comparison studies showed that the VSI chart is more efficient than the traditional chart using the fixed sampling interval (FSI). Further studies showed similar results. Moreno and Vargas [37] show that the VSI scheme for monitoring process dispersion is better than the FSI scheme. Reynolds and Stoumbos [50] study various combinations of VSI control charts for detecting changes in process level and / or dispersion.

Besides the VSI schemes, control charts with variable sample sizes (VSS) have also been proposed. The main goal in this case aims to increase sample size when a plotting point falls in a certain warning region and to reduce sample size when it is close to CL. The performance of VSS charts has been studied by Prabhu et al. [47] and Costa [11].

1.3.3 CUSUM charts for the mean

Cumulative sum (CUSUM) charts were first proposed by Page [40]. Let us suppose that detecting shifts from the target value μ_0 of the mean level of the quality characteristic $X \sim N(\mu; \sigma^2)$ with stable $\sigma = \sigma_0$ is wanted. Basically, a CUSUM procedure consists of plotting the cumulative sums of the standardized values Z_j of the variable X obtained at the $j-$th, $j = 1, 2, \cdots$, monitoring moment. This is, the procedure is based on the sums

$$S_{U,j} = \max\left[0; S_{U,j-1} + Z_j - K\right] \tag{1.3}$$

and

$$S_{L,j} = \min\left[0; S_{L,j-1} + Z_j + K\right] \tag{1.4}$$

where $Z_j = \frac{X_j - \mu_0}{\sigma_0}$; $S_{U,0} = S_{L,0} = 0$ and K is the reference value.

The monitoring is stopped when any of the sums in (1.3) or (1.4) lies beyond the threshold given by $(-h; h)$, where h is chosen to reach a desirable ARL_0. The scheme indicates a possible increase in the mean if $S_{U,j} > h$ and a possible decrease if $S_{L,j} < -h$. CUSUM charts are proved to be effective in detecting small or moderate sustained shifts in the

mean of the quality characteristic in phase II clearly. In Figure 1.2, a CUSUM chart for standard normal observations is illustrated.

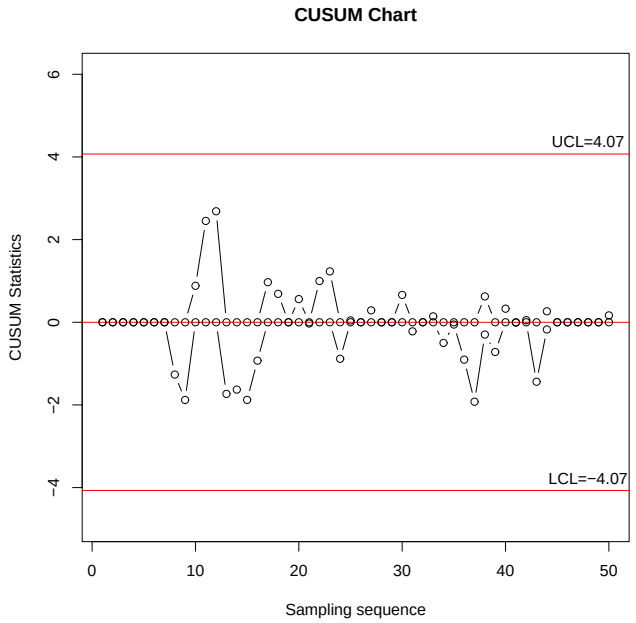

FIGURE 1.2. CUSUM chart for standard normal observations with $K = 0.5$ and $h = 4.07$.

1.3.4 EWMA charts for the mean

Exponentially weighted moving average (EWMA) charts were first proposed by Roberts [51]. Let us still suppose that detecting shifts from the target value μ_0 of the mean level of the quality characteristic $X \sim N(\mu; \sigma^2)$ with stable $\sigma = \sigma_0$ is wanted. At the $j-$th, $j = 1, 2, \cdots$, monitoring moment, the EWMA statistic is set to be

$$EW_j = \lambda X_j + (1 - \lambda) EW_{j-1} \tag{1.5}$$

where $0 < \lambda \leq 1$ is the smoothing constant and $Z_0 = \mu_0$. It is recommended to set the value of the smoothing constant λ as small as possible. In this case, the EWMA statistic is a weighted function that gives less relevance to newer observations. The performance of the EWMA chart is more similar to that of the Shewhart chart as the smoothing constant λ is closer to unity.

When the X_j are independent observations of the in-control process, we have that the variance of the EWMA statistic (1.5) is given by

$$Var(EW_j) = \sigma^2_{EW_j} = \frac{\lambda \left[1 - (1 - \lambda)^{2j}\right]}{2 - \lambda} \sigma_0^2 \tag{1.6}$$

The chart is then given by

$$\mu_0 \pm L \sigma_{EW_j} \tag{1.7}$$

where the constant L is chosen to reach a desirable ARL_0. The scheme indicates a possible increase in the mean if $EW_j > UCL$ and a possible decrease if $EW_j < LCL$. EWMA charts are proved to be effective in detecting small or moderate sustained shifts in the mean of the quality characteristic in phase II. In Figure 1.3, an EWMA chart for standard normal observations is illustrated.

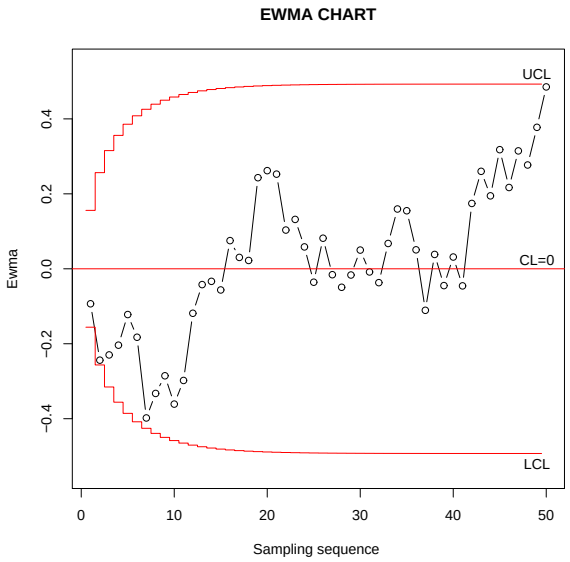

FIGURE 1.3. EWMA chart for standard normal observations with $\lambda = 0.1$ and $L = 2.148$.

1.4 Monitoring multivariate characteristics

In some applications, it is needed to monitor two or more quality characteristics of the same product or process simultaneously. Let us suppose that the quality of a process is formally represented by a $p-$dimensional random vector $\mathbf{X} = (X_1, \cdots, X_p)'$. In this case, the interest is focused on how to use those p variables simultaneously to check the stability of the process over time. In the following, it is assumed that the random vector $\mathbf{X}$ follows a $p-$dimensional normal distribution with mean vector $\boldsymbol{\mu}$ and covariance matrix $\boldsymbol{\Sigma}$. Shifts from the target value $\boldsymbol{\mu} = \boldsymbol{\mu}_0$, for instance, can be detected by control charts based on the Hotelling's T^2 statistic.

1.4.1 Hotelling's T^2-based methods

As in the case of monitoring quality variables, Alt and Smith [3] have established two phases of analysis in the design of a multivariate chart for the mean. Phase I is divided into two stages: a retrospective and a prospective one. The main goal of the retrospective stage aims to verify process stability when initial multivariate observations were taken. In the prospective stage, it is tested whether the process still remains under control when future observations are being collected.

At first stages of monitoring, process parameters are usually unknown and have to be estimated from a set of m observations of the quality vector $\mathbf{X}$. Let $\mathbf{X}_j = (X_{j1}, \cdots, X_{jp})$ be the $j-$th, $j = 1, \cdots, m$, observation of $\mathbf{X}$. Let also $\bar{\mathbf{X}}$ and $\mathbf{S}$ be the estimates of the mean vector $\boldsymbol{\mu}$ and the covariance matrix $\boldsymbol{\Sigma}$, respectively, based on the available m observations. The Hotelling's T^2 statistic for the $j-$th observation is defined to be

$$T_j^2 = (\mathbf{X}_j - \bar{\mathbf{X}})' \mathbf{S}^{-1} (\mathbf{X}_j - \bar{\mathbf{X}}) \tag{1.8}$$

In the retrospective stage of phase I, the UCL of the chart is set to be

$$UCL = \frac{(m-1)^2}{m} \mathcal{B}\left(\frac{p}{2}, \frac{m-p-1}{2}, 1-\alpha\right) \tag{1.9}$$

where $\mathcal{B}(a, b, 1-\alpha$ is the $(1-\alpha)\times 100\%$ percentile of the beta distribution with parameters a and b and α is the nominal false alarm rate.

When the chart signals, the corresponding multivariate must be investigated for possible assignable causes. Observations corresponding to signaling points due to assignable causes have to deleted from the initial set of observations and the UCL has to be recalculated based on the remaining observations. This procedure must be continued until there are no signaling points.

In the prospective stage of phase I, the UCL is set to be

$$UCL = \frac{p(m'+1)(m'-1)}{m'(m'-p)} F_{(p,m'-p,1-\alpha)} \tag{1.10}$$

where $F_{(p,m'-p,1-\alpha)}$ is the $(1-\alpha)\times 100\%$ percentile of the Fisher's distribution with p and $m'-p$ degrees of freedom and m' is the number of remaining observations with which the process parameters were finally estimated at the end of the prospective stage of phase I.

Once the process is assumed to be stable, monitoring is continued in phase II with the help of the statistic

$$T_j^2 = (\mathbf{X}_j - \boldsymbol{\mu}_0)' \boldsymbol{\Sigma}_0^{-1} (\mathbf{X}_j - \boldsymbol{\mu}_0) \tag{1.11}$$

where $\boldsymbol{\mu}_0$ and $\boldsymbol{\Sigma}_0$ are the last estimates of the process parameters obtained at the end of the prospective stage of phase I.

The upper control limit for phase II is set to be

$$UCL = \chi^2_{(p,1-\alpha)} \tag{1.12}$$

The chart signals as soon as $T_j^2 > UCL$ indicating a possible out-of-control situation.

Other Hotelling's T^2-based methods have been studied in specialized literature. Lowry and Montgomery [29] present a review of multivariate control charts. Sullivan and Woodall [64] recommend to estimate the covariance matrix using the vector of differences between successive single multivariate observations. Vargas [65] shows that multivariate control

charts that use estimators of the minimum volume ellipsoid is efficient in the presence of outliers. Vargas [68] presents a complete overview on T^2-based chart designing.

1.4.2 The multivariate EWMA chart

Lowry *et al.* [30] propose the multivariate EWMA chart often referred to as the MEWMA chart. At the $j-$th monitoring moment, $j = 1, 2, \cdots$, the MEWMA statistic is defined to be

$$\mathbf{Z}_j = \Lambda(\mathbf{X}_j - \boldsymbol{\mu}_0) + (\mathbf{I}_p - \Lambda)\mathbf{Z}_{j-1} \tag{1.13}$$

where $\mathbf{Z}_j = \mathbf{0}_p$ and $\Lambda = diag(\lambda_1, \cdots, \lambda_p)$ with $0 < \lambda_l \leq 1$, $l = 1, \cdots, p$.

The MEWMA chart signals as soon as

$$T_j^2 = \mathbf{Z}_j' \boldsymbol{\Omega}_j^{-1} \mathbf{Z}_j > h \tag{1.14}$$

where $\boldsymbol{\Omega}_j$ is the covariance matrix of $\mathbf{Z}_j$ and h is chosen to reach a desirable ARL_0.

When there are no special reasons for assigning different weights to past observations, it is assumed the same weight λ to all the components of the quality vector $\mathbf{X} = (X_1, \cdots, X_p)'$ and the MEWMA statistic is then given by

$$\mathbf{Z}_j = \lambda(\mathbf{X}_j - \boldsymbol{\mu}_0) + (1 - \lambda)\mathbf{Z}_{j-1} \tag{1.15}$$

and

$$\boldsymbol{\Omega}_j = \frac{\lambda\left[1 - (1-\lambda)^{2j}\right]}{2 - \lambda}\boldsymbol{\Sigma}_0 \tag{1.16}$$

where $\boldsymbol{\Sigma}_0$ is the in-control value of the covariance matrix $\boldsymbol{\Sigma}$.

1.5 Monitoring regression models

In most of the existing literature, the monitoring of regression models is a special case of profile monitoring. However, in industrial or healthcare applications, a regression model cannot always adequately represent a profile data structure in the sense given by Woodall [71]. This is clearly the case of regression models for lifetimes. However, it is clear that profile monitoring and regression monitoring share the same purpose, so techniques from profile monitoring can be used for monitoring regression models for lifetimes as well.

1.5.1 Profile monitoring

There are a number of practical situations, where the state of a process or product is better characterized by a functional relationship between a multivariate response variable and one or more explanatory variables. This relationship is usually referred to as *profile*. The most traditional way to represent profiles is by using an appropriate regression model which can be linear or non-linear.

An increasing attention in recent years has been paid to monitoring profiles. Profile monitoring mainly focuses on checking the stability of the parameter vector characterizing the basic regression model over time based on observed data. In profile monitoring, it is assumed that $N > 1$ values of the response multivariate quality characteristic are measured along with the corresponding values of a $p-$dimensional vector of explanatory variables or covariates, reflecting the location of the measurement on a process. Woodall *et al.* [72] and Woodall [71] provide complete overviews on profile monitoring.

There are many applications where the quality of a process can be expressed as a profile. Linear profiles appear to be more common in industrial applications. Kang and Albin [24], for instance, gives a calibration example in semiconductor manufacturing. Applications of non-linear profiles are given by some other authors. Amiri *et al.* [5] discuss a case study on monitoring polynomial profiles in the automotive industry. William *et al.* [70] consider the non-linear profiles of a dose-response curve to monitor the quality of bioassays. For more examples on profile monitoring please read Noorossana *et al.* [39].

1.5.2 Phases I and II in profile monitoring

As in the case of monitoring variables, monitoring profiles can also be studied via two phases. In profile monitoring, Phase I consists of determining the stability of the process by estimating profile parameters based on available historical data sets. Mahmoud and Woodal [32] present a method for Phase I analysis of linear regression models based on indicator variables. Mahmoud *et al.* [31] propose a change point method to detect sustained shifts in linear profiles in Phase I. Kazemzadeh *et al.* [25] present three methods for monitoring polynomial profiles in Phase I.

In Phase II, the main goal aims to monitor future data sets in order to detect departures from the in-control parameter vector (determined in a Phase I analysis) as soon as possible. For monitoring linear profiles in Phase II, Kang and Albin [24] propose the use of a multivariate chart for checking the stability of parameter vector in combination with an EWMA chart for ckecking the residuals of the classic linear regression model. In the same direction, Zhang *et al.* [76] propose an EWMA chart based on the likelihood-ratio test (LRT) and Saghaei *et al.* [54] propose a CUSUM chart. In Amiri *et al.* [4], a dimension reduction method for monitoring multiple linear regression profiles is presented.

1.5.3 Generalized linear profiles

Generalized linear models (GLM) have also been used for representing profiles. Monitoring GLM profiles is completely feasible by taking into account the asymptotic distributional properties of the maximum likelihood estimator (MLE) of the parameter vector characterizing the basic model. Yeh *et al.* [74] and Shang *et al.* [58] propose methods for monitoring logistic profiles in Phase I and Phase II processes, respectively. The Poisson response has been studied by Amiri *et al.* [6], Shadman *et al.* [55, 56]. A method based on the use of U statistics for phase II monitoring of general linear profiles with autocorrelation in the error terms is presented in Khedmati and Niaki [26].

Different methodologies have been developed and modified in order to be applied for monitoring GLM profiles. The use of LRT-based methods for monitoring GLM profiles is quite common in recent years. As our interest is focused on LRT-based charts for monitoring Weibull regression models (WRM) in Phase II, we will briefly review the LRT, LRT-EWMA and MEWMA control charts proposed in Soleymanian *et al.* [61] for monitoring the parameter vector $\boldsymbol{\xi}$ of binary profiles in Phase II processes. At the $j-$th monitoring moment, $j = 1, 2, \cdots$, the LRT statistic can be expressed as

$$LRT_j = 2\left[\ell(\hat{\boldsymbol{\xi}}_j) - \ell\left(\boldsymbol{\xi}_{IC}\right)\right] \tag{1.17}$$

where $\ell(\centerdot)$ is the log-likelihood function of the basic regression model and $\hat{\boldsymbol{\xi}}$ and $\boldsymbol{\xi}_{IC}$ are the MLE and the in-control value of the parameter vector $\boldsymbol{\xi}$, respectively. For the case of large sample sizes, the LRT statistic given by (1.17) follows a chi-square distribution with p degrees of freedom $\left(\chi^2_p\right)$. Accordingly, if $LRT_j \leq \chi^2_{1-\alpha;p}$ then the $j-$th profile is ruled to be in-control.

Soleymanian *et al.* [61] also propose first normalize the LRT values obtained in (1.17) and then evaluate the LRT-EWMA statistic by

$$LE_j = \lambda NL_j + (1-\lambda)LE_{j-1} \quad j = 1, 2, \cdots \tag{1.18}$$

where NL is the normalized value of the corresponding LRT statistic, λ is the smoothing parameter and $LE_0 = 0$. The proposed charts signals when $LE_j > L\frac{\lambda}{2-\lambda}$. The designing constant L is chosen in such a way that a specified ARL_0 is achieved.

The MEWMA monitoring statistic is defined to be

$$M_j = \mathbf{E}_j'\mathbf{E}_j \quad j = 1, 2, \cdots \tag{1.19}$$

where

$$\mathbf{E}_j = \lambda\mathbf{Z}_j + (1-\lambda)\mathbf{E}_{j-1} \quad j = 1, 2, \cdots \tag{1.20}$$

and

$$\mathbf{Z}_j = \Im^{1/2}(\hat{\boldsymbol{\xi}} - \boldsymbol{\xi}_{IC}) \quad j = 1, 2, \cdots \tag{1.21}$$

with $\Im$ being the asymptotic information matrix. Soleymanian's version of the MEWMA chart signals due to out-of-control state as soon as $M_j > L\frac{\lambda}{2-\lambda}$, where the constant L is chosen to reach a desirable ARL_0.

1.6 Monitoring lifetimes

In some practical situations the time from a well-defined starting point until certain event occurs, often referred to as *lifetime*, is of interest. The Weibull model, due to its flexibility, has been found to provide a good description of many types of lifetime data. It has been widely used to model durability of manufactured items or the occurrence of tumours in medical studies.

In the context of statistical process control (SPC), Woodall and Montgomery [73] see lifetime monitoring as a research area with considerable potential. Control charts for monitoring the mean value of lifetime observations have been developed in last decades. Steiner and MacKay [63] proposed five Shewhart-type charts to detect shifts in the process mean with censored lifetimes for Weibull and exponential models. Zhang and Chen [75] propose one-sided EWMA charts and Johnson [23] propose CUSUM charts for detecting shifts in the Weibull mean assuming that the shape parameter is known. Vargas and Montaño [67] extended the study by Steiner and MacKay [63] to the case of Weibull-distributed lifetimes.

In more recent research, Dickinson *et al.* [15] present charting procedures for monitoring shifts in the scale parameter of Type I right-censored Weibull lifetime data for a fixed value of the shape parameter. They are especially interested in detecting decreases in the scale parameter that lead to decreases in the mean value of Weibull-distributed lifetimes. Shafae *et al.* [57] compare CUSUM control charts for monitoring the mean of time between events of Weibull distributed observations.

Monitoring the shape parameter of Weibull distributed observations has also been a research topic of great concern. Pascual [42] presents EWMA schemes based on two different unbiased estimators of the Weibull shape parameter. Pascual and Zhang [45] suggest Shewhart-type control charts based on the extreme value sample range. Pascual and Nguyen [44] and Akhundjanov and Pascual [2] present control charts based on moving range of single observations. Pascual and Li [43], Guo and Wang [19] and Chan *et al.* [10] developed different methods for monitoring the Weibull shape parameter when available samples are type II censored. Haghighi and Castagliola [20] proposed the monitoring of the Weibull shape parameter under progressively type II censored data. Haghighi *et al.* [21] proposed the monitoring of Weibull quantiles under type II censoring.

In other applications, a set of variables that could be correlated to lifetimes are involved. The most effective way to assess the effect of these explanatory variables on lifetimes is by using an appropriate regression model. The WRM with common shape parameter is the most traditionally used parametric model to do so. Actually, there are not sufficiently developed techniques for monitoring any kind of regression models beyond the research area of profile monitoring.

1.7 Motivation

Monitoring regression models for lifetimes is a topic of great relevance. In last two decades, companies have been asked to implement quality improvement programs. These programs often include annually or semi-annually conducted essays consisting of accelerated tests to determine the elapsed time until an event of interest occurs. Observed elapsed times can depend on the experimental conditions they are measured. These experimental conditions can be formally represented by n different fixed values of a set of covariates. We would be interested in checking the stability of the elapsed times measured in the same conditions over time. This is clearly a control process issue.

In this document, some methodologies for monitoring WRM are presented. We propose LRT-based procedures for monitoring the mean response of the WRM throughout the monitoring of one or more of the regression coefficients in some special cases. In the case of monitoring regression models with uncensored times, these methodologies represent adaptations of the existing ones to the case of our particular interest. The fact is that these methodologies are based on the asymptotic normality of the MLE of the parameter vector characterizing the WRM. However, for on-line monitoring, we are really dealing with finite sizes of the available data sets. In addition, distributions for modelling lifetimes are often severely skewed and, in this case, the asymptotic distributional properties of the parameter vector MLE just hold for quite large sample sizes. Thus, the existing methodologies have to be modified in order to make them work as fair as in the asymptotic case but with finite data-set dimensions.

1.8 Outline of the thesis

Chapters 2 and 3 are devoted to monitoring WRM with uncensored response. In Chapter 2, the monitoring of the common WRM shape parameter is presented. It is assumed that the regression coefficients $\beta_1, \cdots, \beta_{p-1}$ are stable but not necessarily known. It is proposed the monitoring by adapting the conventional EWMA, CUSUM and Shewhart-type charts for single normal observations to the case of the WRM shape parameter. The monitoring is completely feasible by taking into account the asymptotic distributional properties of the MLE of the log-transformation of the WRM shape parameter. However, this circumstance has to be faced carefully. In the case of the Weibull distributed-response, preliminary simulations suggest that the normal approximation of the marginal distribution of the log-transformation of the shape parameter MLE is just valid for regression models whose dimension is greater than 1500 approximately. Having such a data-set dimension for monitoring purposes is not a realistic issue.

The main goal in Chapter 2 aims to monitor the common WRM shape parameter when relatively small and moderate data sets are available. This is possible by using control charts based on the relative LRT statistic defined for the log-scale parameter of the log-transformation of the Weibull-distributed response. Some existing adjustments of order $O_P(N^{-3/2})$, where N is the data-set dimension, are needed in order to correct the LRT statistic for monitoring purposes when non-large enough data sets are available. It was found out that the resulting schemes work fairly acceptable for $N \geq 30$. Detection skills of the studied schemes improve as data-set dimension increases.

In Chapter 3, the monitoring of the entire WRM parameter vector is presented. As in this case the main purpose of monitoring aims to check the stability of the WRM parameter vector over time, we feel that techniques from profile monitoring can be adapted for successfully monitoring the WRM parameter vector with not sufficiently large data sets. This is completely possible by using one-sided control charts based on the deviance form of the relative LRT statistic for the log-transformation of the Weibull-distributed response. As in the case of monitoring a single parameter, some existing adjustments of order $O_P(N^{-3/2})$, often referred to as Bartlett's adjustments, are needed in order to correct the deviance form of the LRT statistic for monitoring purposes when non-large enough data sets are available. It was also found out that the resulting schemes work

fairly acceptable for $N \geq 30$. The detection abilities of the studied control schemes improve when data set dimension increases as well. Actually, the methodology described in Chapter 3, developed for a single scalar parameter ($p = 1$) in the WRM parameter vector, represents a special case of the one presented in this chapter.

In Chapter 4, it is presented a LRT-based CUSUM methodology for monitoring the WRM paremeter vector when a type I right-censoring mechanism is operating. The monitoring of one of the regression coefficients of the WRM parameter vector, leading to decreases in the mean response, is presented for a fixed value of the shape parameter. The fact is that changes in the slope of the linear specification for the scale parameter of the WRM lead to changes of the same kind in the mean response. Particularly, the main interest is focused on detecting decreases in the slope that lead to unwanted decreases in the mean of the lifetime response. Thus, one-sided CUSUM charts were designed. The impact that the fixed value of the shape parameter, the data-set dimension, the theoretical censoring rate and the desired shift to be detected have on the performance of the schemes was established via simulation. The resulting schemes can be used for monitoring decreases in the mean response due to changes in all regression coefficients. Increases in the mean response due to changes in the parameter vector for a fixed value of the shape parameter can be detected as well. However, it is worth mentioning that increases in the mean response lead to undesirable higher censoring rates.

The performance of the proposed CUSUM procedures was compared with that of the MEWMA chart first proposed by Zou *et al.* [78] and adapted by Soleymanian *et al.* [61] for monitoring binary profiles. It was found out that the CUSUM chart outperform the adapted version of the MEWMA chart in most of the studied cases.

An illustrating example and some concluding remarks referring to a particular methodology are provided at the end of the respective chapter. General conclusions and some directions of our future research work are present in the last two sections of this document.

CHAPTER 2

Monitoring the WRM shape parameter

2.1 The problem

Let us suppose that at the $j-$th moment in time, $j = 1, 2, ...$, a data set with the structure shown in Table 2.1 is available. In Table 2.1, $\mathbf{x}_i'$, $i = 1, ..., n$, represent n different levels or settings of the same experimental situation. These may be n different values of a $(p-1)$-dimensional vector of explanatory variables. This is, $\mathbf{x}_i' = (x_{1i}, \ldots, x_{p-1,i})$. The values of $\mathbf{x}_i'$ are assumed to be fixed in repeated sampling. In the $i-$th level, $i = 1, \ldots, n$, $y_{ik}^{(j)}$ represent the $k-$th observation, $k = 1, \ldots, m_i$, of the random variable Y_i measured at the $j-$th moment. The variables Y_i, $i = 1, ..., n$, represent the response variable in the $i-$th experimental level. The quantities m_i are the total observations in the $i-$th level and are also set to be fixed for every j value. Thus, for a given experimental level $i = 1, \cdots, n$, the set of values $y_{ik}^{(j)}$ can be treated as a random sample of size m_i taken from the population Y_i at the $j-$th moment. We have $\sum_i^n m_i = N$ observations at the $j-$th moment. In the following, we will refer to N as the data-set dimension and will treat it as a sample size.

$\mathbf{x}_1'$	$\mathbf{x}_2'$	$\cdots$	$\mathbf{x}_n'$
$y_{11}^{(j)}$	$y_{21}^{(j)}$	$\cdots$	$y_{n1}^{(j)}$
$y_{12}^{(j)}$	$y_{22}^{(j)}$	$\cdots$	$y_{n2}^{(j)}$
$\vdots$	$\vdots$	$\cdots$	$\vdots$
$y_{1m_1}^{(j)}$	$y_{2m_2}^{(j)}$	$\cdots$	$y_{nm_n}^{(j)}$

TABLE 2.1. Data structure at the $j-$th moment

For further discussion, in order to simplify the writing, the time super index will be avoided hereafter. It will be assumed that the reader understands that the analysis we will present has to be made at every $j-$th moment. We will write the time super index again if it is needed. Let us suppose that the variables Y_i share the same distribution

with parameter vector depending on the level they are observed. Let $\boldsymbol{\Theta}_i$ be the parameter vector characterizing the distribution of Y_i at the $i-$th level. As the parameter vector $\boldsymbol{\Theta}_i$ may likely define the mean and the variance of Y_i, we may be interested in verifying whether the estimations $\hat{\boldsymbol{\Theta}}_i$ obtained at every $j-$th moment come from a known basic model.

In the context of GLM, the interest is often focused on another parameter vector $\boldsymbol{\xi}$ whose dimension is lower than n and links one or more of the parameters in $\boldsymbol{\Theta}_i$ with the experimental settings $\mathbf{x}_i'$. In other words, we can indirectly know about the distributions of the variables Y_i over time by knowing what is exactly happening with the parameter vector $\boldsymbol{\xi}$ at the $j-$th moment. This is clearly a control process issue.

Formally, let be a process in which, at the $j-$th moment, a linear dependence between the response variables Y_i and the fixed $\mathbf{x}_i'$ values reasonably satisfies the data structure in Table 2.1. This relationship can be analytically written as

$$y_{ik}^{(j)} = \mathbf{x}_i'\boldsymbol{\beta} + \sigma z_{ik}^{(j)}, \quad j = 1, 2, \ldots \tag{2.1}$$

where $\boldsymbol{\beta} = (\beta_1, ..., \beta_{p-1})'$ is a vector of unknown constants. It is usual to set $x_{i1} = 1$ such that β_1 is the intercept of the model. In model (2.1), $\sigma > 0$ is the scale parameter and the terms z_{ik} at the $j-$th moment are independent observations of the random variable Z having a known distribution. For further discussion, it will be assumed that the vector $\boldsymbol{\xi} = (\boldsymbol{\beta}', \varphi)'$, where $\varphi = \log\sigma$, characterizes model (2.1). The reparametrization $\varphi = \log\sigma$ is needed because the variables Y_i we will be interested in represent a log-transformation of Weibull-distributed time measurements.

Let us suppose further that we are interested in testing over time the hypothesis

$$\begin{aligned} H_0 &: \sigma^{(j)} = \sigma_0 \\ H_1 &: \sigma^{(j)} = d_3\sigma_0, \quad d_3 > 0 \end{aligned} \tag{2.2}$$

This is, we are interested in detecting a $d_3 \times 100\%$ shift (increase or decrease) in the known value of the scale parameter σ_0. As it will be seen later, for stable regression coefficients $\beta_1, \cdots, \beta_{p-1}$, both increases and decreases in σ_0 imply a lower mean value of the responses Y_i at all experimental levels and, consequently, the deterioration of the process. It is clear that hypothesis (2.2) can be equivalently expressed in terms of $\varphi = \log\sigma$.

Hypothesis (2.2) can be tested over time by using LRT-based procedures. In this case, the use of LRT-based methods can lead to the use of conventional schemes for monitoring a continuous quality variable. However, distributions for modeling times-to-event data are often skewed, so that the use of the LRT statistic for designing control charts may be restrictive to large enough data sets. As it will be explained later, some adjustments to the LRT statistic are needed so that it can be used in conventional charting procedures for monitoring the parameter φ when non-large enough data sets are available.

2.2 Using existing methods for monitoring the WRM shape parameter

In general linear modeling, LRT-based procedures allow partitioning the parameter vector characterizing the basic model in order to make inferences about the parameters we are interested in. The rest of the parameters in the vector are assumed to be nuisance parameters. In model (2.1), let us suppose that we are interested in the parameter $\varphi = \log \sigma$ of $\boldsymbol{\xi} = (\beta_1, \cdots, \beta_{p-1}, \varphi)'$ and let $R(\varphi)$ be the signed square root of the LRT statistic defined for the single parameter φ as it is indicated in expression (2.9). It is known that $R(\varphi)$ approximately follows the standard normal distribution as $N \to \infty$.

In the context of SPC, it is possible to check the stability of model (2.1) over time by checking the stability of the parameter φ if the parameters $\beta_1, \cdots, \beta_{p-1}$ are known to be stable. This can be achieved, for instance, by taking advantage of the asymptotic distributional properties of $R(\varphi)$ with the help of a conventional EWMA control chart.

	Crowder's	EWMA of R(φ)			EWMA of $R_c(\varphi)$		
L	method	$N = 30$	$N = 50$	$N = 100$	$N = 30$	$N = 50$	$N = 100$
2.00	73.28	22.66	30.50	42.27	72.64	73.17	73.30
	(68.45)	(17.47)	(25.03)	(36.86)	(67.70)	(68.19)	(68.67)
2.25	125.10	29.18	41.10	60.79	124.18	125.59	124.91
	(119.26)	(22.76)	(24.26)	(54.11)	(118.18)	(119.37)	(118.93)
2.50	223.35	37.94	56.23	89.10	220.37	223.50	222.75
	(216.45)	(30.16)	(48.13)	(80.66)	(213.11)	(215.58)	(215.80)
2.75	420.78	50.19	67.43	101.26	414.79	420.51	421.30
	(412.83)	(40.53)	(59.18)	(98.04)	(404.96)	(413.14)	(413.00)
3.00	842.15	68.30	84.54	121.19	823.55	832.73	846.74
	(833.19)	(57.56)	(73.18)	(110.49)	(815.39)	(827.77)	(840.54)

TABLE 2.2. Approximated ARL_0 for the EWMA charts based on $R(\varphi)$ and $R_c(\varphi)$ with $\lambda = 0.1$ and different N and L values.

For illustrating purposes, let us suppose for a moment that $N = 30$ is a large enough value of the data-set dimension so that the standard normal approximation of $R(\varphi)$ defined as in (2.9) is valid. We built an EWMA chart based on $R(\varphi)$ with smoothing parameter $\lambda = 0.1$ for checking the stability of φ in a simple WRM with $x_i = \log(10i)$ and $\boldsymbol{\xi} = (\beta_1, \beta_2, \varphi)' = (3; 2; 0.4055)'$. Approximated ARL_0 for different values of the data-set dimension $N \leq 30$ and the chart designing constant L are shown in Table 2.2. For each combination of designing parameters, ARL_0 in the table were obtained via simulation by generating 50000 run length values. The corresponding UCL was set to be that of the conventional EWMA chart with smoothing parameter $\lambda = 0.1$ for single normal observations. An estimation of the respective standard deviation of the run length values is reported in brackets.

The second column of Table 2.2 contains the ARL_0 values of the conventional EWMA chart with $\lambda = 0.1$ for single normal observations. Reported ARL_0 values were obtained by solving a Fredholm's integral of the second kind for different values of the chart designing parameter L. The values were taken from Crowder [12]. As we have assumed

that $N = 30$ is a sufficiently large value of the data-set dimension, then $R(\varphi)$ should be normal-distributed approximately and the EWMA chart based on $R(\varphi)$ should exhibit a similar performance to that reported in the second column of Table 2.2 for the same explored chart designing parameters and $N \geq 30$. As it can be seen in Table 2.2, the performance of the EWMA chart based on $R(\varphi)$ is substantially different from that of the conventional EWMA chart for single normal observations for all reported N values. Although it is noted that chart performance is closer to the expected one as N increases.

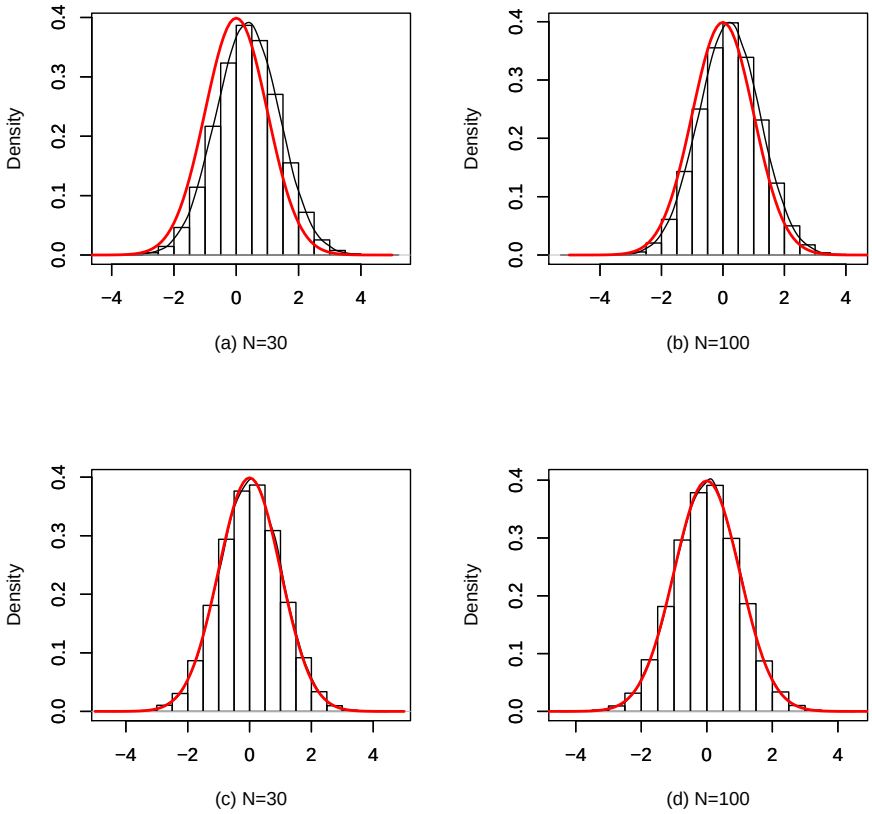

FIGURE 2.1. Normal approximation for the distribution of $R(\varphi)$, graphics (a)-(b), and the distribution of $R_c(\varphi)$, graphics (c)-(d), for different values of the data-set dimension N of the WRM model $y_{ik} = 3 + 2\log(10i) + 1.5z_{ik}$.

The fact is that the standard normal approximation of $R(\varphi)$ holds just asymptotically and the reported values of N are not large enough. Graphics (a) and (b) of Figure 2.1 clearly illustrate the departure of the distribution of $R(\varphi)$ (in black) from the standard normal distribution (in red) when $N = 30$ and $N = 100$, respectively. For each case, the distribution of $R(\varphi)$ was simulated by generating 100000 values from the simple WRM with $x_i = \log(10i)$ and $\boldsymbol{\xi} = (\beta_1, \beta_2, \varphi)' = (3; 2; 0.4055)'$.

In addition, it is known that the values of $R(\varphi)$ depend on the MLE of φ. Thus, let $\hat{\varphi}$ be the MLE of φ. It is also well known that under certain mild conditions $\hat{\varphi}$ asymptotically follows a normal distribution with mean value φ and variance given by $\Im_{\hat{\varphi}}^{-1}$, where $\Im_{\varphi}^{-1}$ is the corresponding element of the observed covariance matrix $\Im^{-1}$. Table 2.3 shows some

quantiles Q_*, the mean and the variance of the distribution of $U(\varphi) = (\varphi - \hat{\varphi})/\Im_{\hat{\varphi}}^{-1/2}$ for different values of the data-set dimension N. The same quantities for the standard normal distribution are reported in the last row of Table 2.3. It can be noted that the distribution of $U(\varphi)$ is close to the standard normal distribution just for $N \geq 1500$ approximately. This has a relevant practical implication: for monitoring the parameter φ of a simple WRM, we should have a data set with the structure in Table 2.1 containing 1500 observations at least at every monitoring moment $j = 1, 2, \cdots$. This is clearly not a realistic issue, even less for monitoring purposes.

N	$Q_{0.025}$	$Q_{0.25}$	$Q_{0.75}$	$Q_{0.975}$	Mean	Variance
30	-1.5405	-0.3183	1.0864	2.5528	0.4036	1.0940
50	-1.6181	-0.3931	0.9897	2.4079	0.3137	1.0557
100	-1.7118	-0.4740	0.8902	2.2655	0.2185	1.0276
500	-1.8455	-0.5840	0.7747	2.0918	0.0994	1.0101
1000	-1.8752	-0.6126	0.7372	2.0501	0.0668	1.0038
1500	-1.8920	-0.6227	0.7286	2.0314	0.0555	1.0022
2000	-1.8988	-0.6258	0.7241	2.0184	0.0498	0.9995
N(0;1)	-1.9600	-0.6745	0.6745	1.9600	0.0000	1.0000

TABLE 2.3. Simulated distribution of the MLE of φ for different values of the data-set dimension N of the WRM model $y_{ik} = 3 + 2\log(10i) + 1.5z_{ik}$.

Consequently, the need of making adjustments to the existing charts arises. We proposed to use Bartlett's adjustments to the relative LRT statistic presented in DiCiccio [14] to improve the performance of LRT-based charts. Indications on how to make corrections to the relative LRT satistic and, consequently, to $R(\varphi)$ are addressed in Section 2.3.2. The implementation of such adjustments to $R(\varphi)$ leads to the corrected statistic $R_c(\varphi)$, whose distribution looks more like the standard normal distribution (see the graphics (c) and (d) in Figure 2.1) for relatively small or moderate N values and makes the performance of the EWMA chart based on $R_c(\varphi)$ be closer to that of the EWMA chart for single normal observations (see the last three columns of Table 2.2).

2.3 Theoretical framework

2.3.1 The Weibull and the extreme value models for lifetimes

Let the random variable T denote Weibull-distributed times. The probability density function (pdf) and the survivor function of the Weibull distribution with scale parameter $\theta > 0$ and shape parameter $\gamma > 0$, respectively, are

$$f(t) = \frac{\gamma}{\theta^\gamma} t^{\gamma-1} \exp\left[-\left(\frac{t}{\theta}\right)^\gamma\right], \quad t > 0 \tag{2.3}$$

and

$$S(t) = \exp\left[-\left(\frac{t}{\theta}\right)^\gamma\right], \quad t > 0 \tag{2.4}$$

The mean and the variance of the Weibull distribution are $E(T) = \theta\Gamma\left(1 + \gamma^{-1}\right)$ and $V(T) = \theta^2\left[\Gamma\left(1 + 2\gamma^{-1}\right) - \Gamma^2\left(1 + \gamma^{-1}\right)\right]$, where $\Gamma(\boldsymbol{.})$ is the gamma function.

Let now be $Y = \log T$, where $T \sim W(\theta, \gamma)$. The random variable Y is said to follow the smallest extreme value distribution, often referred to as the Gumbel distribution, with location parameter $-\infty < \beta < \infty$ and scale parameter$\sigma > 0$. Shortly written, we have $Y \sim EV(\beta; \sigma)$ with EV symbolizing the extreme value distribution. The pdf and the survivor function of a random variable Y following the smallest extreme value distribution respectively are

$$f(y) = \frac{1}{\sigma} \exp\left[\frac{y-\beta}{\sigma} - \exp\left(\frac{y-\beta}{\sigma}\right)\right], \quad -\infty < y < \infty \tag{2.5}$$

and

$$S(y) = \exp\left[-\exp\left(\frac{y-\beta}{\sigma}\right)\right], \quad -\infty < y < \infty \tag{2.6}$$

It is easy to show that the parameters of both the Weibull and the smallest extreme value distributions are linked by the expressions $\beta = \log\theta$ and $\sigma = \gamma^{-1}$.

The $EV(0,1)$ distribution is the standardized extreme value distribution. Clearly, if $Y \sim EV(\beta, \sigma)$, then $(Y-\beta)/\sigma \sim EV(0,1)$. The mean and the variance of the general extreme value distribution are $\beta - \nu\sigma$, and $\frac{(\pi\sigma)^2}{6}$, respectively, where $\nu = 0.5772...$ is the Euler's constant. More details about the Weibull and the extreme value distributions can be read in Lawless [27] or Martinussen and Sheike [33].

Data often include explanatory variables related to time measurements. A regression model is an important tool to take into account the heterogeneity of the experimental units. In generalized linear modeling, it is possible to construct a regression model by specifying a relationship between one or more model parameters and a certain covariate pattern. In the context of SPC, let be n independent settings of the same experimental situation at the $j-$th moment. For the $i-$th setting, $i = 1, ..., n$, let $T_i^{(j)}$ denote lifetimes measured at the $j-$th moment. If it is assumed that $T_i^{(j)} \sim W(\theta_i, \gamma)$, then WRM and the EVRM are related by the expression (2.1) by making $y_{ik}^{(j)} = \log t_{ik}^{(j)}$. This is, $y_{ik}^{(j)}$ represents the log-transformation of the $k-$th time observation measured in the $i-$th setting of the experiment at the $j-$th moment. In this case, $Y_i \sim EV(\mathbf{x}_i'\boldsymbol{\beta}, \sigma)$ and the terms $z_{ik}^{(j)}$ are independent observations of the variable $Z \sim EV(0,1)$. More about the WRM and the EVRM can be read in Lawless [27].

2.3.2 Estimation and inference in the WRM

Let $(\mathbf{x}_i', y_{ik})$, $i = 1, \ldots, n; k = 1, \ldots, m_i$, be a random data set of N observations taken from model (2.1) at the $j-$th moment. It is possible to estimate the p-dimensional parameter vector $\boldsymbol{\xi} = (\boldsymbol{\beta}', \sigma)'$ characterizing model (2.1) at every $j-$th moment. The likelihood function for $\boldsymbol{\beta}$ and $\varphi = \log\sigma$ at the $j-$th moment, when there are no censored observations, is given by

$$\ell_j(\boldsymbol{\xi}) = -N\varphi + \sum_{i=1}^{n}\sum_{k=1}^{m_i}\left[\frac{y_{ij} - \mathbf{x}_i'\boldsymbol{\beta}}{e^{\varphi}} - \exp\left(\frac{y_{ij} - \mathbf{x}_i'\boldsymbol{\beta}}{e^{\varphi}}\right)\right] \tag{2.7}$$

The MLE of the parameter vector $\boldsymbol{\xi}$ at the $j-$th moment is obtained by solving the equation system defined by $\mathbf{U}_p = \mathbf{0}_p$, where the components of the $p-$dimensional vector

$\mathbf{U}$ are the first order partial derivatives of the likelihood function (2.7) respect to $\boldsymbol{\xi}$. The system must be solved numerically by a numerical method.

Let $\hat{\boldsymbol{\xi}} = (\hat{\boldsymbol{\beta}}', \hat{\varphi})'$ be the MLE of the parameter vector $\boldsymbol{\xi}$. It is well known that under certain regularity conditions the vector $\hat{\boldsymbol{\xi}}$ follows a $p-$dimensional normal distribution with mean vector $\boldsymbol{\xi}$ and covariance matrix $\Im^{-1}$, where $\Im$ is the information matrix, when $N \to \infty$. Details on how to proceed with the Newton-Raphson method for finding $\hat{\boldsymbol{\xi}}$ and estimating $\Im$ can be read in Lawless [27]. An approximated method for estimating the asymptotic information matrix $\Im$ is presented in Paul and Thiagarajah [46].

DiCiccio [14] presents some interesting results on how to make approximate inference about the parameter vector $\boldsymbol{\xi} = (\boldsymbol{\beta}', \varphi)'$ characterizing model (2.1) for non-large enough N. In the following discussion, we will address to some aspects of his work that we have adapted to the special case of our interest.

According to DiCiccio [14], several authors as Fraser [18] have stated that inference about the parameters $\boldsymbol{\beta}$ and φ should be made conditionally on the vector $\hat{\mathbf{z}}$ of the standardized residuals $\hat{z}_{ij} = (y_{ij} - \mathbf{x}_i'\hat{\boldsymbol{\beta}})/\hat{\sigma}$. The joint conditional density of the pivotal quantities $\mathbf{P}_1 = (\boldsymbol{\beta} - \hat{\boldsymbol{\beta}})/\hat{\sigma}$ and $P_2 = \varphi - \hat{\varphi}$ given the vector $\hat{\mathbf{z}}$ is known to have an intractable form. Accurate approximated LRT-based methods for making inference about $\boldsymbol{\xi} = (\boldsymbol{\beta}', \varphi)'$ are available. For instance, let the parameter vector $\boldsymbol{\xi}$ be partitioned in the form $(\boldsymbol{\phi}', \boldsymbol{\psi}')'$ so that, for convenience and simplicity, the sub-vector $\boldsymbol{\phi}$ consists of the first q components of $\boldsymbol{\xi}$. By fixing the value of $\boldsymbol{\phi}$, the relative LRT statistic for that parameter is defined to be

$$\Lambda(\boldsymbol{\phi}) = 2\ell(\hat{\boldsymbol{\xi}}) - 2\ell(\boldsymbol{\phi}, \tilde{\boldsymbol{\psi}}_{\boldsymbol{\phi}}) \tag{2.8}$$

where $\hat{\boldsymbol{\xi}}$ is the unrestricted MLE of the parameter vector $\boldsymbol{\xi}$ and $\tilde{\boldsymbol{\psi}}_{\boldsymbol{\phi}}$ is the MLE of the parameters $\boldsymbol{\psi}$ when it is assumed that $\boldsymbol{\phi}$ is fixed at the given value.

If the parameter vector $\boldsymbol{\xi} = (\boldsymbol{\beta}', \varphi)'$ is partitioned so that the sub-vector $\boldsymbol{\phi}$ consists of a single parameter, for instance $\boldsymbol{\phi} = \varphi$, then the signed square root of the relative LRT statistic for φ is defined to be

$$R(\varphi) = \text{sign}(\varphi_0 - \hat{\varphi})\sqrt{\Lambda(\varphi)} \tag{2.9}$$

where φ_0 is the assumed fixed value of φ.

It can be shown that the marginal distributions of $\Lambda(\boldsymbol{\phi})$ and $R(\varphi)$ tend to the chi-square distribution with one degree of freedom and to the normal standard distribution, respectively, as N increases. Hinkley [22] has shown that these limits also hold for the distribution of $\Lambda(\boldsymbol{\phi})|\hat{\mathbf{z}}$ and $R(\varphi)|\hat{\mathbf{z}}$. More details about the use of the relative LRT statistic conditioned by the residuals of the basic model for making inference can be read in Lawless [28].

The standard normal approximation to the conditional distribution of $R(\varphi)$ has an error of order $O_P(N^{-1/2})$ that can be reduced to order $O_P(N^{-3/2})$ by taking its conditional mean and variance into account. Formulae for these adjustments are presented in the rest

of this section. Corrections to the signed root of the relative LRT statistics for a single parameter have been discussed very generally by Barndorff-Nielsen [7] and in the case of location-scale models by DiCiccio [13].

In the following, we will adopt the convention according to which the partial derivatives of the likelihood function (2.7) are $d_{lr\ldots} = [\partial^{1+1+\cdots}\ell(\boldsymbol{\xi})/\partial\xi_l\partial\xi_r\ldots]_{\boldsymbol{\xi}=\hat{\boldsymbol{\xi}}}$, $l, r, t, u = 1, ..., p$. Let also $((v_{lr})) = ((d^2_{lr}))^{-1} = ((\Im_{lr}))^{-1}$ be the elements of the observed covariance matrix. Then, according to Sprott [62] and DiCiccio [14], from the Taylor expansion of $\Lambda(\varphi)$ about $\hat{\varphi}$, with an error of order $O_P(N^{-3/2})$, it follows that

$$\Lambda(\varphi) \approx U^2 - \tfrac{1}{3}AU^3 - \tfrac{1}{12}BU^4 \tag{2.10}$$

and

$$R(\varphi) \approx U - \tfrac{1}{6}AU^2 - \tfrac{1}{72}(3B + A^2)U^3 \tag{2.11}$$

where

$$U = \frac{\varphi - \hat{\varphi}}{\sqrt{v_{pp}}} = \frac{\log\sigma - \log\hat{\sigma}}{\sqrt{v_{pp}}} \tag{2.12}$$

$$A = v_{pp}^{-3/2}\sum_{l=1}^{p}\sum_{r=1}^{p}\sum_{t=1}^{p} d_{lrt}v_{lp}v_{rp}v_{tp} \tag{2.13}$$

and

$$B = v_{pp}^{-1/2}\left(\sum_{l=1}^{p}\sum_{r=1}^{p}\sum_{t=1}^{p}\sum_{u=1}^{p} d_{lrtu}v_{lp}v_{rp}v_{tp}v_{up} + 3\sum_{l=1}^{p}\sum_{r=1}^{p} S_lS_rJ_{lr}\right) \tag{2.14}$$

with

$$S_l = \sum_{r=1}^{p}\sum_{t=1}^{p} d_{lrt}v_{rp}v_{tp} \tag{2.15}$$

and

$$J_{lr} = v_{lr} - v_{pp}^{-1}v_{lp}v_{rp} \tag{2.16}$$

By making calculations similar to those described in Hinkley [22], the conditional mean of $R(\varphi)$ is

$$m \approx \frac{1}{6}v_{pp}^{-1/2}\sum_{l=1}^{p}\sum_{r=1}^{p}\sum_{t=1}^{p} d_{lrt}v_{lp}\left(3v_{rt} - \frac{v_{rp}v_{tp}}{v_{pp}}\right) \tag{2.17}$$

and the conditional variance of $R(\varphi)$ is

$$s^2 \approx 1 + \tfrac{1}{4}C + \tfrac{1}{12}D - m^2 \tag{2.18}$$

where

$$C = \sum_{l=1}^{p}\sum_{r=1}^{p}\sum_{t=1}^{p}\sum_{u=1}^{p} d_{lrtu}(v_{lr}v_{tu} - J_{lr}J_{tu}) \tag{2.19}$$

and

$$D = \sum_{l=1}^{p}\sum_{r=1}^{p}\sum_{t=1}^{p} d_{lrt}\left(\sum_{a=1}^{p}\sum_{b=1}^{p}\sum_{c=1}^{p} d_{abc}\left[3M_1 + 2M_2\right]\right) \tag{2.20}$$

where $M_1 = v_{lr}v_{ta}v_{bc} - J_{lr}J_{ta}J_{bc}$ and $M_2 = v_{la}v_{rb}v_{tc} - J_{la}J_{rb}J_{tc}$.

According to DiCiccio [14], the quantity m is of order $O_P(N^{-1/2})$, whereas s^2 is of order $1 + O_P(N^{-1})$. Thus, with an error of order $O_P(N^{-3/2})$, it can be obtained for relatively small and moderate data-set dimensions that

$$R_C(\varphi) = \frac{R(\varphi) - m}{s} \underset{\text{appr.}}{\sim} N(0;1) \tag{2.21}$$

where the acronym "appr." means "approximately".

From DiCiccio [14] with an error of order $O_P(N^{-3/2})$ for relatively small and moderate samples it can be also obtained that

$$\Lambda_C(\varphi) = \frac{\Lambda(\varphi)}{m^2 + s^2} \underset{\text{appr.}}{\sim} \chi^2_1 \tag{2.22}$$

Moreover, by inverting expression (2.11), the α quantile of U, given by (2.12), correct to order $O_P(N^{-3/2})$, is found to be

$$u_\alpha = r_\alpha + \tfrac{1}{6}A(r_\alpha)^2 + \tfrac{1}{72}(3B + 5A^2)(r_\alpha)^3 \tag{2.23}$$

where $r_\alpha = m + sz_\alpha$ with z_α being the α quantile of the standard normal distribution. Expression (2.23) provides the same order of accuracy as the direct use of the standard normal approximation for $R_C(\varphi)$ in making inference about the parameter φ. However, as DiCiccio [14] states, in very small datasets, expression (2.23) may suffer from failure of monotonicity and produce inaccurate results.

2.4 Control charts for monitoring the parameter φ

2.4.1 Preliminary considerations

According to the fact that $\sigma = \gamma^{-1}$, it is clear that monitoring the EVRM scale parameter σ is equivalent to monitoring the WRM shape parameter γ. Thus, the monitoring of the WRM shape parameter is proposed via the log-transformation of the Weibull-distributed response. Thus, model (2.1) is of interest. Actually, chart designing is based on the EVRM log-scale parameter $\varphi = \log\sigma$. Such parameterization does not substantially change the essence of the design but does make it an easier task to address instead.

In the context of SPC, let us suppose a process characterized by model (2.1) and let $\boldsymbol{\xi}_0 = (\boldsymbol{\beta}_0', \varphi_0)'$, with $\varphi_0 = \log\sigma_0$, be the in-control parameter vector. For the $i-$th level of the experiment at the $j-$th moment, we have

$$E(Y_i^{(j)}) = \mathbf{x}_i'\boldsymbol{\beta}_0 - \sigma_0\nu \tag{2.24}$$

$$Var(Y_i^{(j)}) = \frac{(\pi\sigma_0)^2}{6} \tag{2.25}$$

where $\nu = 0.5772...$ is the Euler's constant.

Let us assume further that detecting departures from the known value of the scale parameter σ_0 is wanted. From expressions (2.24) and (2.25), changes in the extreme value scale parameter σ will generate changes in both the mean, for stable $\boldsymbol{\beta}$, and the variance of the log-transformed times Y_i. Particularly, increases (or decreases) in σ result in a lower mean value of the log-transformed times with a greater (or a lower) variance. Both cases imply the deterioration of the process.

Let us suppose that at the $j-$th moment, $j = 1, 2, \cdots$, a sample $(y_{ik}^{(j)}, \mathbf{x}_i)$, $i = 1, ..., n$, $k = 1, \cdots, m_i$, from model (2.1) is available. Adjustments to ancillaries (2.8) and (2.9) and pivotal (2.12) can be used to design control schemes for detecting departures from $\sigma = \sigma_0$ (or, equivalently, from $\varphi = \varphi_0$). It is clear that chart designing is based on approximations of order $O_P(N^{-3/2})$, so the effectiveness of the schemes are correct to that order. The design does not require the parameters β_l, $l = 1, \cdots, p-1$, to be known, only requires them to be stable.

At this point, it should be noted that the EWMA and CUSUM schemes proposed further are based on functions of $R(\varphi)$ or $\Lambda(\varphi)$ rather than on φ directly. So, the behaviors of the ancillary quantities (2.21) and (2.22) as functions of φ have to be well understood. The fact is that increases (or decreases) in the EVRM log-scale parameter φ lead to decreases (or increases) in $R_C(\varphi)$. Thus, when increases in φ occur, a decrease in the mean value of $R_C(\varphi)$ is expected and viceversa. In the other hand, increases or decreases in φ lead to increases in both the mean and the variance of $R_C^2(\varphi)$ and $\Lambda_C(\varphi)$. Consequently, shifts in φ can be detected by detecting either changes in the mean level of $R_C(\varphi)$ or increases in the variance of $R_C^2(\varphi)$ or $\Lambda_C(\varphi)$. The following methodologies take into account these facts.

2.4.2 The $CU-$Chart

From the adjustment (2.23) to the α quantile of pivotal U given by (2.12), it is approximately obtained that

$$P\left(u_{\alpha/2} \leq \frac{\varphi_0 - \hat{\varphi}}{\sqrt{v_{\varphi\varphi}}} \leq u_{1-\alpha/2}\right) = 1 - \alpha \tag{2.26}$$

where φ_0 is the in-control value of the EVRM log-scale parameter φ. From expression (2.26), it is obtained the Shewhart-type control chart whose central line is $CL = \varphi_0$ and control limits are

$$LCL_j = \varphi_0 - v_{\varphi\varphi}^{1/2}\left[r_{1-\alpha/2}^{(j)} + \frac{A_j}{6}\left(r_{1-\alpha/2}^{(j)}\right)^2 + \frac{3B_j + 5A_j^2}{72}\left(r_{1-\alpha/2}^{(j)}\right)^3\right] \tag{2.27}$$

$$UCL_j = \varphi_0 - v_{\varphi\varphi}^{1/2}\left[r_{\alpha/2}^{(j)} + \frac{A_j}{6}\left(r_{\alpha/2}^{(j)}\right)^2 + \frac{3B_j + 5A_j^2}{72}\left(r_{\alpha/2}^{(j)}\right)^3\right]$$

where $j = 1, 2, \cdots$, and α is the false alarm rate.

This scheme will be called the CU-Chart (Shewhart–type chart based on the corrected α quantile of pivotal U). Note that the quantities $v_{\varphi\varphi}$, A, B, m and s are calculated each

time for the given data set, so the control limits of the chart are variable. If for any j value, $\hat{\varphi}_j < LCL_j$ the chart signal indicating a possible decrease in φ. If $\hat{\varphi}_j > UCL_j$, an increase in φ could happen.

2.4.3 The CR–EChart

Since the standard normal approximation to the conditional distribution of $R_C(\varphi)$ is feasible, it is thus possible to define the EWMA statistic

$$EW_j = \lambda \frac{R_j(\varphi) - m_j}{s_j} + (1-\lambda) EW_{t-1} \tag{2.28}$$

where $0 < \lambda \leq 1$ is the smoothing constant and $EW_0 = 0$. By taking into account approximation (2.21), when samples are taken from the process independently, we have that

$$Var(EW_j) \approx \frac{\lambda[1-(1-\lambda)^{2j}]}{2-\lambda} \tag{2.29}$$

The control chart is then defined by

$$\begin{aligned} LCL_j &= -L\sqrt{\frac{\lambda[1-(1-\lambda)^{2j}]}{2-\lambda}} \\ CL &= 0 \\ UCL_j &= L\sqrt{\frac{\lambda[1-(1-\lambda)^{2j}]}{2-\lambda}} \end{aligned} \tag{2.30}$$

where $j = 1, 2, \cdots$, and L is a positive constant.

This scheme will be called the CR-EChart (EWMA chart based on the standard normal approximation of the corrected $R(\varphi)$ statistic). The chart signals if, for any j, $EW_j < LCL_j$ indicating a possible increase in φ. If $EW_j > UCL_j$, it could be a decrease in φ.

2.4.4 The CR–CChart

The standard normal approximation to the distribution of $R_C(\varphi)$ also makes possible the design of the CUSUM procedure given by

$$SU_j = \max\left[0; \frac{R_j(\varphi) - m_j}{s_j} - C^+ + SU_{j-1}\right] \tag{2.31}$$

$$SL_j = \min\left[0; \frac{R_j(\varphi) - m_j}{s_j} + C^- + SL_{j-1}\right] \tag{2.32}$$

where $j = 1, 2, \cdots$, $SU_0 = SL_0 = 0$, C^+ and C^- are reference values that are chosen as in the coventional CUSUM for single normal observations.

This scheme will be called the CR-CChart (CUSUM chart based on the standard normal approximation of the corrected $R(\varphi)$ statistic). If for any j, $SL_j < LCL$ the procedure

indicates a possible increase in φ. If $SU_j > UCL$, a possible decrease in φ could take place.

2.4.5 The CP–CUSUM charts

As it was stated in Section 2.4.1, shifts in φ can also be detected by detecting increases in the variance of $R_C^2(\varphi)$ or $\Lambda_C(\varphi)$. Acosta-Mejía and Pignatiello [1] proposed the CP-CUSUM chart for monitoring the dispersion of a normal process with single observations. Let $X_j \sim N(\mu, \zeta)$ be a single observation from a normal process at the j-th sampling moment. The CP-CUSUM chart is based on the statistic $Z_j^2 = (X_j - \mu)^2/\zeta^2$ which follows a chi-squared distribution with one degree of freedom.

The distributional properties of Z_j^2, and the fact that at each sampling moment a unique value of the corrected relative LRT statistic $\Lambda_C(\varphi)$ or the corrected square root $R_C(\varphi)$ is available, suggest that Acosta-Mejía and Pigniatello's chart can be adapted for monitoring the log-scale parameter φ of the EVRM by using the ancillaries given in (2.21) or (2.22).

As the variances of $R_C^2(\varphi)$ and $\Lambda_C(\varphi)$ increase when φ increases or decreases, upper CP-CUSUM charts based on (2.21) or (2.22) could be designed for detecting both increases or decreases in the EVRM log-scale parameter φ. The scheme based on (2.21) is given by

$$SU_j = \max\left[0; \left(\frac{R_j(\varphi) - m_j}{s_j}\right)^2 - C^{\pm} + SU_{j-1}\right] \tag{2.33}$$

The scheme based on (2.22) is given by

$$SU_j = \max\left[0; \frac{\Lambda_j(\varphi)}{m_j^2 + s_j^2} - C^{\pm} + SU_{j-1}\right] \tag{2.34}$$

For both schemes given by (2.33) and (2.34), $SU_0 = 0$ and the reference values $C^{\pm}$ are defined as

$$C^{\pm} = \frac{c^{\pm} \log c^{\pm}}{c^{\pm} - 1}$$

and $c^{\pm}$ represents a specified standardized increase or decrease in φ, respectively, that is to be detected quickly. These charts signal as SU_j exceeds its respective control limit h_U.

For further discussion, the scheme based on ancillary (2.21) will be called the CP-CUSUM of CR (the CP-CUSUM chart based on the standard normal approximation of the corrected $R(\varphi)$ statistic) and the scheme based on ancillary (2.22) will be called the CP-CUSUM of CL (the CP-CUSUM chart based on chi-squared with one degree of freedom approximation of the corrected $\Lambda(\varphi)$ statistic).

2.5 Performance evaluation of the control charts

In phase II processes, the ARL is the traditionally used measure to evaluate control chart performance. This is the mean number of inspected samples until the scheme first signals.

Large values of ARL_0 are desirable. When the process is out-of-control, the shorter the ARL is, the better the ability of the scheme to detect an out–of–control state. When the process is in control, a short ARL implies an increase of the false alarm rate. In this work, ARL for each scheme was obtained by simulation.

One of the main purposes of this research is to find a value of the data-set dimension N from which approximations (2.21), (2.22) and (2.23) can be applied for monitoring phase II processes. Reported results suggest that the schemes work reasonably well for relatively small and moderate data-set dimensions.

2.5.1 Simulation settings

For simplicity, it is assumed that $p = 3$. This is, model (2.1) has an intercept β_1, a slope β_2 and a scale parameter σ. At the $j-$th moment, the model can be written in the form

$$y_{ik}^{(j)} = \beta_1 + \beta_2 x_i + \sigma z_{ik}^{(j)} = \beta_1 + \beta_2 \log(10i) + \sigma z_{ik}^{(j)} \tag{2.35}$$

where z_{ik} at every $j-$th moment are independent observations from $EV(0;1)$ and $x_i = \log(10i)$, $i = 1, 2, ..., n$, where $n = 10$ are the numeric levels of the unique covariate in the study. The parameters β_1 and β_2 are supposed to be stable. In-control values of the components of the parameter vector are $(\beta_{10}, \beta_{20}, \sigma_0)' = (3; 2; 1.5)'$ or, equivalently, $(\beta_{10}, \beta_{20}, \varphi_0)' = (3; 2; 0.40546)'$. These simulation settings are similar to those used by Yeh *et al.* [74] for carrying out their simulation study in phase I processes for the logistic profile. The number of observations in each level of the unique covariate is set to be $m_i = 3$, 5 or 10 so that explored values for the data-set dimension are $N = 30$, 50 or 100, respectively. For a given N, covariate values are assumed to be the same in repeated sampling.

For convenience, model (2.35) will be rewritten in the form

$$y_{ik}^{(j)} = 3 + 2\log(10i) + 1.5 d_3 z_{ik}^{(j)} \tag{2.36}$$

or equivalently

$$y_{ik}^{(j)} = 3 + 2\log(10i) + z_{ik}^{(j)} e^{0.40546 + \Delta_3} \tag{2.37}$$

This is, we are interested in detecting a $d_3 \times 100\%$ change in the in-control value of σ (or, equivalently, a departure of $\Delta_3 = \log d_3$ from the in-control value of φ). Decreases in the value σ_0 are obtained when $0 < d_3 < 1$. Increases in the value σ_0 are obtained when $d_3 > 1$. The in-control model is obtained when $d_3 = 1$.

2.5.2 ARL estimation

Approximated ARL were obtained via simulation as it is described below:

1. A single observation z_{ik} is generated from the standardized extreme value distribution. Then, for the given values of the simulation settings and the contamination constant d_3, the generated observation z_{ik} is replaced in (2.36) to obtain a log-transformed lifetime y_{ik}. Repeat until a set of N observations is completed.

2. Once a data set is completed, fit the model (2.35). The fit results in the MLE of $\boldsymbol{\xi} = (\beta_1, \beta_2, \varphi)$ and the observed information matrix $\Im^{-1}$.

3. With the help of the third– and fourth–order derivatives of the likelihood function (2.7) evaluated at the MLE of $\boldsymbol{\xi}$, find the quantities U, A, B, C and D by using formulae (2.12), (2.13), (2.14), (2.19) and (2.20).

4. Compute $R(\varphi)$, m and s throughout expressions (2.11), (2.17) and (2.18).

5. (a) For the CU–Chart, control limits are found by (2.27) for a given α.

   (b) For the rest of the schemes, let G denote either the quantity given by (2.21) or by (2.22). Compute G and, subsequently, the EWMA statistic (2.28), the CUSUM statistics (2.31) and (2.32) and the CP–CUSUM statistics (2.33) or (2.34).

6. For a given scheme, repeat steps 1–5 until the signaling condition first holds. The total number of data sets generated this way is called a run length. A lot of run length values are needed to obtain. The mean of these values is an ARL estimate.

2.5.3 Simulations results

Described procedure for ARL estimation was run out for $N = 30, 50$ and 100. All the schemes were calibrated to reach $ARL_0 = 200$. This is obtained by choosing $\alpha = 0.005$ for the CU–Chart; $\lambda = 0.1$ and $L = 2.4536$ for the CR–EChart; $C^+ = C^- = 0.5$ and $UCL = -LCL = 4.07$ for the CR–CChart; $C^{\pm} = 1.09393$ and $h_U = 14.10$ for the upper CP–CUSUM of CR. It is worth mentioning that these designing parameters are approximately the same used for monitoring single normal observations.

Designing parameters for the CP–CUSUM of CL depend on the data-set dimension N and were set to be $C^{\pm} = 1.19337$ and $h_U = 12.11$ for $N = 30$, $h_U = 12.00$ for $N = 50$ and $h_U = 11.92$ for $N = 100$. In this case, the designing parameters for the largest studied N are approximately those of the unbiased chart for monitoring dispersion of a normal process with single observations.

Designing parameters ARL_0, α, λ and C^* were set to be fixed. The rest of the designing parameters: L, UCL, LCL and h_U, were found via simulation by using a bisection search algorithm in order to achieve the desired ARL_0 value. In the bisection search algorithm, for each intermediary value of the designing parameters, 20000 run lengths were simulated. If the estimated ARL_0 was sufficiently close to 200, the current value of the corresponding designing parameter was retained. Otherwise, the search was continued.

Approximated ARL values were obtained by generating 50000 run-length values and are presented in Tables 2.4 and 2.5. These tables also contain an estimation of the respective standard deviation of the run lengths in brackets. Results for decreases in σ_0 greater than 50% and increases greater than twice the in-control value are not reported because these large shifts are detected as soon as they occur in mean terms.

Table 2.4 shows the performance of the CU–Chart, the CR–EChart and the CR–CChart when sustained shifts (increases or decreases) in the log–scale parameter φ of the EVRM

	CU–Chart			CR–EChart			CR–CChart		
d_3	N=30	N=50	N=100	N=30	N=50	N=100	N=30	N=50	N=100
0.5	1.06	1.00	1.00	2.01	1.72	1.01	1.83	1.23	1.00
	(0.25)	(0.02)	(0.00)	(0.20)	(0.45)	(0.08)	(0.38)	(0.42)	(0.01)
0.6	1.62	1.07	1.00	2.46	2.01	1.46	2.19	1.81	1.09
	(1.00)	(0.28)	(0.01)	(0.23)	(0.23)	(0.50)	(0.46)	(0.41)	(0.29)
0.7	4.18	1.86	1.06	3.40	2.60	1.99	3.06	2.31	1.74
	(3.64)	(1.27)	(0.26)	(0.83)	(0.59)	(0.25)	(0.86)	(0.54)	(0.45)
0.8	15.75	6.79	2.28	5.49	4.06	2.12	5.24	3.72	2.50
	(15.25)	(6.27)	(1.71)	(1.84)	(1.15)	(0.67)	(2.07)	(1.22)	(0.66)
0.9	71.85	43.22	17.84	14.00	9.70	6.15	16.20	10.24	5.96
	(70.68)	(42.71)	(17.34)	(7.88)	(4.62)	(2.30)	(11.18)	(5.89)	(2.63)
1.0	198.62	199.20	199.81	199.04	199.55	200.15	198.69	199.76	200.22
	(198.12)	(198.70)	(199.31)	(192.81)	(192.99)	(192.51)	(196.96)	(197.60)	(197.75)
1.1	52.22	31.83	15.15	15.67	10.50	6.58	17.83	11.08	6.42
	(51.72)	(31.33)	(14.64)	(9.84)	(5.57)	(2.77)	(13.26)	(7.00)	(3.19)
1.2	12.94	6.70	2.80	6.43	4.63	3.15	6.22	4.31	2.85
	(12.43)	(6.18)	(2.24)	(2.76)	(1.67)	(0.92)	(3.13)	(1.79)	(0.93)
1.3	5.03	2.64	1.35	4.15	3.10	2.22	3.81	2.78	1.96
	(4.50)	(2.08)	(0.69)	(1.45)	(0.93)	(0.52)	(1.53)	(0.93)	(0.55)
1.4	2.70	1.58	1.07	3.15	2.42	1.82	2.83	2.15	1.52
	(2.14)	(0.96)	(0.27)	(0.97)	(0.63)	(0.44)	(0.99)	(0.63)	(0.51)
1.5	1.81	1.22	1.01	2.60	2.05	1.48	2.31	1.79	1.21
	(1.21)	(0.51)	(0.10)	(0.73)	(0.48)	(0.50)	(0.73)	(0.54)	(0.41)
1.6	1.41	1.08	1.00	2.25	1.81	1.20	1.99	1.52	1.06
	(0.76)	(0.29)	(0.03)	(0.58)	(0.46)	(0.40)	(0.61)	(0.52)	(0.23)
1.7	1.22	1.03	1.00	2.02	1.60	1.06	1.75	1.31	1.01
	(0.51)	(0.17)	(0.01)	(0.50)	(0.50)	(0.24)	(0.56)	(0.47)	(0.10)
1.8	1.11	1.01	1.00	1.85	1.40	1.01	1.57	1.17	1.00
	(0.36)	(0.01)	(0.00)	(0.48)	(0.49)	(0.12)	(0.54)	(0.37)	(0.04)
1.9	1.06	1.00	1.00	1.70	1.24	1.00	1.41	1.08	1.00
	(0.25)	(0.05)	(0.00)	(0.50)	(0.43)	(0.05)	(0.51)	(0.27)	(0.02)
2.0	1.03	1.00	1.00	1.55	1.13	1.00	1.29	1.04	1.00
	(0.18)	(0.31)	(0.00)	(0.51)	(0.34)	(0.02)	(0.46)	(0.18)	(0.01)

TABLE 2.4. Approximated performance of the proposed charts for detecting a $d_3 \times 100\%$ shift in the parameter $\sigma = 1.5$ of the simple WRM $y_{ik} = 3 + 2\log(10i) + 1.5z_{ik}$ with different dimensions N. Shifts in σ are detected via drops in the mean value of the corrected monitoring statistic.

are detected by detecting shifts in the mean level of the respective plotting statistics. All the schemes detect changes (increases or decreases) in φ. For all studied cases, changes are detected earlier as N increases. As it was expected, the CR–EChart and the CR–CChart detect small changes faster with a lower standard deviation of the run lengths than the CU–Chart. The CU–Chart, instead, detects large shifts faster with a lower standard deviation. In general, the CR–CChart performs slightly better than the CR–EChart except for small shifts (increases or decreases) and small and moderate N values.

The performance of the CP–CUSUM of CR and the CP–CUSUM of CL schemes are presented in Table 2.5. In this case, sustained shifts in the EVRM log-scale parameter φ are detected by detecting increases in the variability of the quantities $R^2_C(\varphi)$ and $\Lambda_C(\varphi)$. Simulations suggest that the CP–CUSUM of CL detects decreases in φ faster than the CP–

	CP–CUSUM of CR			CP–CUSUM of CL		
d_3	N=30	N=50	N=100	N=30	N=50	N=100
0.5	1.47 (0.52)	1.04 (0.19)	1.00 (0.00)	1.26 (0.44)	1.01 (0.10)	1.00 (0.00)
0.6	2.25 (0.79)	1.47 (0.53)	1.00 (0.00)	1.88 (0.67)	1.26 (0.45)	1.00 (0.05)
0.7	3.99 (1.61)	2.46 (0.91)	1.40 (0.52)	3.07 (1.23)	2.03 (0.77)	1.23 (0.43)
0.8	9.32 (4.58)	5.43 (2.41)	2.81 (1.11)	6.30 (3.02)	4.07 (1.82)	2.31 (0.95)
0.9	41.25 (29.72)	23.01 (14.28)	10.85 (5.68)	20.90 (13.82)	14.01 (8.50)	7.87 (4.22)
1.0	198.68 (183.67)	200.73 (183.87)	200.02 (183.15)	198.99 (189.36)	199.79 (189.61)	199.84 (190.01)
1.1	32.99 (23.13)	20.59 (13.00)	10.79 (5.99)	148.90 (139.05)	48.02 (39.85)	14.59 (9.50)
1.2	9.95 (5.55)	6.13 (3.16)	3.30 (1.54)	19.91 (13.92)	8.37 (4.87)	3.54 (1.78)
1.3	5.06 (2.60)	3.18 (1.51)	1.81 (0.78)	7.55 (4.34)	3.73 (1.92)	1.84 (0.82)
1.4	3.24 (1.58)	2.10 (0.94)	1.28 (0.48)	4.23 (2.24)	2.30 (1.10)	1.28 (0.49)
1.5	2.36 (1.10)	1.58 (0.67)	1.08 (0.27)	2.86 (1.44)	1.67 (0.74)	1.07 (0.26)
1.6	1.86 (0.84)	1.30 (0.49)	1.01 (0.10)	2.15 (1.03)	1.35 (0.54)	1.01 (0.12)
1.7	1.55 (0.67)	1.14 (0.35)	1.00 (0.05)	1.74 (0.79)	1.17 (0.39)	1.00 (0.04)
1.8	1.35 (0.54)	1.06 (0.24)	1.00 (0.02)	1.48 (0.63)	1.08 (0.27)	1.00 (0.01)
1.9	1.22 (0.44)	1.02 (0.15)	1.00 (0.00)	1.31 (0.52)	1.03 (0.17)	1.00 (0.00)
2.0	1.14 (0.35)	1.01 (0.10)	1.00 (0.00)	1.20 (0.42)	1.01 (0.11)	1.00 (0.00)

TABLE 2.5. Approximated performance of the proposed CP–CUSUM charts for detecting a $d_3 \times 100\%$ shift in the parameter $\sigma = 1.5$ of the simple WRM $y_{ik} = 3 + 2\log(10i) + 1.5z_{ik}$ with different dimensions N. Shifts in σ are detected via drops in the dispersion of the corrected monitoring statistic.

CUSUM of CR but takes longer to detect increases in φ for all reported N. For the largest reported data-set dimension, both schemes exhibit similar performances approximately.

2.6 Example

Nelson [38] describes a life test experiment in which specimens of an electrical insulating fluid were subjected to a constant high-voltage stress. The elapsed time until each specimen failed was observed. There were seven groups of specimens tested at voltages ranging from 26 to 38 kilovolts. There were 76 specimens at 7 defined voltage levels. Data are presented in Table A.1 of Appendix A.1.

A preliminary analysis suggested a Weibull accelerated failure time model (2.1) with $\mathbf{x}_i'\beta = \beta_1 + \beta_2 \log V_i$, where V is the voltage level. The likelihood ratio test for $H_0 : \beta_2 = 0$ gives $LRT = 77.6$ ($p = 0.0000; d.f. = 1$) what suggests that part of the variability observed in failure times can be explained by the voltage stress. The fitted model is

$$\hat{y}_{ik} = \log \hat{t}_{ik} = 64.8472 - 17.7296 x_i + 1.2877 z_{ik} \tag{2.38}$$

For further illustration and monitoring purposes, it will be assumed that fit (2.38) represents the in-control model and it is wanted to detect departures from $\sigma = 1.2877$ (or, equivalently, from $\varphi = 0.2529$). Thus, 20 independent samples were generated with the same covariate pattern; first 10 from the in-control model and the last ones from the model whose shape parameter shifts to the value $1.2877 d_3$.

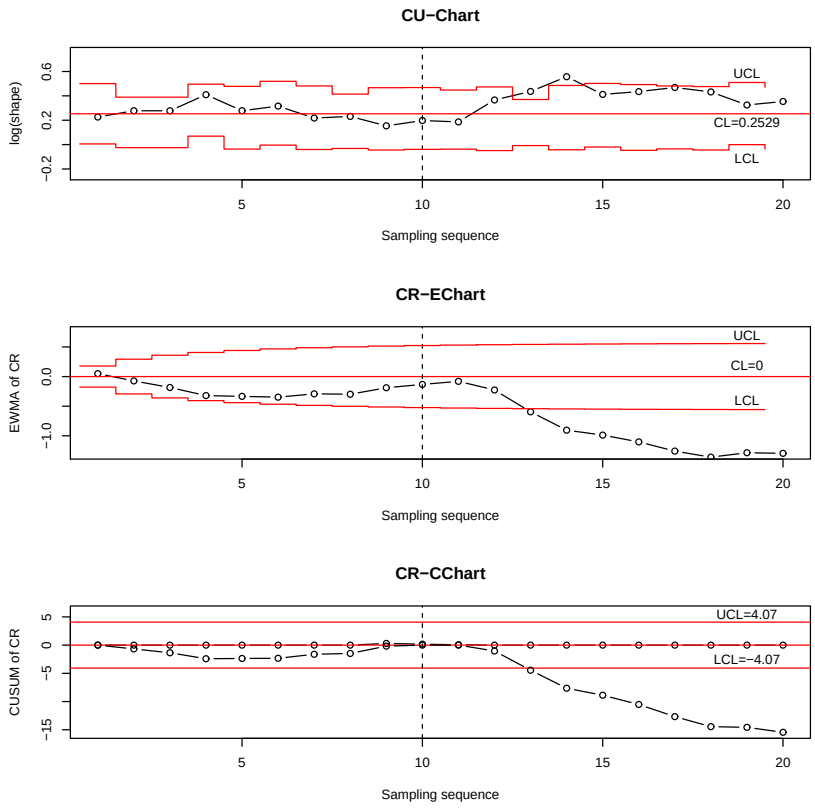

FIGURE 2.2. Control charts for detecting a 15% increase in $\varphi_0 = 0.2529$ for the failure time data. There are shown the charts for detecting shifts via changes in the mean value of the corrected $U(\varphi)$ or $R(\varphi)$ statistics.

The proposed Shewhart-type, EWMA, CUSUM and CP-CUSUM control schemes based on the corrected statistics were built for verifying the out-of-control detection ability. The CU–Chart was designed for $\alpha = 0.005$; the CR–EChart, for $\lambda = 0.1$ and $L = 2.4536$; the CR–CChart, for $C^+ = C^- = 0.5$ and $UCL = LCL = 4.07$; the upper CP–CUSUM of CR, for $C^{\pm} = 1.09393$ and $h_U = 14.10$ and the upper CP–CUSUM of CL, for $C^{\pm} = 1.19337$ and $h_U = 11.92$. All designs result in a nominal $ARL_0 = 200$.

The schemes for detecting a 15% increase in the scale parameter of the EVRM are presented in Figure 2.2 and Figure 2.3, respectively. In Figure 2.2, there are shown the charts for detecting the increase in φ via the increase in the mean value of the corrected $U(\varphi)$ statistic or the decrease in the mean value of the corrected $R(\varphi)$ statistic. All the schemes detect the planned increase at the 13−th monitoring moment, three moments later than it actually occurs. However, the CR-EChart and the CR-CChart show a sustained increase. The CU-Chart, instead, shows a stable process after having signaled when it really is out-of-control.

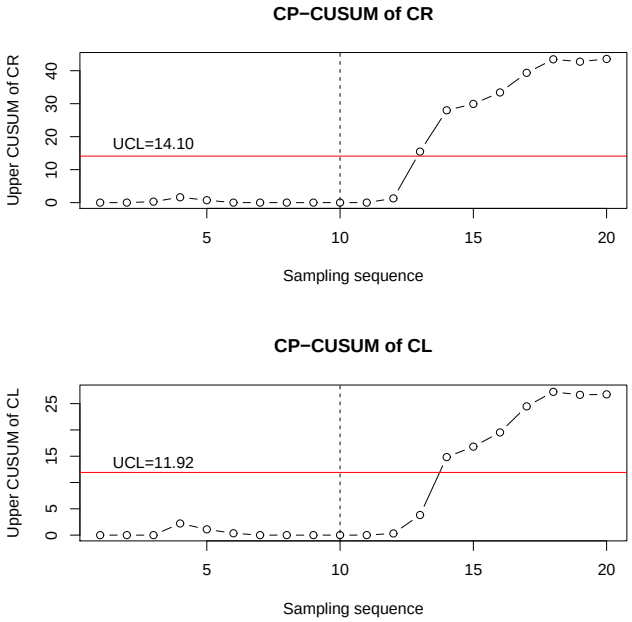

FIGURE 2.3. Control charts for detecting a 15% increase in $\varphi_0 = 0.2529$ for the failure time data. There are shown the charts for detecting shifts via increases in the dispersion of the corrected $R(\varphi)$ or $\Lambda(\varphi)$ statistics.

In Figure 2.3, the planned increase in φ is detected via the increase in the dispersion of the corrected $R(\varphi)$ and $\Lambda(\varphi)$ statistics. As it can be seen, both the CP-CUSUM charts detect the planned increase. However, the CP-CUSUM chart based on the corrected $R(\varphi)$ statistic signals one monitoring moment earlier than the CP-CUSUM chart based on the corrected $\Lambda(\varphi)$ statistic. The CP-CUSUM of CR delays two monitoring moments to detect the planned increase.

The schemes for detecting a 10% decrease in the scale parameter of the EVRM are presented in Figure 2.4 and Figure 2.5, respectively. In Figure 2.4, there are shown the charts for detecting the planned decrease in φ via the decrease in the mean value of the corrected $U(\varphi)$ statistic or the increase in the mean value of the corrected $R(\varphi)$ statistic. All these schemes detect the planned decrease at the 16-th monitoring moment, six moments after it really occurs. Again, the CR-EChart and the CR-CChart show the sustained pattern of the simulated decrease, the CU-Chart does not. However, although the CU-Chart takes longer to detect the planned decrease in φ, a trend in the values of the plotting statistic to lie below the central line of the chart can be observed.

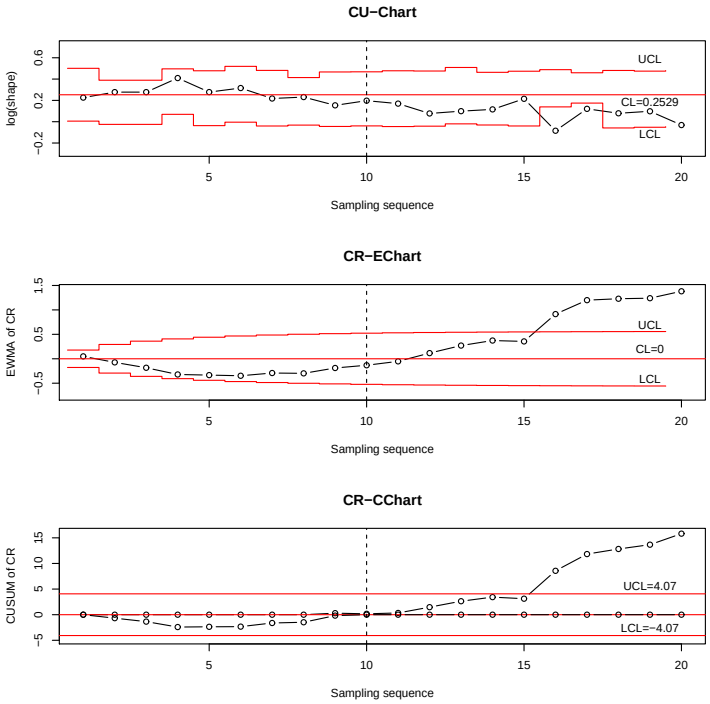

FIGURE 2.4. Control charts for detecting a 10% decrease in $\varphi_0 = 0.2529$ for the failure time data. There are shown the charts for detecting shifts via changes in the mean value of the corrected $U(\varphi)$ or $R(\varphi)$ statistics.

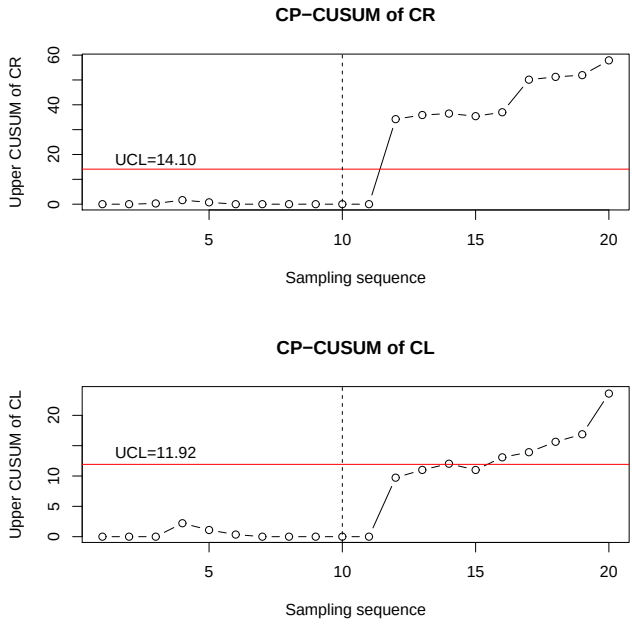

FIGURE 2.5. Control charts for detecting a 10% decrease in $\varphi_0 = 0.2529$ for the failure time data. There are shown the charts for detecting shifts via increases in the dispersion of the corrected $R(\varphi)$ or $\Lambda(\varphi)$ statistics.

Figure 2.5 shows the detection of the planned decrease via the increase in the dispersion of the corrected $R(\varphi)$ and $\Lambda(\varphi)$ statistics. Both of the charts detect the decrease but not at the same monitoring moment. The CP-CUSUM of CR detects the decrease substantially earlier than the CP-CUSUM of CL. The CP-CUSUM of CR signals at the 12-th monitoring moment, whilst the CP-CUSUM of CL takes three more monitoring moments to detect the simulated decrease.

2.7 Recommendations

The presented methodology strongly depends on the amount of covariates in the model being monitored and the assessment of the quantities A, B, C and D depends on the number of third– and fourth–order derivatives of the underlying likelihood function. Thus, when a covariate is added, calculations for obtaining mentioned quantities become a hard task. However, this drawback could be overcome by designing a specialized software.

Due to particular theoretical aspects of the methodology for making Bartlett's corrections, we believe that the proposed methodology could be successfully extended to new monitoring conditions, rather than the ones presented herein, since:

- It turns the problem of monitoring the parameter vector of a WRM into the simpler problem of monitoring the mean level or the dispersion of a continuous quality characteristic whose distribution is known.
- With the exception of the *CU*–Chart, resulting control schemes are based on ancillary statistics. So, chart designing does not depend on the true value of the parameter being monitored.
- It could be used for monitoring regression models with response variable in the log-scale family.
- Although the methodology is developed for the special case of monitoring the EVRM log–scale parameter, it can be used for monitoring any single parameter of a parameter vector. This is, resulting schemes do not depend directly on the nature of the parameter being monitored. This fact has an important implication: regardless the parameter (a scale, a location or a shape one), the methodology always leads to simple schemes based on the same type of ancillary statistics.
- When monitoring a single parameter from a parameter vector, the rest of the parameters are treated as nuisance and do not need to be known.
- The methodology could represent an approximated but fairly acceptable procedure for monitoring a single parameter from a parameter vector when non-large enough data sets are available from regression models with response in the log-scale family.

2.8 Conclusions

In this chapter, some different control mechanisms were studied for monitoring the log-scale parameter of the EVRM in phase II processes. This is equivalent to monitoring

the shape parameter of the WRM. Simulation results suggest that Bartlett's adjustments to the relative LRT statistic (2.8), to the signed square root defined for the log-scale parameter $R(\varphi)$ given by (2.9) and to the $(\alpha \times 100\%)$-th quantile of U given by (2.12) make the resulting schemes a fairly acceptable procedure to carry out the monitoring for detecting sustained shifts in the log-scale parameter of the EVRM. None of the schemes exhibited an overall best performance. Each of them can be used upon certain conditions depending on the need of practitioners.

Although the presented methodology was developed for the particular case of the log-scale parameter of the EVRM, they could be applied for successfully monitoring one single parameter, not necessarily a scale one, of any regression model with response in the location-scale family. For instance, the monitoring of one of the coefficients β_l, $j = 1, ..., p-1$, of the EVRM can be carried regardless the value of the rest of the parameters including the scale one. At this point, this fact has a relevant importance because monitoring the parameters β_l, $j = 1, ..., p-1$, would be equivalent to monitoring risks.

REMARK

Part of the results presented in this chapter are reported in the paper "Monitoring the shape parameter of a Weibull regression model in Phase II processes" published in 2016 in *Journal of Quality and Reliability Engineering International*, volume 36, pages $195-207$.

CHAPTER 3

Monitoring the WRM parameter vector

3.1 The problem

Let us suppose again that at the $j-$th moment in time, $j = 1, 2, ...$, a data set with the structure in Table 2.1 is available. All the quantities in the table retain their primary meanings. Let us suppose further that we are still interested in the stability of the distributions of the variables Y_i, $i = 1, \cdots, n$ over time. In the preceding chapter, we made the same assumptions and proposed the monitoring of the WRM shape parameter in order to achieve our objective. As in a given moment in time, all the parameters of the model can change, in the following, we will propose the monitoring of the entire parameter vector linking the distributions of all the variables Y_i.

In some applications, the Y_i are time-to-event variables so that the data collection process may require the deterioration of the experimental units in which they are being measured. Thus, the measurements $y_{ik}^{(j)}$ at every $j-$th moment can be obtained just once at most from the same produced item or individual. Although under the definition provided by Woodall [71], the structure in Table 2.1 cannot be qualified as a profile, the statistical analysis in such situations aims to the same goal of profile monitoring.

For instance, the example from the food industry reviewed in Section 3.7 perfectly illustrates our point of view. In this example, we are interested in the stability of the distribution of the shelf life of sweet cookies in different storage conditions over time. This is, we would like to know whether the shelf time of different produced items subjected to the same storage conditions at different moments in time has the same distribution.

Moreover, from a preliminary graphical analysis of the 17 annually collected data batches in the example, it can be noted a decreasing linear trend for the log-transformation of the shelf life in accelerated conditions as temperature level increases. This trend is shown in solid lines for each annual batch in Figure 3.1. We have found enough reasons to think that methodologies from the monitoring of GLM profiles can be adapted for successfully monitoring regression models with time-to-event response.

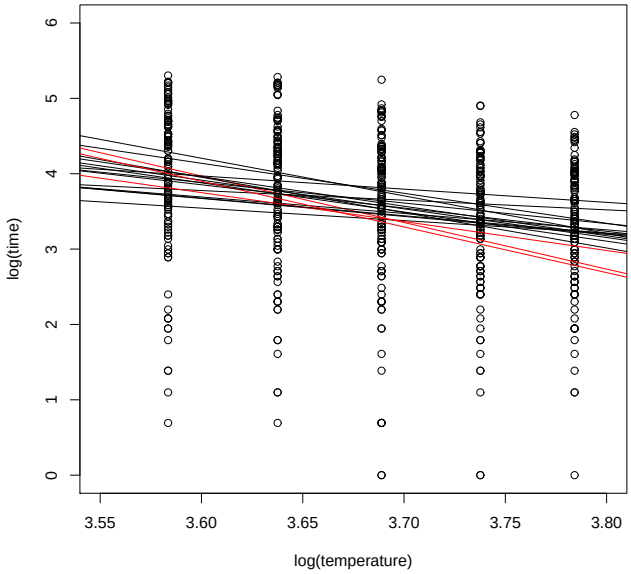

FIGURE 3.1. Preliminary graphical analysis for the food industry example

If a linear dependence between the response variables Y_i and the fixed $\mathbf{x}_i'$ values is assumed at the $j-$th moment, then this relationship can be analytically expressed by model (2.1) and we would be interested in testing over time the hypothesis

$$\begin{aligned} H_0 &: \boldsymbol{\xi}^{(j)} = \boldsymbol{\xi}_0 \\ H_1 &: \boldsymbol{\xi}^{(j)} = \boldsymbol{\xi}_0 + \boldsymbol{\Delta} \end{aligned} \tag{3.1}$$

This is, we would be interested in detecting departures $\boldsymbol{\Delta}$ from a known value $\boldsymbol{\xi}_0$. Departures can take place in one or more components of the parameter vector characterizing model (2.1). At this point, this fact has a great relevance because changes in the value of $\boldsymbol{\xi}$ will necessarily imply changes in the distributions of the responses Y_i at all experimental levels.

The hypothesis (3.1) can be tested over time by using LRT-based procedures. However, as it was stated earlier, distributions for modeling times-to-event data are often skewed, so that the use of the LRT statistic for designing control charts may be restrictive to large enough data sets. The need of making adjustments to the LRT statistic arises again for monitoring purposes when non-large enough data sets are available.

3.2 Using techniques from profile monitoring

As it was stated in Section 3.1, profile monitoring and monitoring regression models share the same objective. Thus, we feel that techniques from profile monitoring can be adapted for checking the stability of the parameter vector characterizing a regression model.

Different methodologies have been developed in order to be applied for monitoring GLM profiles. Soleymanian *et al.* [61] and Qi *et al.* [48] propose the monitoring of GLM profiles by using LRT-based charts. It is easy to realize that in most of the existing work on GLM monitoring the main purpose is focused on profiles with counting response. Maybe either the binary or the Poisson responses make the MLE of the parameter vector characterizing the model quickly converge to the asymptotic normality. That is perhaps the reason for the charts based on this asymptotic property to work reasonably well even for non-large enough profile dimensions.

Although in some of afore-cited articles it is stated that the proposed methodologies can be extended to the case of continuous response variable, they cannot be directly applied in the case of severely skewed response variables. For instance, we calculated ARL_0 for the Shewhart-type LRT chart presented in Soleymanian *et al.* [61] for monitoring the parameter vector of a simple WRM with the structure in Table 2.1 for different values of the data-set dimension N. In all cases, the upper control limit was set to be $UCL = \chi^2_{(0.995;3)} = 12.83816$, regardless the N value. This should lead to $ARL_0 = 200$. Estimated ARL_0 were obtained by setting $\mathbf{x}_i = (1, \log(10i))'$ and $\boldsymbol{\xi} = (\beta_1, \beta_2, \varphi)' = (3; 2; 0.4055)'$. Results are shown in the last row of Table 3.1.

	$\chi^2_{(3)}$	$N = 30$	$N = 50$	$N = 100$	$N = 300$	$N = 500$	$N = 1000$
$Q_{0.25}$	1.2125	1.2883	1.2507	1.2367	1.2207	1.2179	1.2169
$Q_{0.5}$	2.3659	2.5066	2.4439	2.4113	2.3844	2.3752	2.3682
$Q_{0.75}$	4.1083	4.3452	4.2472	4.1848	4.1389	4.1201	4.1071
$Q_{0.995}$	12.8381	13.5255	13.2889	13.0197	12.9533	12.8926	12.8152
$Mean$	3.0000	3.1772	3.1013	3.0528	3.0207	3.0117	3.0007
$Variance$	6.0000	6.7035	6.4242	6.1898	6.0862	6.0429	5.9999
ARL_0	200.10	134.41	165.56	179.05	185.55	190.84	197.08

TABLE 3.1. Numerical characteristics of the distribution of the LRT statistic for different dimensions N of the simple WRM $y_{ik} = 3 + 2\log(10i) + 1.5z_{ik}$.

Table 3.1 also contains some approximated quantiles Q_*, the mean and the variance of the distribution of the LRT statistic defined for the WRM parameter vector for different N values. These approximated results were also obtained by simulation. The same numeric characteristics for the chi-square distribution with three degrees of freedom are reported in the second column of Table 3.1. As it can be seen, ARL_0 values are far from the nominal one for small and moderate N dimensions. ARL_0 values begin to be close to the nominal $ARL_0 = 200$ just for $N = 1000$. The fact is that the distribution of the LRT statistic is not exactly that of the chi-square distribution. This is due to the skewness of the response variable in the WRM. This fact has the same practical implication that we faced while were trying to monitor a single parameter and can be overcome in the same way.

Table 3.2 shows the simulated distribution of the adjusted LRT statistic for different N values. Note that the distribution of the adjusted LRT is now closer to the chi-square distribution for all reported N values practically. Approximated ARL_0 of the Shewhart-type LRT chart in Soleymanian *et al.* [61] with $UCL = \chi^2_{(0.995;3)} = 12.83816$ are also reported. All results were obtained by setting $\mathbf{x}_i = (1, \log(10i))'$ and $\boldsymbol{\xi} = (\beta_1, \beta_2, \varphi)' = (3; 2; 0.4055)'$. It is clear that the chart that uses the corrected monitoring statistic performs fairly ac-

ceptable even for non-large enough N. This is, with the help of Bartlett's adjustments, the monitoring of the WRM parameter vector can be now carried out with a data structure whose dimension is approximately 33 times smaller. Indications on how to use Bartlett's adjustments for correcting the LRT statistic in a WRM will be addressed in the following sections.

	$\chi^2_{(3)}$	$N = 30$	$N = 50$	$N = 100$
$Q_{0.25}$	1.2125	1.2165	1.2150	1.2136
$Q_{0.5}$	2.3660	2.3741	2.3702	2.3669
$Q_{0.75}$	4.1083	4.1173	4.1191	4.1065
$Q_{0.995}$	12.8381	12.9154	12.8434	12.8378
$Mean$	3.0000	3.0095	3.0020	3.0002
$Variance$	6.0000	6.0473	6.0126	5.9997
ARL_0	200.10	193.75	197.32	198.12

TABLE 3.2. Numerical characteristics of the distribution of the corrected LRT statistic for different dimensions N of the simple WRM $y_{ik} = 3 + 2\log(10i) + 1.5z_{ik}$.

3.3 Theoretical framework

We are still interested in regression models of the form

$$y_{ik}^{(j)} = \log t_{ik}^{(j)} = \mathbf{x}_i'\boldsymbol{\beta} + \sigma z_{ik}^{(j)} \tag{3.2}$$

where $j = 1, 2, \ldots$ is the monitoring moment and $t_{ik}^{(j)}$, $k = 1, \cdots, m_i$, are observations of the variables $T_i \sim W(\theta_i; \gamma)$ measured at the $j-$th moment. Some details about the WRM (3.2) were already discussed in Section 2.3.1. Among other things, there was pointed that the $p-$dimensional vector $\boldsymbol{\xi} = (\boldsymbol{\beta}', \varphi)'$, where $\varphi = \log\sigma$, characterizes the WRM.

In previous chapter, the main objective was to monitor a single component of the parameter vector $\boldsymbol{\xi}$. Thus, the vector $\boldsymbol{\xi}$ was partitioned so that one of the resulting sub-vectors was formed by the single parameter we were interested in. The relative LRT-statistic defined for that parameter helped us to carry out the monitoring. We are now interested in monitoring the entire WRM parameter vector $\boldsymbol{\xi}$. Then, we will turn back to DiCicio's methodology based on Bartlett's adjustments to the LRT-statistic and will develop it for the special case of a sub-vector having dimension $2 \leq q \leq p$. This is, let the WRM parameter vector be partitioned of the form $\boldsymbol{\xi} = (\boldsymbol{\phi}', \boldsymbol{\psi}')'$, so that the sub-vector $\boldsymbol{\phi}$ with dimension $2 \leq q \leq p$ is of interest. In Section 2.3.2, it was stated that when we fix the value of $\boldsymbol{\phi}$, the relative LRT statistic for that parameter is defined to be

$$\Lambda(\boldsymbol{\phi}) = 2\ell(\hat{\boldsymbol{\xi}}) - 2\ell(\boldsymbol{\phi}, \tilde{\boldsymbol{\psi}}_{\boldsymbol{\phi}}) \tag{3.3}$$

where $\hat{\boldsymbol{\xi}}$ is the unrestricted MLE of the parameter vector $\boldsymbol{\xi}$ and $\tilde{\boldsymbol{\psi}}_{\boldsymbol{\phi}}$ is the MLE of the parameters $\boldsymbol{\psi}$ when it is assumed that $\boldsymbol{\phi}$ is fixed at the given value.

It was also stated that under some mild conditions $\Lambda(\boldsymbol{\phi}) \sim \chi^2_q$ when $N \to \infty$. This limit also holds for the conditional distribution of $\Lambda(\boldsymbol{\phi})|\hat{\mathbf{z}}$, where the vector $\hat{\mathbf{z}}$ consists of the residuals of model 3.2. The chi-square approximation to the conditional distribution of $\Lambda(\varphi)$ has an error of order $O_P(N^{-1})$ that can be reduced to order $O_P(N^{-3/2})$ by using a scaling factor that takes into account its conditional mean. A formula for this adjustment is given in the following paragraphs. This correction to the relative LRT statstic, often referred to as Bartlett's adjustment, has been discussed in [8].

For further discussion, we will return to the convention presented in Section 2.3.2, so the high-order partial derivatives of the likelihood function (2.7) for the WRM are assumed to be $d_{lr\ldots} = [\partial^{1+1+\cdots}\ell(\boldsymbol{\xi})/\partial\xi_l\partial\xi_r\ldots]_{\boldsymbol{\xi}=\hat{\boldsymbol{\xi}}}$, $l, r, t, u = 1, ..., p$. Let also the elements of the observed covariance matrix be $((v_{lr})) = ((d^2_{lr}))^{-1} = ((\Im_{lr}))^{-1}$. Let be the partitioned observed information matrix

$$\Im = \begin{bmatrix} \Im_{\boldsymbol{\phi}\boldsymbol{\phi}} & \Im_{\boldsymbol{\phi}\boldsymbol{\psi}} \\ \Im_{\boldsymbol{\psi}\boldsymbol{\phi}} & \Im_{\boldsymbol{\psi}\boldsymbol{\psi}} \end{bmatrix}$$

According to DiCiccio [14], it can be shown that, with an error of order $O_P(N^{-3/2})$, the conditional expectation of the relative LRT statistic defined for $\boldsymbol{\phi}$ can be approximated by the expression

$$b_\phi \approx q + \tfrac{1}{4}C + \tfrac{1}{12}D \tag{3.4}$$

where

$$C = \sum_{l=1}^{p}\sum_{r=1}^{p}\sum_{t=1}^{p}\sum_{u=1}^{p} d_{lrtu}(v_{lr}v_{tu} - K_{lr}K_{tu}) \tag{3.5}$$

and

$$D = \sum_{l=1}^{p}\sum_{r=1}^{p}\sum_{t=1}^{p} d_{lrt}\left(\sum_{a=1}^{p}\sum_{b=1}^{p}\sum_{c=1}^{p} d_{abc}\,[3M_1 + 2M_2]\right) \tag{3.6}$$

where $M_1 = v_{lr}v_{ta}v_{bc} - K_{lr}K_{ta}K_{bc}$, $M_2 = v_{la}v_{rb}v_{tc} - K_{la}K_{rb}K_{tc}$ and $K = ((K_{lr})) = \text{diag}\,(0, \Im^{-1}_{\psi\psi})$.

The χ^2_q approximation to the conditional distribution of $\Lambda(\boldsymbol{\phi})|\hat{\mathbf{z}}$ is of order $O_P(N^{-1})$, whereas the error in the approximation for $\frac{q}{b_\phi}\Lambda(\boldsymbol{\phi})$ is of order $O_P(N^{-3/2})$. Thus, with an error of order $O_P(N^{-3/2})$, it can be obtained for relatively small and moderate data-set dimensions that

$$\frac{q}{b_\phi}\Lambda(\boldsymbol{\phi}) \underset{\text{appr.}}{\sim} \chi^2_q \tag{3.7}$$

It is easy to see that for $q = p$, it is obtained the deviance form of the relative LRT statistic (3.3) defined for $\boldsymbol{\xi}$ and, with the help of Bartlett's adjustments, the χ^2_p distribution will better approximate the distribution of $\frac{p}{b_\xi}\Lambda(\boldsymbol{\xi})$ for non-large enough samples, with an error of order $O_P(N^{-3/2})$. In this case, $K_{lr} = 0$, $l, r = 1, ..., p$.

Moreover, from Lawless [27], it can be stated that the random variable $V^2 = \log\left[\frac{p}{b_\xi}\Lambda(\boldsymbol{\xi})\right]$ follows approximately a normal distribution whose mean and variance can be approximated by the expressions $E(V^2) = \log 2 + g(\frac{p}{2})$ and $Var(V^2) = g'(\frac{p}{2})$, respectively. In these expressions, $g(\centerdot)$ and $g'(\centerdot)$ are the digamma and the trigamma functions, respectively.

3.4 Control charts for monitoring WRM parameter vector

3.4.1 Preliminary considerations

As it was done in the case of monitoring a single parameter, monitoring the WRM parameter vector is proposed via the log-transformation of the Weibull-distributed response. Thus, the EVRM in the form given by (3.2) is of interest. In the context of SPC, let us suppose again a process characterized by the relationship (3.2) and let $\boldsymbol{\xi}_0 = (\boldsymbol{\beta}_0', \varphi_0)'$, with $\varphi_0 = \log \sigma_0$, be the in-control parameter vector. For the $i-$th level of the experiment at the $j-$th moment, the in-control mean and variance of the log-transformed Weibull-distributed lifetimes are given by expressions (2.24) and (2.25).

Other quantities related to the distribution of the log-transformed Weibull lifetimes in the $i-$th level at the $j-$moment are presented below. The in-control $r \times 100\%$ percentile, $r \in (0, 1)$, of the distribution of Y_i is

$$y_{i,r}^{(j)} = \mathbf{x}_i' \boldsymbol{\beta}_0 + \sigma_0 \log\left[-\log\left(1 - r\right)\right] \tag{3.8}$$

Note that the in-control $r \times 100\%$ percentile of the Weibull distribution is $t_{i,r} = \exp\left(y_{i,r}\right)$. Note also that the mean and/or the median of the variables Y_i can be verified with the help of (3.8) by making $r = 0.4296$ and/or $r = 0.5$.

The in-control survival probability corresponding to a particular value $y_{i0}^{(j)}$ is

$$S(y_{i0}^{(j)}) = \exp\left[-\exp\left(\frac{y_{i0}^{(j)} - \mathbf{x}_i' \boldsymbol{\beta}_0}{\sigma_0}\right)\right] \tag{3.9}$$

Let us assume further that detecting departures from the known value of the parameter vector $\boldsymbol{\xi}_0 = (\boldsymbol{\beta}_0', \varphi_0)'$ is wanted. It is clear that changes in the parameter vector will generate changes in all quantities of main interest related to the distribution of Y_i. It is also clear that changes (increases or decreases) in the mean of log-transformed times depend on the combinations of increases and decreases in all or several components of $\boldsymbol{\xi}$. We are particularly interested in detecting decreases in the mean response value of Y_i because they lead to the deterioration of a process characterized by model (3.2).

Let us suppose that at the $j-$th moment a data set $(\mathbf{x}_i', y_{ik}^{(j)})$, from model (3.2) is available. Adjustments to ancillary (3.3) and the log–transformation V^2 can be used to adapt existing control schemes for detecting departures from the known value $\boldsymbol{\xi} = \boldsymbol{\xi}_0$.

Chart designing has to take into account the behaviors of the ancillary quantity (3.7) and V^2 as functions of $\boldsymbol{\xi}$. Simulations suggest that whatever the combinations of increases and decreases in the components of $\boldsymbol{\xi}$ are, they lead to increases in the mean value of $\frac{p}{b_\xi}\Lambda(\boldsymbol{\xi})$. Consequently, shifts in $\boldsymbol{\xi}$ can be detected by detecting increases in the mean level of either $\frac{p}{b_\xi}\Lambda(\xi)$ or V^2. Thus, upper–sided control schemes has to be designed.

3.4.2 The LRT–Chart

Based on approximation (3.7), it is possible to design the Shewhart-type chart whose UCL is given by

$$UCL_j = \frac{b_{\xi,j}}{p} Q_{N,1-\alpha} \tag{3.10}$$

or

$$UCL = Q_{N,1-\alpha} \tag{3.11}$$

where α is the desired false alarm rate and $Q_{N,1-\alpha}$ is the $(1-\alpha)\times 100\%$ percentile of a large enough set of values of $CW = \frac{p}{b_\xi}\Lambda(\boldsymbol{\xi})$ corresponding to the data-set dimension N. It is worth mentioning that $Q_{N,1-\alpha}$ is closer to the chi-squared percentile $\chi^2_{p;1-\alpha}$ as N increases. Simulations suggest that the $\chi^2_{(p;1-\alpha)}$ percentile works fairly acceptable for $N \geq 50$. As we are dealing with an approximated methodology, it is preferable to take the UCL as it is indicated in (3.10) for $N < 50$.

When the UCL of the scheme is established as in (3.10), the LRT-Chart has varying in time control limit. In this case, the chart signals if $\Lambda_j(\hat{\boldsymbol{\xi}}) > UCL_j$ for a given j, where $\Lambda_j(\hat{\boldsymbol{\xi}})$ is the relative LRT statistic (3.3) defined for the entire parameter vector $\boldsymbol{\xi}$ evaluated at the MLE of $\boldsymbol{\xi} = (\boldsymbol{\beta}', \varphi)'$ obtained from the j-th data set.

When the UCL of the scheme is established as in (3.11), the LRT-Chart has a constant control limit and signals if $C\hat{W}_j = \frac{p}{b_{\xi,j}}\Lambda(\hat{\boldsymbol{\xi}}_j) > UCL$, where the quantities $b_{\xi,j}$ and $\Lambda(\hat{\boldsymbol{\xi}}_j)$ are obtained from the $j-$th data set.

Both of the charts in (3.10) and (3.11) represent the adapted version of the LRT chart in Soleymanian *et al* [61] in which Bartlett's corrections have been implemented. For further discussion, the formulation given in (3.11) is adopted.

3.4.3 The LRT–EChart

It was established that $CW = \frac{p}{b_\xi}\Lambda(\boldsymbol{\xi}) \sim \chi^2_p$ for non-large enough data sets, so it is possible to define the EWMA statistic

$$EW_j = \lambda \frac{\widehat{CW}_j - \mathsf{med}}{\mathsf{sd}} + (1-\lambda) EW_{j-1} \tag{3.12}$$

where $\widehat{CW}_j$ is the value of the corrected LRT statistic CW evaluated at the MLE of $\boldsymbol{\xi}$ at the $j-$th moment, $0 < \lambda \leq 1$ is the smoothing constant, $EW_0 = 0$, $\mathsf{med} = \chi^2_{(p;0.5)}$ and $\mathsf{sd} = \sqrt{2p}$. The quantities med and sd can be replaced by the median and the standard deviation of a set of simulated values of CW for a given N but the values of the χ^2_p distribution work quite acceptable for $N \geq 50$.

The UCL is defined to be

$$UCL_j = L\sqrt{\frac{\lambda[1-(1-\lambda)^{2j}]}{2-\lambda}} \tag{3.13}$$

where L is a positive constant that is chosen to reach a desirable ARL_0. This scheme signals if $EW_j > UCL_j$. This is the adapted version of the LRT-EWMA chart in Soleymanian *et al* [61] with the implemented Bartlett's corrections.

3.4.4 The LRT–CChart

The normal approximation of the log-transformation V^2 makes also possible to design the CUSUM procedure given by

$$SU_j = \max\left[0; \frac{V_j^2 - \mu}{\zeta} - K^{\pm} + SU_{j-1}\right] \tag{3.14}$$

where $SU_0 = 0$ and $K^{\pm}$ is the reference value that is chosen as for the conventional CUSUM chart for single normal observations. For further discussion, this scheme will be called the LRT–CChart (CUSUM chart based on the log-transformation of the scaled relative LRT statistic). This scheme signals when it holds that $SU_j > h$. The upper control limit h has to be chosen to reach a desirable ARL_0. This chart is introduced to verify the performance of the conventional CUSUM chart under the implemented corrections to the monitoring statistic.

3.4.5 The MEWMA chart

In this section, we adapt the MEWMA scheme first developed by Zou *et al.* [78] for GLM profiles to the case of monitoring the WRM parameter vector. First of all, it is needed to define the vectors

$$\mathbf{A}_j = \Im^{1/2}\left(\hat{\boldsymbol{\xi}}_j - \boldsymbol{\xi}_0\right) \tag{3.15}$$

where $\hat{\boldsymbol{\xi}}_j$ is the MLE of the parameter vector $\boldsymbol{\xi}$ at the $j-$ moment and $\Im$ is the asymptotic information matrix.

The MEWMA statistic is then define to be

$$\mathbf{E}_j = \lambda \mathbf{A}_j + (1-\lambda)\mathbf{E}_{j-1} \tag{3.16}$$

where $0 < \lambda \leq 1$ is the smoothing constant and $\mathbf{E}_0 = \mathbf{0}_{(p)\times 1}$. The MEWMA control chart signals as soon as $M_j = \mathbf{E}_j'\mathbf{E}_j > UCL$. The UCL is determined to reach a desirable ARL_0.

When monitoring EVRM, the multivariate normality of $\hat{\boldsymbol{\xi}}$ holds just asymptotically, so it will be needed to obtain $\Im$ in an appropriate way for a given data-set dimension N.

3.5 Performance evaluation of the control charts

As in the case of monitoring a single parameter, the ARL was used to evaluate control charts performance. This is the mean number of inspected samples until the scheme first signals.

3.5.1 Simulation settings

As in the simulation settings for the case of monitoring a single parameter, it is assumed that $p = 3$. Thus, at the $j-$th moment, the model can be written in the form given by (2.35) and the values of n and m_i are the ones established then. Thus, that explored values for the data-set dimension also are $N = 30$, 50 or 100. For a given N, covariate values are assumed to be the same in repeated sampling.

For convenience, model (2.35) will be rewritten in the form

$$y_{ik}^{(j)} = (\beta_{10} + \Delta_1) + (\beta_{20} + \Delta_2)\log(10i) + z_{ik}^{(j)} e^{\varphi_0 + \Delta_3} \tag{3.17}$$

This is, let $\boldsymbol{\xi}_0 = (\beta_{10}, \beta_{20}, \varphi_0)' = (3, 2, 0.4055)'$ be the in-control parameter vector. Let us also define the vector $\boldsymbol{\Delta} = (\Delta_1, \Delta_2, \Delta_3)'$, so that the vector $\boldsymbol{\xi}_0 + \boldsymbol{\Delta}$ represents an out–of–control situation. The quantities in the vector $\boldsymbol{\Delta}$ are determined as follows: $\Delta_f = C_f \sqrt{Var\left(\hat{\beta}_f\right)}$, for $f = 1, 2$, and $\Delta_3 = \log C_3$. The contamination constants C_f are such that, for $f = 1, 2$, a decrease (or an increase) in the parameter β_f occurs when $C_f < 0$ (or $C_f > 0$) and a decrease (or an increase) in the parameter σ occurs for $0 < C_3 < 1$ (or $C_3 > 1$). The in-control model is obtained for $C_f = 0$, $f = 1, 2$, and $C_3 = 1$.

The asymptotic information matrix can be approximated for each needed case by simulation or by using the methodology presented in Paul and Thiagarajah [46]. The variances $Var\left(\hat{\beta}_f\right)$, $f = 1, 2$, were taken from the diagonal of these approximations.

3.5.2 Estimation algorithm

For a given scheme, ARL values were simulated as it is described below:

1. Set $j = 1$ and proceed as follows. A single observation $z_{ik}^{(1)}$ is generated from $EV(0; 1)$. Then, for given values of the contamination constants C_f, the generated observation is replaced in expression (3.17) to obtain a log-transformed time $y_{ik}^{(1)}$. Repeat this procedure until a data set of N log-transformed times is completed.
2. Once a data set is completed, fit the model $y_{ik} = \beta_1 + \beta_2 x_i + \sigma z_{ik}$. The fit results in the MLE $\hat{\boldsymbol{\xi}}^{(1)} = (\hat{\beta}_1^{(1)}, \hat{\beta}_2^{(1)}, \hat{\varphi}^{(1)})$ and the observed information matrix $\Im_j$.
3. With the help of the third– and fourth–order derivatives of the likelihood function (2.7) evaluated at the MLE of $\boldsymbol{\xi}$, find the quantity b_ξ by using formula (3.4) for the case $q = 3$.
4. Compute the corresponding scaled value of $\Lambda_j(\hat{\boldsymbol{\xi}})$ by (3.7) for the case $q = 3$ or its corresponding log-transformation V^2.
5. For the Shewhart-type chart, establish the respective control limit for the available sample by (3.11). For the rest of the schemes, let G denote either the quantity given in (3.7) defined for the case $q = 3$ or its corresponding log-transformation V^2. Compute G and, subsequently, the EWMA statistic given by (3.12) or the upper CUSUM statistic given by (3.14).

6. For a given scheme, repeat steps 1–5 increasing the value of j in a unit until the signaling condition first holds. The total number of samples generated this way is called a run length. A lot of run length values is needed to obtain. The mean of the run length values is an estimate of the ARL of the scheme.

In-control $\Im_0$ needed for carrying out the monitoring was obtained by simulation for each studied data-set dimension N. Software needed for carrying out the study, including the one based on the simulation algorithm described above, was designed in R language.

data set	LRT–Chart	LRT–EChart	LRT–CChart	MEWMA
dimension	$\alpha = 0.005$	$\lambda = 0.1$	$K^{\pm} = 0.5$	$\lambda = 0.1$
30	12.915	0.8044	2.6911	0.6298
50	12.843	0.8042	2.6740	0.6056
100	12.837	0.8042	2.6740	0.5853

TABLE 3.3. UCL of the proposed schemes, leading to $ARL_0 = 200$, for monitoring the WRM $y_{ik} = 3 + 2\log(10i) + 1.5z_{ik}$.

3.5.3 Simulation results

All the schemes were calibrated to reach $ARL_0 = 200$. This is obtained by choosing chart designing parameters as it is presented in Table 3.3 for the special case of $p = 3$. Chart parameters in the second row of Table 3.3 were set to be fixed, the corresponding UCL were obtained via simulation by a bisection search algorithm based on 20000 run length values. Note that for $N \geq 50$ the difference in the UCL values is negligible for the LRT–based schemes. Thus, it is possible to conclude about the robustness of these schemes respect to the data-set dimension N. The UCL of the MEWMA chart depends on N.

As it was stated earlier, we are especially interested in the deterioration of the process. This is, in decreases in the mean of the response variables Y_i, $i = 1, \ldots, n$. Simulated ARL's for decreases in the mean response were obtained, for instance, by planning increases in the scale parameter σ and/or decreases in one or both β_1 and β_2 coefficients. For fixed values of the contamination constants C_3 and C_2, out-of-control ARL's were estimated for several values of C_1. Further, the contamination constant C_2 was shifted to a larger decrease with the given values of C_1 and C_3 remaining at their previous values. Thus, the mean values $E_{OC}(Y_i)$ for out-of-control situations are expected to decrease and, subsequently, corresponding out-of-control ARL's to be shorter. Alternative ways for planning changes in the parameter vector leading to decreases in the mean response are possible.

Out-of-control ARL's are based on 50000 run-length values and are reported in Tables 3.4–3.9 for some studied shifting patterns. In each table, approximated ARL are reported for a given shift in the WRM shape parameter σ and the shifting patterns shown in the first two columns. Tables also show results for the mean value of the first experimental level $E(Y_1)$ in the fourth column for the shifting pattern given in the preceding columns. The rest of the columns contain the respective out-of-control ARL's with an estimate of the standard deviation of the run lengths in brackets for each proposed chart.

Shifting pattern			LRT-Chart		LRT-EChart		LRT-CChart		MEWMA	
C_1	C_2	$E(Y_1)$	ARL	SD	ARL	SD	ARL	SD	ARL	SD
0.00	0.0	6.75	200.14	(199.16)	199.97	(198.87)	200.41	(198.76)	199.92	(198.14)
0.00	-0.1	6.65	137.36	(136.86)	91.68	(80.20)	99.86	(96.33)	27.92	(19.37)
	-0.2	6.56	60.31	(59.81)	26.37	(19.03)	28.06	(24.14)	10.15	(4.42)
	-0.3	6.47	24.31	(23.81)	11.07	(6.02)	10.06	(6.47)	6.12	(1.96)
	-0.4	6.38	10.58	(10.07)	6.19	(2.77)	5.37	(2.48)	4.44	(1.18)
	-0.5	6.29	5.09	(4.57)	4.12	(1.62)	3.70	(1.26)	3.53	(0.81)
	-0.6	6.20	2.83	(2.27)	3.01	(1.07)	2.90	(0.80)	2.96	(0.63)
	-0.7	6.11	1.80	(1.20)	2.36	(0.78)	2.43	(0.57)	2.55	(0.54)
	-0.8	6.02	1.34	(0.67)	1.95	(0.61)	2.16	(0.37)	2.24	(0.44)
	-0.9	5.93	1.13	(0.38)	1.66	(0.54)	2.04	(0.19)	2.06	(0.28)
	-1.0	5.84	1.04	(0.20)	1.42	(0.50)	2.00	(0.10)	2.04	(0.26)
-0.02	-0.1	6.62	115.34	(114.84)	70.97	(61.64)	79.26	(74.65)	21.22	(13.12)
	-0.2	6.53	48.31	(47.81)	21.54	(14.49)	22.00	(17.77)	8.98	(3.59)
	-0.3	6.44	17.87	(14.83)	9.68	(5.06)	8.61	(5.30)	5.68	(1.75)
	-0.4	6.35	9.07	(8.56)	5.63	(2.46)	4.93	(2.16)	4.22	(1.90)
	-0.5	6.26	4.50	(3.97)	3.82	(1.46)	3.51	(1.16)	3.40	(0.77)
	-0.6	6.17	2.55	(1.99)	2.84	(0.98)	2.80	(0.74)	2.86	(0.60)
	-0.7	6.08	1.69	(1.08)	2.26	(0.73)	2.37	(0.53)	2.48	(0.53)
	-0.8	6.00	1.28	(0.60)	1.89	(0.59)	2.12	(0.33)	2.20	(0.41)
	-0.9	5.90	1.10	(0.33)	1.61	(0.54)	2.02	(0.16)	2.04	(0.25)
	-1.0	5.80	1.03	(0.17)	1.37	(0.49)	1.99	(0.09)	2.03	(0.24)
-0.04	-0.1	6.59	101.42	(100.92)	54.73	(46.04)	60.95	(56.20)	16.84	(9.59)
	-0.2	6.50	41.29	(40.78)	17.80	(11.26)	17.60	(13.77)	8.04	(3.02)
	-0.3	6.41	17.11	(16.61)	8.59	(4.30)	7.53	(4.26)	5.29	(1.55)
	-0.4	6.32	7.84	(7.32)	5.18	(2.18)	4.54	(1.84)	4.03	(1.01)
	-0.5	6.23	3.96	(3.42)	3.60	(1.34)	3.32	(1.04)	3.27	(0.72)
	-0.6	6.14	2.33	(1.77)	2.69	(0.92)	2.68	(0.69)	2.78	(0.59)
	-0.7	6.05	1.58	(0.96)	2.18	(0.70)	2.31	(0.49)	2.42	(0.51)
	-0.8	5.96	1.24	(0.54)	1.82	(0.57)	2.09	(0.30)	2.16	(0.38)
	-0.9	5.87	1.08	(0.29)	1.56	(0.53)	2.02	(0.14)	2.02	(0.23)
	-1.0	5.78	1.02	(0.15)	1.34	(0.48)	1.99	(0.08)	2.01	(0.23)

TABLE 3.4. Performance of the proposed schemes for data-set dimension $N = 30$ of the simple WRM $y_{ik} = 3 + 2\log(10i) + 1.5z_{ik}$ with $C_3 = 1$ (no changes in $\sigma = 1.5$) and decreases in both β_1 and β_2.

Shifting pattern			LRT-Chart		LRT-EChart		LRT-CChart		MEWMA	
C_1	C_2	$E(Y_1)$	ARL	SD	ARL	SD	ARL	SD	ARL	SD
0.00	-0.1	6.48	26.19	(26.99)	15.41	(10.0)	16.17	(12.54)	8.21	(3.22)
	-0.2	6.39	22.30	(21.79)	12.97	(7.85)	12.95	(9.67)	7.04	(2.62)
	-0.3	6.29	14.44	(13.93)	8.98	(4.94)	8.50	(5.41)	5.54	(1.86)
	-0.4	6.20	8.36	(7.84)	6.13	(3.01)	5.62	(2.91)	4.40	(1.32)
	-0.5	6.11	4.96	(4.43)	4.38	(1.94)	4.07	(1.71)	3.61	(0.97)
	-0.6	6.02	3.09	(2.54)	3.29	(1.36)	3.16	(1.06)	3.06	(0.76)
	-0.7	5.94	2.11	(1.53)	2.59	(0.99)	2.64	(0.74)	2.65	(0.63)
	-0.8	5.85	1.55	(0.93)	2.12	(0.76)	2.31	(0.52)	2.36	(0.52)
	-0.9	5.76	1.27	(0.59)	1.81	(0.63)	2.12	(0.35)	2.14	(0.40)
	-1.0	5.68	1.12	(0.37)	1.55	(0.55)	2.02	(0.21)	2.06	(0.28)
-0.02	-0.1	6.44	25.23	(24.72)	14.99	(9.64)	15.89	(12.41)	8.06	(3.17)
	-0.2	6.36	20.63	(20.13)	12.13	(7.36)	11.99	(8.65)	6.74	(2.48)
	-0.3	6.27	12.57	(12.06)	8.30	(4.48)	7.76	(4.66)	5.28	(1.72)
	-0.4	6.18	7.41	(6.89)	5.70	(2.77)	5.23	(2.61)	4.23	(1.23)
	-0.5	6.09	4.45	(3.92)	4.14	(1.82)	3.84	(1.52)	3.48	(0.92)
	-0.6	6.00	2.83	(2.28)	3.12	(1.25)	3.05	(0.98)	2.97	(0.73)
	-0.7	5.91	1.97	(1.38)	2.48	(0.94)	2.58	(0.70)	2.59	(0.60)
	-0.8	5.82	1.48	(0.85)	2.05	(0.74)	2.27	(0.48)	2.31	(0.50)
	-0.9	5.73	1.23	(0.53)	1.75	(0.62)	2.10	(0.32)	2.10	(0.37)
	-1.0	5.64	1.10	(0.33)	1.51	(0.54)	2.01	(0.20)	2.05	(0.26)
-0.04	-0.1	6.41	25.33	(24.82)	15.31	(9.86)	15.42	(11.95)	7.92	(3.10)
	-0.2	6.32	18.80	(18.29)	11.34	(6.68)	11.07	(7.77)	6.46	(2.36)
	-0.3	6.23	11.36	(10.85)	7.70	(4.08)	7.19	(4.24)	5.05	(1.62)
	-0.4	6.14	6.72	(6.20)	5.34	(2.53)	4.90	(2.36)	4.05	(1.16)
	-0.5	6.06	4.06	(3.53)	3.86	(1.66)	3.67	(1.40)	3.37	(0.88)
	-0.6	5.97	2.63	(2.07)	2.98	(1.18)	2.95	(0.93)	2.89	(0.70)
	-0.7	5.87	1.85	(1.26)	2.38	(0.89)	2.50	(0.65)	2.53	(0.58)
	-0.8	5.78	1.42	(0.77)	1.98	(0.70)	2.23	(0.45)	2.26	(0.48)
	-0.9	5.70	1.20	(0.49)	1.69	(0.60)	2.08	(0.28)	2.08	(0.36)
	-1.0	5.62	1.08	(0.30)	1.47	(0.53)	2.00	(0.18)	2.04	(0.26)

TABLE 3.5. Performance of the proposed schemes for data-set dimension $N = 30$ of the simple WRM $y_{ik} = 3 + 2\log(10i) + 1.5z_{ik}$ with $C_3 = 1.2$ (20% increase in $\sigma = 1.5$) and decreases in both β_1 and β_2.

Shifting pattern			LRT-Chart		LRT-EChart		LRT-CChart		MEWMA	
C_1	C_2	$E(Y_1)$	ARL	SD	ARL	SD	ARL	SD	ARL	SD
0.00	0.0	6.75	199.69	(198.96)	199.76	(198.87)	200.13	(199.16)	200.90	(199.22)
0.00	-0.1	6.65	130.55	(130.05)	88.81	(78.98)	96.51	(92.08)	27.46	(18.57)
	-0.2	6.56	50.43	(49.92)	24.39	(17.68)	26.37	(18.00)	9.99	(4.27)
	-0.3	6.47	19.07	(19.56)	10.24	(5.64)	9.27	(5.92)	6.04	(1.93)
	-0.4	6.38	8.91	(8.40)	5.86	(2.66)	5.13	(2.36)	4.39	(1.15)
	-0.5	6.29	4.37	(3.83)	3.88	(1.54)	3.57	(1.25)	3.49	(0.80)
	-0.6	6.20	2.48	(1.91)	2.84	(1.02)	2.78	(0.76)	2.93	(0.62)
	-0.7	6.11	1.65	(1.03)	2.23	(0.76)	2.35	(0.53)	2.52	(0.54)
	-0.8	6.02	1.26	(0.57)	1.84	(0.61)	2.12	(0.33)	2.22	(0.42)
	-0.9	5.93	1.09	(0.32)	1.55	(0.54)	2.02	(0.16)	2.05	(0.27)
	-1.0	5.84	1.03	(0.16)	1.32	(0.47)	1.99	(0.14)	2.00	(0.26)
-0.02	-0.1	6.62	107.30	(106.80)	67.90	(57.89)	75.97	(71.94)	20.72	(12.58)
	-0.2	6.53	44.52	(44.02)	20.24	(13.61)	20.50	(16.87)	8.86	(3.56)
	-0.3	6.44	17.22	(16.71)	9.07	(4.73)	8.27	(5.06)	5.16	(1.72)
	-0.4	6.35	7.76	(7.25)	5.31	(2.35)	4.71	(2.06)	4.16	(1.06)
	-0.5	6.26	3.86	(3.32)	3.63	(1.40)	3.36	(1.12)	3.36	(0.72)
	-0.6	6.17	2.25	(1.68)	2.70	(0.96)	2.67	(0.71)	2.84	(0.60)
	-0.7	6.08	1.55	(1.92)	2.14	(0.72)	2.29	(0.49)	2.47	(0.53)
	-0.8	6.00	1.22	(0.51)	1.77	(0.60)	2.09	(0.29)	2.18	(0.40)
	-0.9	5.90	1.07	(0.28)	1.50	(0.53)	2.01	(0.15)	2.03	(0.24)
	-1.0	5.80	1.02	(0.14)	1.28	(0.45)	1.98	(0.14)	2.00	(0.23)
-0.04	-0.1	6.59	92.68	(92.18)	52.16	(43.05)	57.98	(53.77)	16.36	(9.00)
	-0.2	6.50	36.50	(35.99)	16.73	(10.36)	16.69	(13.00)	7.89	(2.94)
	-0.3	6.41	14.50	(13.99)	8.06	(4.02)	7.16	(4.05)	5.24	(1.54)
	-0.4	6.32	6.62	(6.10)	4.86	(2.08)	4.36	(1.79)	3.97	(0.98)
	-0.5	6.23	3.43	(2.89)	3.40	(1.29)	3.19	(1.01)	3.23	(0.71)
	-0.6	6.14	2.06	(1.48)	2.55	(0.89)	2.58	(0.66)	2.76	(0.59)
	-0.7	6.05	1.46	(0.82)	2.05	(0.68)	2.23	(0.45)	2.39	(0.51)
	-0.8	5.96	1.18	(0.46)	1.71	(0.58)	2.06	(0.25)	2.14	(0.36)
	-0.9	5.87	1.06	(0.25)	1.46	(0.52)	2.00	(0.13)	2.01	(0.22)
	-1.0	5.78	1.01	(0.12)	1.25	(0.43)	1.97	(0.12)	1.99	(0.20)

TABLE 3.6. Performance of the proposed schemes for data-set dimension $N = 50$ of the simple WRM $y_{ik} = 3 + 2\log(10i) + 1.5z_{ik}$ with $C_3 = 1$ (no changes in $\sigma = 1.5$) and decreases in both β_1 and β_2.

Shifting pattern			LRT-Chart		LRT-EChart		LRT-CChart		MEWMA	
C_1	C_2	$E(Y_1)$	ARL	SD	ARL	SD	ARL	SD	ARL	SD
0.00	-0.1	6.48	12.28	(11.77)	8.74	(4.92)	8.43	(5.44)	6.03	(1.97)
	-0.2	6.39	11.79	(11.28)	8.22	(4.50)	7.78	(4.83)	5.63	(1.81)
	-0.3	6.29	8.77	(8.26)	6.66	(3.41)	6.17	(3.40)	4.86	(1.47)
	-0.4	6.20	5.93	(5.41)	5.04	(2.39)	4.69	(2.21)	4.08	(1.14)
	-0.5	6.11	3.85	(3.31)	3.80	(1.68)	3.64	(1.43)	3.46	(0.90)
	-0.6	6.02	2.57	(2.01)	2.97	(1.24)	2.95	(0.96)	2.98	(0.72)
	-0.7	5.94	1.85	(1.26)	2.39	(0.92)	2.53	(0.69)	2.61	(0.61)
	-0.8	5.85	1.44	(0.79)	1.98	(0.74)	2.24	(0.47)	2.33	(0.51)
	-0.9	5.76	1.21	(0.51)	1.69	(0.62)	2.08	(0.31)	2.13	(0.38)
	-1.0	5.68	1.00	(0.07)	1.18	(0.38)	1.97	(0.19)	2.03	(0.37)
-0.02	-0.1	6.44	12.63	(12.2)	8.79	(4.90)	8.49	(5.57)	5.99	(1.94)
	-0.2	6.36	11.43	(10.92)	7.97	(4.32)	7.54	(4.64)	5.51	(1.74)
	-0.3	6.27	8.27	(7.76)	6.30	(3.20)	5.85	(3.20)	4.68	(1.39)
	-0.4	6.18	5.45	(4.92)	4.77	(2.25)	4.46	(2.05)	3.97	(1.09)
	-0.5	6.09	3.56	(3.02)	3.64	(1.58)	3.49	(1.30)	3.36	(0.85)
	-0.6	6.00	2.42	(1.85)	2.85	(1.17)	2.86	(0.91)	2.90	(0.69)
	-0.7	5.91	1.75	(1.15)	2.29	(0.87)	2.46	(0.64)	2.56	(0.59)
	-0.8	5.82	1.38	(0.73)	1.92	(0.71)	2.20	(0.44)	2.28	(0.48)
	-0.9	5.73	1.18	(0.47)	1.64	(0.61)	2.06	(0.29)	2.10	(0.36)
	-1.0	5.64	1.00	(0.06)	1.15	(0.35)	1.95	(0.18)	2.01	(0.34)
-0.04	-0.1	6.41	12.89	(12.38)	8.70	(4.83)	8.33	(5.33)	5.95	(1.94)
	-0.2	6.32	10.88	(10.37)	7.74	(4.10)	7.26	(4.37)	5.34	(1.67)
	-0.3	6.23	7.72	(7.20)	5.99	(3.01)	5.53	(2.90)	4.55	(1.34)
	-0.4	6.14	5.07	(4.53)	4.51	(2.09)	4.24	(1.85)	3.82	(1.03)
	-0.5	6.06	3.25	(2.71)	3.45	(1.47)	3.35	(1.22)	3.26	(0.80)
	-0.6	5.97	2.25	(1.68)	2.71	(1.09)	2.77	(0.85)	2.83	(0.68)
	-0.7	5.87	1.66	(1.05)	2.22	(0.84)	2.38	(0.59)	2.50	(0.57)
	-0.8	5.78	1.34	(0.67)	1.86	(0.69)	2.17	(0.40)	2.24	(0.46)
	-0.9	5.70	1.15	(0.42)	1.59	(0.58)	2.05	(0.26)	2.07	(0.34)
	-1.0	5.63	1.00	(0.04)	1.12	(0.32)	1.94	(0.18)	2.99	(0.31)

TABLE 3.7. Performance of the proposed schemes for data-set dimension $N = 50$ of the simple WRM $y_{ik} = 3 + 2\log(10i) + 1.5z_{ik}$ with $C_3 = 1.2$ (20% increase in $\sigma = 1.5$) and decreases in both β_1 and β_2.

All the tables are organized in blocks of ten rows such that each block considers a decreasing pattern in the mean response as decreases in one or both β parameters are larger. For understanding the performance of the proposed schemes, just take a glimpse between columns or between the corresponding rows of different blocks of the same table or between columns or rows of different tables. For instance, given a value of the scale parameter, chart performance for changes in the slope can be established by making a comparison between rows of the first block of each table or comparing first blocks of different tables.

Shifting pattern			LRT-Chart		LRT-EChart		LRT-CChart		MEWMA	
C_1	C_2	$E(Y_1)$	ARL	SD	ARL	SD	ARL	SD	ARL	SD
0.00	0.0	6.75	200.02	(199.69)	199.89	(198.78)	200.23	(199.36)	200.42	(199.01)
0.00	-0.1	6.65	127.23	(126.73)	86.64	(75.93)	95.44	(90.50)	27.31	(18.67)
	-0.2	6.56	48.68	(48.18)	23.94	(16.83)	25.08	(21.01)	9.87	(4.15)
	-0.3	6.47	18.44	(17.93)	9.91	(5.34)	9.16	(5.85)	5.96	(1.87)
	-0.4	6.38	7.76	(7.24)	5.56	(2.51)	4.95	(2.27)	4.35	(1.13)
	-0.5	6.29	3.90	(3.36)	3.71	(1.50)	3.43	(1.19)	3.46	(0.79)
	-0.6	6.20	2.25	(1.67)	2.71	(.99)	2.69	(0.75)	2.90	(0.62)
	-0.7	6.11	1.54	(0.91)	2.11	(0.75)	2.28	(0.49)	2.51	(0.54)
	-0.8	6.02	1.21	(0.51)	1.74	(0.61)	2.09	(0.29)	2.20	(0.41)
	-0.9	5.93	1.07	(0.28)	1.46	(0.52)	2.00	(0.17)	2.04	(0.25)
	-1.0	5.84	1.02	(0.14)	1.25	(0.44)	1.96	(0.20)	1.97	(0.22)
-0.02	-0.1	6.62	105.34	(104.87)	66.16	(53.70)	73.93	(69.31)	20.34	(12.47)
	-0.2	6.53	39.74	(39.24)	19.39	(12.82)	20.07	(16.19)	8.68	(3.46)
	-0.3	6.44	15.39	(14.88)	8.70	(4.48)	7.89	(4.79)	5.56	(1.67)
	-0.4	6.35	6.77	(6.25)	5.08	(2.24)	4.54	(1.95)	4.11	(1.03)
	-0.5	6.26	3.40	(2.86)	3.46	(1.36)	3.25	(1.07)	3.33	(0.74)
	-0.6	6.17	2.06	(1.47)	2.55	(0.93)	2.60	(0.69)	2.82	(0.59)
	-0.7	6.08	1.45	(0.81)	2.04	(0.71)	2.23	(0.45)	2.44	(0.52)
	-0.8	6.00	1.17	(0.45)	1.67	(0.59)	2.06	(0.26)	2.17	(0.39)
	-0.9	5.90	1.06	(0.25)	1.42	(0.51)	1.99	(0.15)	2.03	(0.23)
	-1.0	5.80	1.01	(0.12)	1.22	(0.41)	1.95	(0.22)	1.96	(0.23)
-0.04	-0.1	6.59	88.10	(87.60)	50.70	(42.19)	56.46	(52.19)	16.33	(9.02)
	-0.2	6.50	32.48	(31.94)	16.00	(10.60)	16.08	(12.33)	7.80	(2.88)
	-0.3	6.41	12.75	(12.24)	7.74	(3.89)	6.94	(3.91)	5.17	(1.50)
	-0.4	6.32	5.79	(5.27)	4.64	(1.99)	4.19	(1.72)	3.93	(0.97)
	-0.5	6.23	3.07	(2.52)	3.23	(1.25)	3.09	(0.97)	3.22	(0.71)
	-0.6	6.14	1.90	(1.31)	2.44	(0.89)	2.50	(0.64)	2.73	(0.58)
	-0.7	6.05	1.38	(0.72)	1.95	(0.67)	2.18	(0.41)	2.37	(0.50)
	-0.8	5.96	1.14	(0.40)	1.62	(0.57)	2.04	(0.23)	2.13	(0.35)
	-0.9	5.87	1.04	(0.22)	1.34	(0.50)	1.99	(0.16)	2.01	(0.21)
	-1.0	5.78	1.01	(0.11)	1.19	(0.39)	1.94	(0.24)	1.94	(0.24)

TABLE 3.8. Performance of the proposed schemes for data-set dimension $N = 100$ of the simple WRM $y_{ik} = 3 + 2\log(10i) + 1.5z_{ik}$ with $C_3 = 1$ (no changes in $\sigma = 1.5$) and decreases in both β_1 and β_2.

In Table 3.4, results for data-set dimension $N = 30$, no shifts in $\sigma_0 = 1.5$ ($C_3 = 1$) and decreases in both the intercept and the slope of the linear specification for the WRM scale parameter are reported. As it can be seen, all the schemes detect planned shifts in the parameter vector. The larger the decrease in the mean response, the sooner each scheme detects planned shifts.

However, none of the charts exhibits an overall best performance. The MEWMA chart outperforms its competitors for relatively small and moderate decreases in the mean response. The LRT–EChart and the LRT–CChart are alternative to the MEWMA chart for detecting small and moderate decreases in the mean response. Both of them are substantially less effective in detecting small decreases in the mean response than the MEWMA chart, but almost as effective as the latter in detecting moderate and large decreases. The LRT–EChart is the best option for detecting larger decreases among the non-Shewhart-type charts. The LRT–EChart and the LRT–CChart exhibit a similar performance, but the LRT–CChart is a slightly better option than the LRT–EChart for

Shifting pattern			LRT-Chart		LRT-EChart		LRT-CChart		MEWMA	
C_1	C_2	$E(Y_1)$	ARL	SD	ARL	SD	ARL	SD	ARL	SD
0.00	-0.1	6.48	4.63	(4.02)	4.36	(2.05)	4.20	(1.86)	4.05	(1.04)
	-0.2	6.39	4.52	(3.99)	4.33	(2.07)	4.13	(1.85)	4.02	(1.04)
	-0.3	6.29	4.13	(3.59)	4.05	(1.86)	3.87	(1.60)	3.78	(0.95)
	-0.4	6.20	3.33	(2.79)	3.49	(1.53)	3.41	(1.29)	3.46	(0.85)
	-0.5	6.11	2.56	(1.99)	2.96	(1.25)	2.97	(0.99)	3.10	(0.74)
	-0.6	6.02	1.96	(1.37)	2.48	(1.00)	2.61	(0.76)	2.77	(0.65)
	-0.7	5.94	1.55	(0.93)	2.09	(0.81)	2.32	(0.55)	2.49	(0.57)
	-0.8	5.85	1.30	(0.63)	1.79	(0.68)	2.14	(0.40)	2.26	(0.47)
	-0.9	5.76	1.15	(0.41)	1.55	(0.59)	2.03	(0.27)	2.09	(0.35)
	-1.0	5.68	1.07	(0.27)	1.36	(0.60)	1.96	(0.25)	1.99	(0.29)
-0.02	-0.1	6.44	4.56	(3.93)	4.33	(2.06)	4.16	(1.85)	4.05	(1.03)
	-0.2	6.36	4.51	(3.97)	4.31	(2.05)	4.07	(1.77)	3.99	(1.02)
	-0.3	6.27	3.96	(3.42)	3.96	(1.82)	3.76	(1.55)	3.73	(0.94)
	-0.4	6.18	3.15	(2.60)	3.38	(1.48)	3.34	(1.24)	3.40	(0.82)
	-0.5	6.09	2.42	(1.86)	2.87	(1.20)	2.90	(0.95)	3.04	(0.72)
	-0.6	6.00	1.87	(1.27)	2.39	(0.96)	2.54	(0.71)	2.72	(0.63)
	-0.7	5.91	1.50	(0.87)	2.03	(0.79)	2.29	(0.52)	2.44	(0.55)
	-0.8	5.82	1.26	(0.58)	1.75	(0.67)	2.12	(0.37)	2.22	(0.44)
	-0.9	5.73	1.13	(0.38)	1.50	(0.57)	2.02	(0.27)	2.06	(0.33)
	-1.0	5.68	1.05	(0.24)	1.33	(0.49)	1.95	(0.26)	1.97	(0.28)
-0.04	-0.1	6.41	4.53	(4.00)	4.34	(2.05)	4.14	(1.86)	4.06	(1.04)
	-0.2	6.32	4.43	(3.90)	4.26	(2.01)	4.04	(1.78)	3.95	(1.01)
	-0.3	6.23	3.88	(3.34)	3.86	(1.77)	3.70	(1.51)	3.67	(0.91)
	-0.4	6.14	3.00	(2.45)	3.28	(1.41)	3.22	(1.16)	3.32	(0.81)
	-0.5	6.06	2.30	(1.73)	2.78	(1.16)	2.82	(0.91)	2.97	(0.70)
	-0.6	5.97	1.78	(1.18)	2.30	(0.93)	2.48	(0.67)	2.39	(0.61)
	-0.7	5.87	1.44	(0.79)	1.96	(0.76)	2.24	(0.49)	2.19	(0.53)
	-0.8	5.78	1.23	(0.53)	1.70	(0.64)	2.09	(0.34)	2.05	(0.42)
	-0.9	5.70	1.11	(0.35)	1.46	(0.55)	2.00	(0.26)	1.99	(0.32)
	-1.0	5.62	1.05	(0.22)	1.30	(0.47)	1.94	(0.25)	1.95	(0.27)

TABLE 3.9. Performance of the proposed schemes for data-set dimension $N = 100$ of the simple WRM $y_{ik} = 3 + 2\log(10i) + 1.5z_{ik}$ with $C_3 = 1.2$ (20% increase in $\sigma = 1.5$) and decreases in both β_1 and β_2.

detecting moderate decreases in the mean response. The LRT–CChart and LRT–CChart detect small decreases in the mean response faster than the LRT–Chart. For larger decreases, the LRT–Chart performs slightly better than the LRT–CChart and LRT–CChart but does not show a substantially better ability.

As it can be noted from Table 3.5, the increase in the scale parameter, for the same decreasing patterns in the β parameters, makes the proposed charts detect small decreases in the mean response substantially faster and detect moderate and larger decreases, slightly slower. Simulations also suggest that large decreases in the mean response are detected the sooner as N increases. However. small decreases in the mean response are detected just slightly sooner as N increases. For details please compare results in Tables 3.4 and 3.5 with those reported in Tables 3.6 and 3.7, for $N = 50$, and with those reported in Tables 3.8 and 3.9, for $N = 100$.

Increases in the mean response can also be monitored by using the same schemes and just taking appropriate values for the contamination constants C_f given in Section 3.5.2. For details see Appendix A.2.

3.6 Diagnostic aid

It was stated in Section 3.4.1 that changes in the WRM parameter vector lead to changes in the distribution of the random variable Y_i measured in the $i-$th, $i = 1, \cdots, n$ experimental setting. Once the control chart signals, from the signaling data set it is possible to evaluate, for instance, the $r \times 100\%$ percentile of the distribution of Y_i in the $i-$th experimental level. Departures from the in-control $r \times 100\%$ percentile of the distribution of Y_i in the $i-$th experimental level, $y_{i,r}$, can be established from the fact that for large data sets we have

$$Z_0 = \frac{\hat{y}_{i,r} - y_{i,r}}{se\left(\hat{y}_{i,r}\right)} \sim N(0;1) \tag{3.18}$$

where $\hat{y}_{i,r} = \mathbf{x}_i'\hat{\boldsymbol{\beta}} + a\hat{\sigma}$ y $se\left(\hat{y}_{i,r}\right) = \left[(\mathbf{x}_i', a)\Im^{-1}(\mathbf{x}_i', a)'\right]^{1/2}$ with $\hat{\boldsymbol{\beta}}$ and $\hat{\sigma}$ being the MLE of the parameter vector and $\Im$, the observed information matrix for the signaling data set, respectively, and $a = \log\left[-\log\left(1-r\right)\right]$.

Although approximation (3.18) just holds asymptotically, simulations suggest that it works quite acceptable for the data-set dimensions explored in this study. Thus, for a given significance level α, a decision about a possible increase in $y_{i,r}$ could be made when $Z_0 > z_{1-\alpha/2}$ and about a possible decrease in $y_{i,q}$, when $Z_0 < z_{\alpha/2}$. In particular, possible increases or decreases in the mean or the median of the distribution of the random variable Y_i in the $i-$th experimental setting can be evaluated with the help of the MLE of the parameter vector for the signaling data set by making $r = 0.4296$ or $r = 0.5$, respectively, in (3.18).

If it is the case, some punctual results of the methodology presented in DiCiccio [13], developed separately for the particular case of the intercept, the slope or the log-scale parameter can be used to identify possible increases or decreases in each parameter once control schemes signal. The procedure is based on the fact that, for large N we have

$$U_f = \frac{\hat{\xi_f} - \xi_f}{\sqrt{\Im_{ff}^{-1}}} \sim N(0,1), \quad f = 1,2,3. \tag{3.19}$$

with $(\xi_1, \xi_2, \xi_3) = (\beta_1, \beta_2, \varphi)$. For non–large enough N, the $\alpha \times 100\%$ percentile of U can be corrected as it is indicated in DiCiccio [13]. Details on how to do it for the particular case of the log-scale parameter were explained in the preceding chapter and can be easily extended to the rest of the cases.

3.7 Example from the food industry

One of the most important aspects of quality improvement in food industry consists of determining the shelf life of processed foods. This is, the elapsed time before a product is deemed to be inappropriate for human consumption. The shelf life of processed foods depends on their storage and exhibition conditions. Temperature and relative humidity are the main causes of deterioration of physical, chemical and organoleptic properties of processed foods.

By following the recommendations of quality authorities, a company dedicated to biscuit production implemented new methods for verifying storage conditions of filled sweet cookies. Besides the usual tests, since 1997 the company has annually conducted accelerated tests to determine the shelf life of cookies in different storage conditions. Seven specimens of 4 g weight are subjected to five different high-temperature levels at a fixed 75% relative humidity level. Temperature levels range from 36 to $44°C$ with a $2°C$ increase between levels. A climatic device is used to control temperature levels, so that one day in the device chamber is equivalent to $4 - 8$ days in normal storage conditions depending on the temperature level.

The response variable is the elapsed time in days until a specimen achieves a 40% moisture gain. There are $N = 35$ uncensored observations in an annual batch. The complete data set consists of 14 annual batches collected in the period $1997 - 2010$ and 3 additional batches of the same dimension collected in 2011 that are known to be out-of-control because of a lack of calibration of the climatic device. The use of data for academic purposes was allowed exclusively. Data are shown in Appendix A.3.

A preliminary graphical analysis is shown in Figure 3.1. It suggests that the problem of verifying the shelf life in different storage conditions can be approached from the perspective of regression models. Different models with a single covariate were proved to fit the available data sets corresponding to the period $1997 - 2010$. The EVRM (2.1) appears to give a good description for the log-transformation of the shelf time in terms of the log-transformation of the temperature levels ($p - value = 0.037$). The fit results in the model

$$\hat{y}_{ij} = 18.1692 - 3.8365x_i + 0.7242z_{ij} \tag{3.20}$$

where x_i is the log-transformation of the temperature level.

For further discussion, and just for illustrating the proposed methodologies, fit (3.20) was assumed to be the in-control model. Corrected control charts were built for all available data sets. All schemes were calibrated to reach $ARL_0 = 200$. Designing parameters for each chart are reported in Table 3.10. Control charts are presented in Figure 3.2.

LRT–Chart	LRT–EChart	LRT–CChart	MEWMA
$\alpha = 0.005$	$\lambda = 0.1$	$K^{\pm} = 0.5$	$\lambda = 0.1$
$UCL =$12.891	$L = 3.518$	$h = 2.683$	$h = 0.621$

TABLE 3.10. Designing parameters of the proposed schemes leading to $ARL_0 = 200$ for the food industry example

As is can be seen in Figure 3.2, LRT-based charts detect the out-of-control situations as soon as they occur. The MEWMA chart does it one sampling moment later. This is perhaps due to the fact that we are dealing with a substantial decrease in the mean response and the LRT-based charts outperform the MEWMA scheme in such cases. It is worth mentioning that the LRT chart is the only one scheme that identifies the last data set as an in-control point when it is really an out-of-control one.

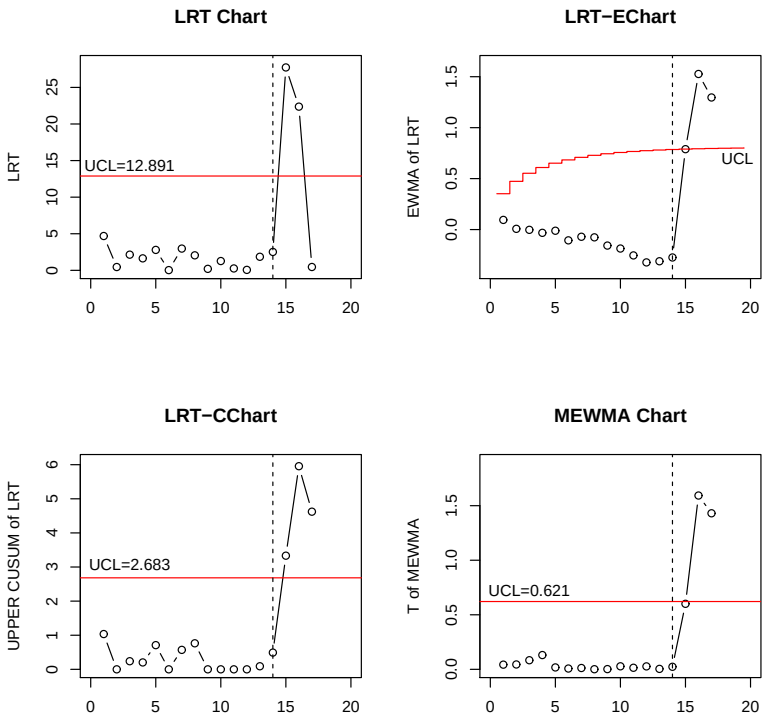

FIGURE 3.2. Control charts for the food industry example

Let us suppose further that we want to know what happened to the mean response as soon as the charts first signal. The in-control mean shelf time in days for the five fixed temperature levels in accelerated conditions are 76, 62, 51, 42 and 35, respectively. The EVRM fit to the 15−th data set results in $\hat{\beta}_1 = 18.439$, $\hat{\beta}_2 = -4.001$ and $\hat{\sigma} = 0.773$ with $(p - value = 0.10147)$. Thus, the approximated mean shelf time based on the information from the signaling data set are 56, 45, 37, 30 and 25, respectively, in accelerated conditions. Thus, cookies should be lasting less time in shelves in mean terms. For instance, cookies at a 44° temperature level in accelerated conditions last 10 days less in mean terms approximately. This is equivalent to $40 - 80$ days in normal conditions. This particular shift in the mean response value was correctly identified by the diagnostic aid.

3.8 Conclusions

In this study, some different control mechanisms were improved for monitoring the parameter vector of the EVRM with uncensored observations in phase II processes. This is equivalent to monitoring the WRM parameter vector. The results of the conducted simulation study suggest that adjustments to the relative LRT statistic (3.3) defined for the entire parameter vector $\boldsymbol{\xi}$ make the proposed schemes a fairly acceptable procedure to carry out the monitoring for detecting sustained shifts in the parameter vector of the EVRM with uncensored observations.

None of the schemes exhibited an overall best performance. For all studied data-set dimensions, the MEWMA chart was found to be the best option for detecting small and moderate decreases in the mean response, whilst the LRT chart is the best option for detecting larger decreases. The LRT-EChart and LRT-CChart exhibit a similar performance. The LRT-EChart may be considered as a good alternative to the LRT chart for detecting large decreases in the mean response. The LRT-CChart is the best alternative to the MEWMA chart for detecting moderate decreases in the mean response.

Special attention has to be paid to the MEWMA chart. It certainly outperforms the rest of the schemes for detecting small and moderate decreases in the mean response. However, the UCL of this chart strongly depends on the data-set dimension N. Furthermore, its performance also depends on the distribution of the MLE of the EVRM parameter vector for non-large enough N values, which is unknown. This drawback makes its use more restrictive than that of the competing methodologies. The fact is that the adjustments introduced into the LRT statistic make the schemes based on them, work approximately as well as in the asymptotic case even for non-large enough N. Moreover, the UCL of the corrected schemes seems to be robust respect to the N values.

Furthermore, once out-of-control signals are obtained while monitoring, it is possible to know approximately what happens to the main quantities related to the distribution in the $i-$th experimental level. An approximated procedure based on the asymptotic distribution of the $r \times 100\%$ percentile in the $i-$th covariate level was presented for making conclusions about the mean (or the median, if it is the case) response in the respective level. It is also possible to judge about the survival probabilities in the $i-$th covariate level.

Although the presented methodology was developed for the special case of the WRM, it could be applied for successfully monitoring regression models with response variable in the location-scale family. Whatever the response in this family is, the parameter vector $\boldsymbol{\beta}$, that measures the effects of covariates on times, can be monitored by taking an adequate partition of the entire parameter vector. This is achieved by letting the parameters that we are not interested in to form a sub-vector and treating them as nuisance parameters that do not have to be known but stable.

REMARK

Part of the results presented in this chapter are reported in the paper "Monitoring the parameter vector of regression models with time-to-event response in phase II processes" published on line in 2017 in *Journal of Statistical Computation and Simulation*, http://dx.doi.org/10.1080/00949655.2017.1344240

CHAPTER 4

Monitoring WRM with censored observations

4.1 The problem

Let us suppose that at the $j-$th moment in time, $j = 1, 2, ...$, a data set with the structure shown in Table 4.1 is available. In Table 4.1, $\mathbf{x}_i'$, $i = 1, ..., n$, represent n different levels or settings of the same experimental situation. These may be n different values of a $p-$dimensional vector of explanatory variables. This is,$\mathbf{x}_i' = (x_{1i}, \ldots, x_{pi})$. The values of $\mathbf{x}_i'$ are considered to be fixed in repeated sampling.

$\mathbf{x}_1'$	$\mathbf{x}_2'$	$\cdots$	$\mathbf{x}_n'$
$(t_{11}^{(j)}, \delta_{11}^{(j)})$	$(t_{21}^{(j)}, \delta_{21}^{(j)})$	$\cdots$	$(t_{n1}^{(j)}, \delta_{n1}^{(j)})$
$(t_{12}^{(j)}, \delta_{12}^{(j)})$	$(t_{22}^{(j)}, \delta_{22}^{(j)})$	$\cdots$	$(t_{n2}^{(j)}, \delta_{n1}^{(j)})$
$\vdots$	$\vdots$	$\cdots$	$\vdots$
$(t_{1m_1}^{(j)}, \delta_{1m_1}^{(j)})$	$(t_{2m_2}^{(j)}, \delta_{2m_2}^{(j)})$	$\cdots$	$(t_{nm_n}^{(j)}, \delta_{nm_n}^{(j)})$

TABLE 4.1. Data structure at the $j-$th moment

Before going further, some notation is needed to clarify. At the $j-$th moment in the $i-$th level, $i = 1, \ldots, n$, a random variable $T_i^{(j)}$ representing lifetimes has to be measured. However, instead of the observed real lifetime values, we have a time $t_i^{(j)}$ that we know is either an observed lifetime or a fixed time value previously established C_i. The values C_i are often referred to in specialized literature as *censoring* times. Let us also define the status indicator $\delta_i^{(j)}$ for $t_i^{(j)}$ that tells us if $t_i^{(j)}$ is an observed lifetime ($\delta_i^{(j)} = 1$) or a censoring time ($\delta_i^{(j)} = 0$). Formally, we have $t_i^{(j)} = \min\left[T_i^{(j)}; C_i^{(j)}\right]$ and $\delta_i^{(j)} = I\left[T_i^{(j)} \leq C_i^{(j)}\right]$. In this formulation we made a mistake by letting t_i represent either a random variable or a realized value but no confusion should arise.

Thus, in Table 4.1, $t_{ik}^{(j)}$ represents the $k-$th observation, $k = 1, \ldots, m_i$, of the random variable t_i at the $j-$th moment and $\delta_{ik}^{(j)}$ is the status indicator for $t_{ik}^{(j)}$. The censoring times c_{ik} are assumed to be the same for every j value. The quantities m_i are the total observations in the $i-$th level and are also set to be fixed for every j value. We have $\sum_i^n m_i = N$ observations at the $j-$th moment. In the following, as in previously reviewed cases, we will refer to N as the data-set dimension.

In the context of GLM, the variables $t_i^{(j)}$ share the same distribution but with parameters depending on the $i-$th experimental level. It is well known that all these distributions are linked by a parameter vector $\boldsymbol{\xi} = (\beta_1, \cdots, \beta_p, \sigma)$ whose dimension $p + 1 < n$. If we assume a linear dependence between the response vector and the experimental levels, then the structure in Table 4.1 can be written in the form

$$y_{ik}^{(j)} = \log t_{ik}^{(j)} = \mathbf{x}_i'\boldsymbol{\beta} + \sigma z_{ik}^{(j)}, \quad j = 1, 2, ... \tag{4.1}$$

This is exactly the same functional dependence as in models (2.1) and (3.2), but with a little difference. There is a right-censoring mechanism operating on the response variables t_i. In addition, it will be assumed that the scale parameter $\sigma > 0$ is fixed at a given known value. The rest of the quantities in model (4.1) have the same meaning as in models (2.1) and (3.2).

In the context of SPC, we are formally interested in testing over time the hypothesis

$$\begin{aligned} H_0 &: \boldsymbol{\beta} = \boldsymbol{\beta}_{IC} = \boldsymbol{\beta}_0 \\ H_1 &: \boldsymbol{\beta} = \boldsymbol{\beta}_{OC} = (\mathbf{1} - \mathbf{d}) \circ \boldsymbol{\beta}_0 \end{aligned} \tag{4.2}$$

where the circle symbol represents the Hadamard product, $\mathbf{d}$ is a $p-$dimensional vector whose components are such that $-1 < d_q < 1$, $q = 1, \cdots, p$, and $\mathbf{1}$ is the $p-$dimensional unitary vector. This is, in the most general case, we would be interested in detecting $\mathbf{d} \times 100\%$ shifts from $\boldsymbol{\beta}_0$. Departures can take place in one or more components of the parameter vector $\boldsymbol{\beta}$. The importance of detecting these drops lies on the fact that changes in the value of $\boldsymbol{\beta}$ will necessarily imply changes in the distributions of the responses t_i at all experimental levels. However, the main goal of this study will be focused on the early detection of decreases in one or more regression coefficients $\beta_1, ..., \beta_p$ because this kind of shifts imply a lower mean value of the response variable. This is achieved by making $0 < d_q < 1$, $q = 1, \cdots, p$.

We propose to test hypothesis (4.2) over time by using a CUSUM procedure based on the LRT statistic defined by

$$LRT_j = \ell_j(\boldsymbol{\beta}_{OC}) - \ell_j(\boldsymbol{\beta}_{IC}), \quad j = 1, 2, ... \tag{4.3}$$

where $\ell_j(\boldsymbol{\beta}_{OC})$ and $\ell_j(\boldsymbol{\beta}_{IC})$ are the likelihood functions for model (4.1) defined for the out-of-control and the in-control states at the $j-$th moment, respectively. This formulation was first used by Dickinson *et al.* [15] for monitoring censored Weibull lifetimes without covariates.

This is one of the first attempts for monitoring regression models with censored lifetimes. Thus, there are no methodologies to compare with. Although the structure in Table 4.1 is not that of a profile, we have adapted the MEWMA chart for monitoring binary profiles to the case of our particular interest. The MEWMA chart for monitoring profiles was first proposed by Zou *et al.* [78] and extended by Soleymanian *et al.* [61] to the case of binary profiles. Soleymanian's version of the MEWMA chart was proved to outperform its LRT-based competitors when detecting small and moderate shifts in the parameter vector characterizing binary profiles is needed.

However, as it will be seen later, the use of Soleymanian's MEWMA chart is restrictive when regression models for censored lifetimes have to be monitored. The fact is that the MEWMA chart is based on the asymptotic normality of the MLE of the parameter vector characterizing the basic model. Panza and Vargas [41] have shown by simulations that in the case of the WRM for uncensored lifetimes this property just holds for $N > 1500$. In addition, for relatively small and moderate data-set dimensions and theoretical censoring rates $p_C \geq 50\%$, the expected value of the parameter vector MLE is substantially different from that of the in-control value. For instance, Table 4.2 shows the approximated expected value of the MLE of both the intercept and the slope of simple linear WRM for different data-set dimensions N, theoretical censoring rates p_C and fixed shape parameter γ. Reported results were obtained by simulating random data sets with the structure in Table 4.1 for the WRM with $x_i = \log(10i)$ and $\boldsymbol{\beta}_{IC} = (\beta_{10}, \beta_{20})' = (3, 2)'$.

N	$\gamma = 0.5$			$\gamma = 1.0$			$\gamma = 1.5$		
	$p_C = 30\%$	$p_C = 50\%$	$p_C = 70\%$	$p_C = 30\%$	$p_C = 50\%$	$p_C = 70\%$	$p_C = 30\%$	$p_C = 50\%$	$p_C = 70\%$
30	3.1439	3.4209	3.9430	2.9977	3.1029	3.3642	3.0841	3.3099	3.7554
	1.9930	1.9771	1.9298	2.0009	1.9809	1.9306	1.9958	1.9778	1.9278
50	3.1282	3.3672	3.7616	3.0001	3.0566	3.1856	3.0761	3.2607	3.5673
	1.9961	1.9873	1.9648	2.0002	1.9896	1.9647	1.9970	1.9870	1.9644
100	3.1162	3.3298	3.6567	3.0021	3.0272	3.0827	3.0679	3.2219	3.4629
	1.9984	1.9944	1.9848	1.9997	1.9950	1.9845	1.9986	1.9946	1.9845

TABLE 4.2. Expected value of the MLE of the WRM parameter vector for different data-set dimensions N, theoretical censoring rates p_C and fixed shape parameter γ. The expected value of MLE of the intercept (or the slope) is reported in the upper (lower) row for each data-set dimension value N.

As it can be seen in Table 4.2, $E(\hat{\boldsymbol{\beta}}) \approx \boldsymbol{\beta}_{IC}$ for theoretical censoring rates $p_C < 50\%$ and all the reported γ values. For greater p_C values, the approximation holds as N increases. The design of the adapted MEWMA chart takes into account this circumstance.

4.2 Theoretical framework

Details about the Weibull and the extreme value models were already presented in Section 2.3. We will refer instead to some particular aspects of the WRM with censored observations.

4.2.1 Censoring mechanisms

While dealing with lifetimes, it may not be possible to assess when exactly a failure or an event of interest occurs, because time needed to observe the lifetimes of all items or individuals involved in the study may be large enough that researchers cannot make all measurements. This leads to so called *censoring*, in which the lifetime of an individual is known only to exceed a certain fixed value.

Several censoring mechanisms can operate while observing lifetimes. We are in the presence of a right-censoring mechanism when only lower bounds on lifetime are available for some individuals. A Type I censoring mechanism is said to apply when each individual has a fixed censoring time $c_{ik} > 0$ such that the lifetime t_{ik} is observed if $t_{ik} \leq c_{ik}$; otherwise, it is only known that $t_{ik} > c_{ik}$. Type I censoring often arises when a study is conducted over a specified time period. In clinical trial, for instance, there are entries of individuals to a study combined with a specified ending date. Type II censoring appears when only the r smallest lifetimes in a random sample of N are observed. This mechanism arises when N individuals start on a study at the same time and the study ends once r lifetimes have been observed.

There are other censoring mechanisms in specialized literature. However, we will not refer to them since our interest is focused on Type I right censoring for being the most presented mechanism in practical situations. For more details about censoring please address to Lawless [27] or Meeker and Escobar [34].

4.2.2 Estimation in the WRM

At every $j-$th moment, based on a censored data set (t_{ik}, δ_{ik}) of dimension N, it is possible to estimate the regression parameters $\beta_1, \cdots, \beta_p$ characterizing model (4.1) for a fixed value of the shape parameter $\gamma = \sigma^{-1}$. The likelihood function for the parameter vector $\boldsymbol{\beta} = (\beta_1, \cdots, \beta_p)'$ with right censored observations and fixed γ is

$$Ł_j(\boldsymbol{\beta}) = \prod_{i=1}^{n} \prod_{k=1}^{m_i} \left[f\left(t_{ik}^{(j)}\right) \right]^{\delta_{ik}^{(j)}} \left[S\left(t_{ik}^{(j)}\right) \right]^{\left(1-\delta_{ik}^{(j)}\right)}$$

and the log-likelihood function is

$$\ell_j(\boldsymbol{\beta}) = \sum_{i=1}^{n} \sum_{k=1}^{m_i} \left[\delta_{ik}^{(j)} \log f\left(t_{ik}^{(j)}\right) + \left(1 - \delta_{ik}^{(j)}\right) \log S\left(t_{ik}^{(j)}\right) \right]$$

$$= r_j \log \gamma + \sum_{i=1}^{n} \sum_{k=1}^{m_i} \delta_{ik}^{(j)} \left[(\gamma - 1) \log t_{ik}^{(j)} - \gamma \log \theta_i^{(j)} \right] + \sum_{i=1}^{n} \sum_{k=1}^{m_i} \left[- \left(\frac{t_{ik}^{(j)}}{\theta_i^{(j)}} \right)^{\gamma} \right] \qquad (4.4)$$

where $\theta_i^{(j)} = \theta(\mathbf{x}_i') = \exp\left(\mathbf{x}_i' \boldsymbol{\beta}^{(j)}\right)$ and $r_j = \sum_{i=1}^{n} \sum_{k=1}^{m_i} \delta_{ik}^{(j)}$.

At every $j-$th moment, the MLE of the parameter vector $\boldsymbol{\beta}$ is obtained by solving numerically the equation system defined by the scores $U_l = \frac{\partial \ell(\boldsymbol{\beta})}{\partial \beta_l} = 0$, $l = 1, 2, ..., p$.

Let $\hat{\boldsymbol{\beta}}$ be the MLE of the parameter vector $\boldsymbol{\beta}$. The components of the observed information matrix $\Im_{\hat{\boldsymbol{\beta}}}$ are of the form

$$\Im_{lm} = \left[-\frac{\partial^2 \ell(\boldsymbol{\beta})}{\partial \beta_l \partial \beta_m} \right]_{\boldsymbol{\beta}=\hat{\boldsymbol{\beta}}}, \quad l, m = 1, 2, ..., p \tag{4.5}$$

It is also well known that under certain regularity conditions the vector $\hat{\boldsymbol{\beta}}$ follows a $p-$dimensional normal distribution with mean vector $\boldsymbol{\beta}$ and covariance matrix $\Im_{\hat{\boldsymbol{\beta}}}^{-1}$ as $N \to \infty$.

4.3 Particularities of the monitoring

Let $T_i \sim W(\theta_i, \gamma)$, $i = 1, ..., n$, be random variables denoting lifetimes. The regression model (4.1) can be written in the form

$$t_{ik}^{(j)} = \exp\left(\mathbf{x}_i' \boldsymbol{\beta}^{(j)} + \gamma^{-1} z_{ik}^{(j)} \right) \tag{4.6}$$

For $p = 2$, this is $\mathbf{x}_i' \boldsymbol{\beta} = \beta_1 + \beta_2 x_i$, simulations suggest that increases (or decreases) in one of the components of the parameter vector $\boldsymbol{\beta} = (\beta_1; \beta_2)'$ generates increases (or decreases) in the mean value of t_i for a given value of the shape parameter γ. Moreover, for theoretical censoring rates $p_C \geq 10\%$, it was also observed that increases (or decreases) in the slope β_2 generate increases (or decreases) in the mean response regardless the changes in the intercept β_1. For $p_C < 10\%$, changes in the mean response due to combinations of different shifting patterns in all parameters, especially those with small shifts in one of them, need more careful investigation.

In addition, as it was stated earlier, we are interested in detecting decreases in the mean time response. The deterioration of the process is achieved by considering decreases in just one of the regression coefficients or combinations of changes in all of them. Although the methodologies that will be introduced in next section is proposed to deal with simultaneous shifts in the regression coefficients, the decrease in the slope β_2 is the only one case to be considered. When simultaneous changes are taken into account, additional changes in the intercept β_1, for instance, could lead to a faster reaction of the control schemes due to larger decreases in the mean time response. However, if it is desired, the redesign of the prosposed methodologies in order to consider new monitoring needs is straightforward.

Above mentioned circumstances allow us to design control schemes for detecting decreases in the slope that imply the deterioration of the mean response. Although increases in the slope could imply the improvement of the process, increases in the mean response also lead to undesirable higher censoring rates. In the following, for designing purposes, we will consider that $\beta_2 = \beta_{21} = (1 - d_2)\beta_{20}$ for out-of-control states, where β_{20} is the known stable value of the slope. The constant d_2 represents a $d_2 \times 100\%$ shift in the slope. Decreases in the slope can be obtained for $0 < d_2 < 1$. If it is desired, increases in the slope can be modeled by making $d_2 < 0$. The in-control state is obtained for $d_2 = 0$.

4.4 Control charts for the WRM

4.4.1 The WRM–CUSUM chart

A CUSUM scheme based on the LRT statistic (4.3) has the form

$$D_j = \max\left[0; D_{j-1} + LRT_j\right], \quad j = 1, 2, ... \tag{4.7}$$

with $D_0 = 0$. The chart signals when, for any j, the corresponding value D_j exceed a threshold h that is chosen to reach a desired ARL_0.

For the WRM, the LRT statistic (4.3) for testing the hypothesis (4.2) takes the form

$$LRT_j = -\sum_{i=1}^{n}\sum_{k=1}^{m_i}\left[\delta_{ik}^{(j)}\log\omega_i - a_i\left(\frac{t_{ik}^{(j)}}{\exp\left(\mathbf{x}_i'\boldsymbol{\beta}_0\right)}\right)^{\gamma}\right] \tag{4.8}$$

where $\omega_i = \exp\left[-\gamma\mathbf{x}_i'(\mathbf{d}\circ\boldsymbol{\beta}_0)\right]$ and $a_i = \left(\omega_i - 1\right)/\omega_i$.

It has to be noted that, in general, the performance of the CUSUM charts based on the LRT statistic (4.8) depends on the data-set dimension N, the fixed value of the shape parameter γ, the in-control value of the parameter vector $\boldsymbol{\beta}_0$, the nominal shift to be detected $\mathbf{d}$, the fixed covariate pattern and the amount of censored observations in the available data set. However, no concern should arise because all these quantities are supposed to be known in phase II monitoring.

When we are interested in monitoring the slope β_2 of the simple WRM, in expression (4.8) we have $\mathbf{d} = (d_1, d_2)' = (0, d_2)$ and then $\omega_i = \exp\left(-\gamma d_2\beta_{20}x_i\right)$. Other shifting patterns leading to decreases of the mean response value are easy to design by taking an appropriate form of vector $\mathbf{d}$.

At this point, it is worth mentioning that simulations suggest the increase of the mean of the second weighted sum in the right part of expression (4.8) when β_2 decreases. Thus, for detecting decreases in β_2, it can be used the upper CUSUM chart defined by

$$D_j^{+} = \max\left[0; D_{j-1}^{+} - K_j + \sum_{i=1}^{n}\sum_{k=1}^{m_i} a_i\left(\frac{t_{ik}^{(j)}}{\exp\left(\mathbf{x}_i'\boldsymbol{\beta}_0\right)}\right)^{\gamma}\right], \quad j = 1, 2, ... \tag{4.9}$$

where $D_0^{+} = 0$ and $K_j = \sum_{i=1}^{n}\sum_{k=1}^{m_i}\delta_{ik}^{(j)}\log\omega_i$ is the reference value for the $j-$th data set. The chart signals if $D_j^{+} > h^{+}$, for any j, indicating a possible decrease in β_2. This scheme will be called the WRM-CUSUM chart.

4.4.2 The adapted MEWMA chart

Soleymanian [61] proposed a MEWMA chart for monitoring the parameter vector of binary profiles. Soleymanian's version of the MEWMA chart was found to detect small shifts in the parameter vector substantially faster than the Shewhart-type and EWMA charts based

on the deviance form of the LRT statistic. To design the chart, it is first needed to define the vectors

$$\mathbf{V}_j = \Im^{1/2}\left(\hat{\boldsymbol{\beta}}_j - \boldsymbol{\beta}_0\right) \tag{4.10}$$

where $\hat{\boldsymbol{\beta}}_j$ is the MLE of the parameter vector $\boldsymbol{\beta}$ at the $j-$ moment and $\Im$ is the asymptotic information matrix. In order to use the most of the information in the available data sets, we propose to replace the asymptotic matrix $\Im$ in (4.10) by the observed information matrix for the $j-$th data set $\Im_{\hat{\boldsymbol{\beta}}}$.

The MEWMA statistic is then defined to be

$$\mathbf{E}_j = \lambda \mathbf{V}_j + (1-\lambda)\mathbf{E}_{j-1} \tag{4.11}$$

where $0 < \lambda \leq 1$ is the smoothing constant and $\mathbf{E}_0 = \mathbf{0}_{p\times 1}$. The MEWMA control chart signals as soon as $M_j = \mathbf{E}_j'\mathbf{E}_j > h$, where h is the UCL that is determined to reach a desirable ARL_0.

It is clear that MEWMA chart performance strongly depends on the distribution of the parameter vector MLE for a given data-set dimension N, a fixed shape parameter γ and the amount of censored observations in the available datasets. As the distribution of the parameter vector MLE is unknown, we take into account the results in Table 4.2 for designing the corresponding MEWMA charts. Because of these circumstances, we feel that the use of the MEWMA chart is very restrictive for monitoring WRM with censored observations, but we do introduce it for comparing purposes.

4.5 Performance evaluation of the control charts

As it was done in the case of monitoring the WRM with uncensored observations, the ARL was used to evaluate control chart performance. This is the mean number of inspected samples until the scheme first signals. In this study, ARL for each scheme was obtained by simulation.

4.5.1 Simulation settings

For simulation purposes, model (4.1) will be written in the form

$$t_{ik}^{(j)} = \exp\left[\beta_1 + \beta_2 \log(10i) + \gamma^{-1} z_{ik}^{(j)}\right] \tag{4.12}$$

It is set that at every $j-$th moment we have $n = 10$ fixed in repeated sampling levels of the same experimental situation. Thus, for $i = 1, \cdots, 10$, we have that $T_i \sim W(\theta_i, \gamma)$, with scale parameter $\theta_i = \exp[\beta_1 + \beta_2 \log(10i)]$, and z_{ik} being independent observations of the variable $Z_i \sim EV(0;1)$. The in-control regression coefficients are set to be $\beta_{10} = 3$ and $\beta_{20} = 2$. These settings are similar to those used by Yeh *et al.* [74] in their Phase I study for monitoring binary profiles.

To take into account out-of-control states, model (4.12) will be rewritten in the form

$$t_{ik}^{(j)} = \exp\left[3 + 2(1 - d_2)\log(10i) + \gamma^{-1} z_{ik}^{(j)}\right] \tag{4.13}$$

The performance of the proposed schemes depend on the scenario of interest. These scenarios include combinations of different values of the fixed Weibull shape parameter γ, the data-set dimension N, the in-control theoretical censoring rate p_C and the decrease size d_2. To evaluate the impact of these factors in chart performance, were considered values for the fixed shape parameter $\gamma = 0.5, 1.0$ and 1.5; censoring rates $p_C = 30\%, 50\%$ or 70% and decreases of size $d_2 \in [0.0(0.01)0.2]$. We also set the fixed total amount of observations per level $m_i = 3, 5$ or 10 leading to explored data-set dimensions $N = 30, 50$ and 100, respectively

For each considered scenario, censoring times C_i, $i = 1, ..., n$, were generated, for given values of the shape parameter γ, the in-control scale parameter $\theta_i = \exp[3 + 2\log(10i)]$ and the in-control censoring rate p_C, by using the expression

$$C_i = \theta_i \left[-\log(p_C)\right]^{1/\gamma} \tag{4.14}$$

A similar expression to that in (4.14) was used by Dickinson *et al.* [15] to generate censoring times for monitoring Weibull-distributed observations without covariates. As these censoring times represent an in-control situation, they will be assumed to be fixed in repeated sampling.

4.5.2 Obtaining control limits

The control limits for the studied charts were estimated using a bisection search algorithm so that each scheme reach $ARL_0 = 200$. For each scenario of interest, in-control data sets of a given dimension N, that included Type I right-censored observations, were generated. For intermediary values of the control limit, 20000 run-length values were simulated. When the obtained ARL_0 was sufficiently close to 200, the current value of the corresponding control limit was retained. Otherwise, the search was continued.

4.5.3 ARL estimation algorithm

For a scenario of interest, proceed as follows:

1. Set the values for λ, γ, N, p_C and d_2.

2. Generate a single observation z_{ik} from the standardized extreme value distribution and replace it in expression (4.13) to obtain a lifetime t_{ik}. Repeat until a set of N uncensored lifetimes is completed.

3. Generate the censoring times c_{ik} by formula (4.14).

4. Compare each t_{ik} with its corresponding c_{ik}. If $t_{ik} < c_{ik}$, retain t_{ik} and consider it as an exact lifetime with $\delta_{ik} = 1$. Otherwise, make $t_{ik} = c_{ik}$ and consider it as a censored observation for which $\delta_{ik} = 0$.

5. For a given scheme, proceed as follows:

   (a) For the CUSUM charts, compute the upper CUSUM statistic (4.9) for the obtained censored data set.

   (b) For the MEWMA charts, fit the model $t_{ik} = \exp\left(\beta_1 + \beta_2 x_i + \gamma^{-1} z_{ik}\right)$ and compute the MEWMA statistic (4.11) and the corresponding plotting statistic M_j.

6. Repeat steps 2–5 until the signaling condition holds. The total number of generated data set is a run length. A lot of run-length values are needed to obtain. The mean of them is an estimate of the scheme ARL.

For carrying out simulations, all the schemes were calibrated to reach $ARL_0 = 200$. Estimated ARL's were obtained by generating 50000 run-length values for each scenario of interest. Needed software was designed in *R* language.

4.5.4 Simulation results

In Tables 4.3, 4.4 and 4.5, simulated ARL of the WRM-CUSUM charts for detecting a nominal 1% decrease in the slope β_2 of the linear specification for the WRM scale parameter are presented. Tables include the results for three values of the fixed WRM shape parameter, $\gamma = 0.5, 1.0$ and 1.5. It can be noted that the larger the decrease is, the sooner each CUSUM scheme detects it. As it was expected, the increase of the theoretical censoring rate makes the schemes work less effective in detecting decreases in β_2. For a given censoring rate, the schemes take shorter to detect an out-of-control state as data-set dimension N increases. Charts designed for larger values of the fixed shape parameter react faster to out-of-control states for all reported censoring rates and data-set dimensions.

d_2	$p_c = 30\%$			$p_c = 50\%$			$p_c = 70\%$		
	$N = 30$	$N = 50$	$N = 100$	$N = 30$	$N = 50$	$N = 100$	$N = 30$	$N = 50$	$N = 100$
0.00	199.92	200.30	200.59	199.58	199.54	200.16	199.39	200.82	198.91
0.01	60.28	47.42	32.68	68.85	55.05	39.11	83.22	68.84	50.42
0.02	30.61	22.67	14.68	36.18	27.26	17.94	46.43	35.89	24.24
0.03	20.02	14.63	9.32	23.83	17.59	11.43	31.19	23.54	15.54
0.04	14.84	10.78	6.87	17.58	12.92	8.34	23.16	17.32	11.35
0.05	11.80	8.57	5.45	13.96	10.23	6.60	18.30	13.63	8.90
0.06	9.80	7.12	4.55	11.51	8.43	5.44	15.04	11.18	7.29
0.07	8.40	6.11	3.92	9.82	7.17	4.66	12.74	9.46	6.18
0.08	7.37	5.36	3.47	8.53	6.24	4.07	11.03	8.19	5.36
0.09	6.57	4.80	3.12	7.56	5.54	3.63	9.70	7.21	4.72
0.10	5.95	4.35	2.86	6.78	4.98	3.28	8.64	6.43	4.23
0.20	3.28	2.45	1.97	3.46	2.62	1.98	4.05	3.08	2.08

TABLE 4.3. Approximated performance of the WRM–CUSUM charts for the fixed shape parameter $\gamma = 0.5$ and different values of the data-set dimension N, censoring rate p_C and nominal 1% decrease in the slope of the linear specification of the scale parameter.

For instance, when $\gamma = 0.5$, the WRM-CUSUM for detecting decreases in slope in data sets of dimension $N = 30$ with a 30% of censored observations has $ARL_1 = 11.80$ for $d_2 = 0.05$. This means that this chart detects a 5% decrease in the slope at the $12-$th sampling moment, in mean terms, from the beginning of the monitoring, approximately.

d_2	$p_c = 30\%$			$p_c = 50\%$			$p_c = 70\%$		
	$N = 30$	$N = 50$	$N = 100$	$N = 30$	$N = 50$	$N = 100$	$N = 30$	$N = 50$	$N = 100$
0.00	200.99	200.61	200.60	201.01	200.55	199.30	200.51	200.11	198.79
0.01	29.35	21.65	13.59	35.20	26.17	16.79	45.93	34.72	23.20
0.02	12.96	9.18	5.58	15.75	11.27	6.72	21.28	15.39	9.73
0.03	8.24	5.82	3.56	9.94	7.05	4.34	13.40	9.58	6.01
0.04	6.08	4.32	2.67	7.23	5.14	3.20	9.66	6.90	4.35
0.05	4.87	3.47	2.19	5.69	4.06	2.55	7.50	5.36	3.41
0.06	4.09	2.94	1.97	4.70	3.38	2.17	6.10	4.38	2.81
0.07	3.57	2.56	1.80	4.02	2.90	1.97	5.13	3.70	2.39
0.08	3.19	2.26	1.55	3.53	2.55	1.81	4.11	3.21	2.12
0.09	2.93	2.08	1.27	3.17	2.77	1.58	3.88	2.83	1.96
0.10	2.71	2.01	1.08	2.89	2.10	1.31	3.46	2.53	1.82
0.20	2.00	1.06	1.00	2.00	1.04	1.00	1.99	1.16	1.00

TABLE 4.4. Approximated performance of the WRM–CUSUM charts for the fixed shape parameter $\gamma = 1.0$ and different values of the data-set dimension N, censoring rate p_C and nominal 1% decrease in the slope of the linear specification of the scale parameter.

d_2	$p_c = 30\%$			$p_c = 50\%$			$p_c = 70\%$		
	$N = 30$	$N = 50$	$N = 100$	$N = 30$	$N = 50$	$N = 100$	$N = 30$	$N = 50$	$N = 100$
0.00	200.81	199.54	199.87	200.08	198.97	200.33	200.51	199.77	200.50
0.01	17.65	12.50	7.53	21.45	15.36	9.57	28.97	21.02	13.33
0.02	7.40	5.11	3.09	8.98	6.27	3.80	12.29	8.71	5.36
0.03	4.70	3.28	2.06	5.62	3.92	2.42	7.58	5.35	3.29
0.04	3.53	2.48	1.59	4.10	2.88	1.88	5.41	3.82	2.41
0.05	2.88	2.09	1.18	3.26	2.33	1.49	4.17	2.99	1.96
0.06	2.44	1.94	1.02	2.73	2.03	1.31	3.42	2.46	1.64
0.07	2.14	1.76	1.00	2.35	1.88	1.02	2.88	2.13	1.31
0.08	2.03	1.47	1.00	2.11	1.66	1.00	2.49	1.94	1.09
0.09	2.00	1.20	1.00	2.01	1.37	1.00	2.22	1.77	1.01
0.10	1.99	1.05	1.00	1.99	1.14	1.00	2.05	1.53	1.00
0.20	1.03	1.00	1.00	1.00	1.00	1.00	1.00	1.00	1.00

TABLE 4.5. Approximated performance of the WRM–CUSUM charts for the fixed shape parameter $\gamma = 1.5$ and different values of the data-set dimension N, censoring rate p_C and nominal 1% decrease in the slope of the linear specification of the scale parameter.

When there are more censored observations in data sets of the same dimension $N = 30$, the chart detects the mentioned 5% decrease approximately at the $14-$th sampling moment ($ARL_1 = 13.96$) for $p_C = 50\%$ or approximately at the $18-$th sampling moment ($ARL_1 = 18.30$) for $p_C = 70\%$. For a given censoring rate, say $p_C = 30\%$, a faster detection is achieved by increasing the data-set dimension. The WRM-CUSUM for data sets containing 50 observations detects the mentioned 5% decrease a little earlier than that for $N = 30$, approximately at the $9-$th sampling moment ($ARL_1 = 8.57$). The WRM-CUSUM for $N = 100$ detects such decrease approximately at the $5-$th sampling moment ($ARL_1 = 5.45$). The 5% decrease is detected sooner when the shape parameter increases. When $\gamma = 1.0$, the decrease is detected at the $5-$th sampling moment ($ARL_1 = 4.87$), at the $4-$th sampling moment ($ARL_1 = 3.47$) or at the $2-$nd sampling moment ($ARL_1 = 2.19$), for $N = 30$, $N = 50$ or $N = 100$, respectively.

Similar performance to that described in the preceding paragraphs was observed for the WRM-CUSUM designed for detecting larger nominal decreases in β_2. In particular, in Tables B.1,B.2 and B.3 of Appendix B.1, simulated ARL of the WRM-CUSUM charts designed for detecting a nominal 3% decrease in β_2 are shown. It can be seen that these

d_2	$p_c = 30\%$			$p_c = 50\%$			$p_c = 70\%$		
	$N = 30$	$N = 50$	$N = 100$	$N = 30$	$N = 50$	$N = 100$	$N = 30$	$N = 50$	$N = 100$
0.00	200.02	200.10	200.12	199.37	199.23	200.05	200.91	200.87	200.64
0.01	75.73	59.39	29.22	83.68	73.50	57.71	101.27	88.87	72.10
0.02	39.31	29.18	16.85	45.97	42.14	33.69	62.99	53.31	43.17
0.03	25.01	18.80	11.86	33.11	29.94	24.93	45.53	38.46	32.19
0.04	18.10	13.90	9.21	26.05	23.63	20.33	35.65	30.68	26.29
0.05	14.14	11.02	7.51	21.76	19.78	17.32	29.76	25.89	22.57
0.06	11.57	9.11	6.36	18.70	17.14	15.12	25.63	22.58	19.96
0.07	9.83	7.78	5.52	16.51	15.10	13.52	22.59	20.10	17.97
0.08	8.52	6.80	4.89	14.74	13.58	12.24	20.24	18.12	16.36
0.09	7.51	6.01	4.37	13.38	12.35	11.16	18.35	16.60	15.06
0.10	6.71	5.41	3.97	12.23	11.32	10.27	16.90	15.28	13.96
0.20	3.25	2.74	2.03	6.54	6.14	5.71	9.30	8.62	8.05

TABLE 4.6. Approximated performance of the MEWMA chart with $\lambda = 0.1$ for the fixed WRM shape parameter $\gamma = 0.5$ and different values of the data-set dimension N and censoring rate p_C.

d_2	$p_c = 30\%$			$p_c = 50\%$			$p_c = 70\%$		
	$N = 30$	$N = 50$	$N = 100$	$N = 30$	$N = 50$	$N = 100$	$N = 30$	$N = 50$	$N = 100$
	$\gamma = 1.0$								
0.00	199.35	199.85	200.64	200.49	199.99	199.22	200.60	199.92	200.67
0.01	36.56	26.24	16.37	44.30	31.76	20.13	60.52	45.21	28.21
0.02	14.67	10.43	6.76	18.84	12.89	8.21	25.70	18.89	11.47
0.03	8.75	6.36	4.29	11.18	7.84	5.12	15.06	11.32	7.00
0.04	6.24	4.61	3.17	7.89	5.57	3.71	10.34	7.91	5.00
0.05	4.84	3.61	2.55	6.05	4.34	2.94	7.82	6.09	3.89
0.06	3.97	3.00	2.15	4.90	3.55	2.44	6.18	4.90	3.17
0.07	3.38	2.57	1.97	4.12	3.02	2.13	5.10	4.09	2.70
0.08	2.96	2.26	1.82	3.56	2.62	1.96	4.36	3.50	2.32
0.09	2.62	2.06	1.57	3.14	2.32	1.81	3.78	3.07	2.09
0.10	2.37	1.96	1.29	2.81	2.11	1.59	3.34	2.72	1.95
0.20	1.15	1.00	1.00	1.49	1.00	1.00	1.67	1.16	1.00

TABLE 4.7. Approximated performance of the MEWMA chart with $\lambda = 1.0$ for the fixed WRM shape parameter $\gamma = 1.0$ and different values of the data-set dimension N and censoring rate p_C.

d_2	$p_c = 30\%$			$p_c = 50\%$			$p_c = 70\%$		
	$N = 30$	$N = 50$	$N = 100$	$N = 30$	$N = 50$	$N = 100$	$N = 30$	$N = 50$	$N = 100$
0.00	199.56	200.59	200.50	199.60	199.34	200.23	200.32	200.95	200.93
0.01	21.63	15.44	9.90	27.53	19.33	12.23	40.74	28.41	17.11
0.02	9.03	6.56	4.42	11.50	8.12	5.30	17.63	11.73	7.17
0.03	5.62	4.18	2.94	7.05	5.05	3.42	10.57	7.06	4.40
0.04	4.12	3.13	2.22	5.03	3.69	2.54	7.32	4.93	3.16
0.05	3.31	2.53	1.97	3.94	2.92	2.08	5.48	3.78	2.49
0.06	2.77	2.14	1.75	3.24	2.42	1.89	4.34	3.04	2.08
0.07	2.40	1.99	1.34	2.77	2.10	1.60	3.57	2.55	1.86
0.08	2.12	1.91	1.06	2.41	1.98	1.22	3.02	2.20	1.60
0.09	2.01	1.73	1.00	2.14	1.88	1.03	2.62	1.99	1.28
0.10	1.98	1.44	1.00	2.02	1.67	1.00	2.32	1.86	1.07
0.20	1.00	1.00	1.00	1.00	1.00	1.00	1.01	1.00	1.00

TABLE 4.8. Approximated performance of the MEWMA chart with $\lambda = 0.1$ for the fixed WRM shape parameter $\gamma = 1.5$ and different values of the data-set dimension N and censoring rate p_C.

charts perform slightly better than those designed for detecting a 1% decrease in β_2 for decreases that are closer or greater than the nominal decrease value they are designed to detect. Approximated performance of the WRM-CUSUM charts for detecting decreases in the intercept β_1 of the lineal specification for the WRM scale parameter is presented in Appendix B.2.

Tables 4.6, 4.7 and 4.8 report simulated ARL for the MEWMA charts with $\lambda = 0.1$ and three different values of the fixed shape parameter γ. The MEWMA charts were not optimized because our interest is focused on the WRM-CUSUM. However, it is worth mentioning that the performance of the MEWMA charts with $\lambda = 0.05$ and $\lambda = 0.15$ were also investigated. Simulations suggest that the performance of these charts is not quite different from that of the MEWMA chart with $\lambda = 0.1$. As there are no reasons to think that MEWMA control charts with smoothing parameter $\lambda > 0.15$ would exhibit a substantially better performance to those of the explored MEWMA schemes, we decided to report in this document obtained results for the MEWMA chart with $\lambda = 0.1$.

The MEWMA charts show a similar performance to that of the WRM-CUSUM. This is, they react sooner to the increase of the shift value, the data-set dimension and the shape parameter value. As in the case of the WRM-CUSUM, detecting skills of the MEWMA charts become less effective as the censoring rate increases. However,in general, except for the planned 1% decrease in β_2, the MEWMA charts react slower than the WRM-CUSUM charts to the same combination of factors determining out-of-control states. For instance, the above mentioned 5% decrease in the slope is detected at the $14-$th ($ARL_1 = 14.14$), $11-$th ($ARL_1 = 11.02$) and $8-$th ($ARL_1 = 7.51$) sampling moments from the beginning of the monitoring for $N = 30$, $N = 50$ or $N = 100$, respectively, when $p_C = 30\%$ and $\gamma = 0.5$; a little slower than the corresponding WRM-CUSUM charts.

4.6 Example

In recent years, production companies have been asked to implement quality improvement programs. Conducting experiments has been turned an effective way for verifying desired properties of products. The results of an annually conducted accelerated experiment in the laboratory of a pharmaceutical company were collected during the period 1999–2013. In this experiment, specimens of certain type of tick were exposed to different concentrations of a solution used for aspersion baths in domestic animals against mite infection. The elapsed time, in hours, until death was observed.

The interest focuses on verifying whether the distribution of the elapsed time until death in each of the six experimental levels does not change over time. This would guarantee that the mean elapsed time until death of ticks treated with different concentrations of the same solution is holding at the same assessment level over time. For that, six specimens of the selected type of ticks were tested at six different concentration levels of the active principle of the solution ranging from 2% to 12% with a 2% increase between levels. For instance, the first experimental level, $i = 1$, corresponds to a 2% solution used against tick infection in small dogs. The 12% solution is used in cattle.

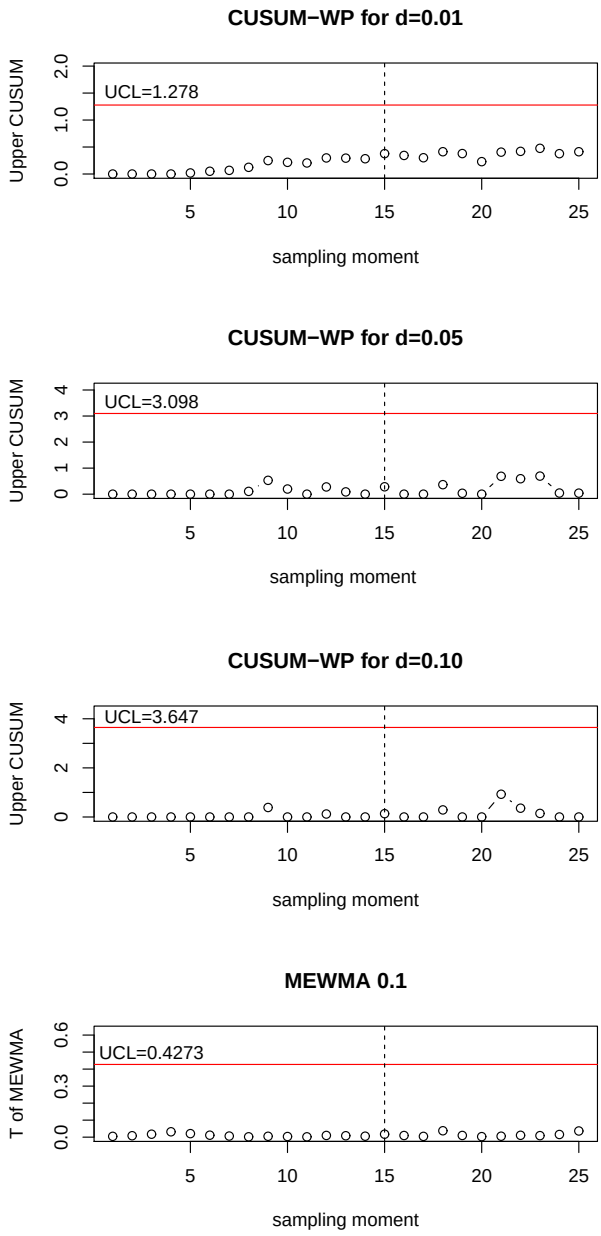

FIGURE 4.1. Control charts for the in–control process in the pharmaceutical industry example

The experiment is planned to terminate testing after a fixed time in hours, that depends on the concentration level, had elapsed. Thus, for instance, the censoring time in accelerated conditions for ticks treated with the 2% solution is 75.2 hours, while for those treated with the 12% solution is 25.1 hours. Times measured in accelerated conditions correspond approximately to half the elapsed times in normal conditions. The complete data set consists of 15 annually collected batches of $N = 36$ observations each with the same covariate pattern and an operating Type I censoring mechanism. Data were provided by the Quality Laboratory of a pharmaceutical company and can be used under request for academic purposes only. The use of these data for other purposes is not allowed. Data are reported in Appendix B.3.

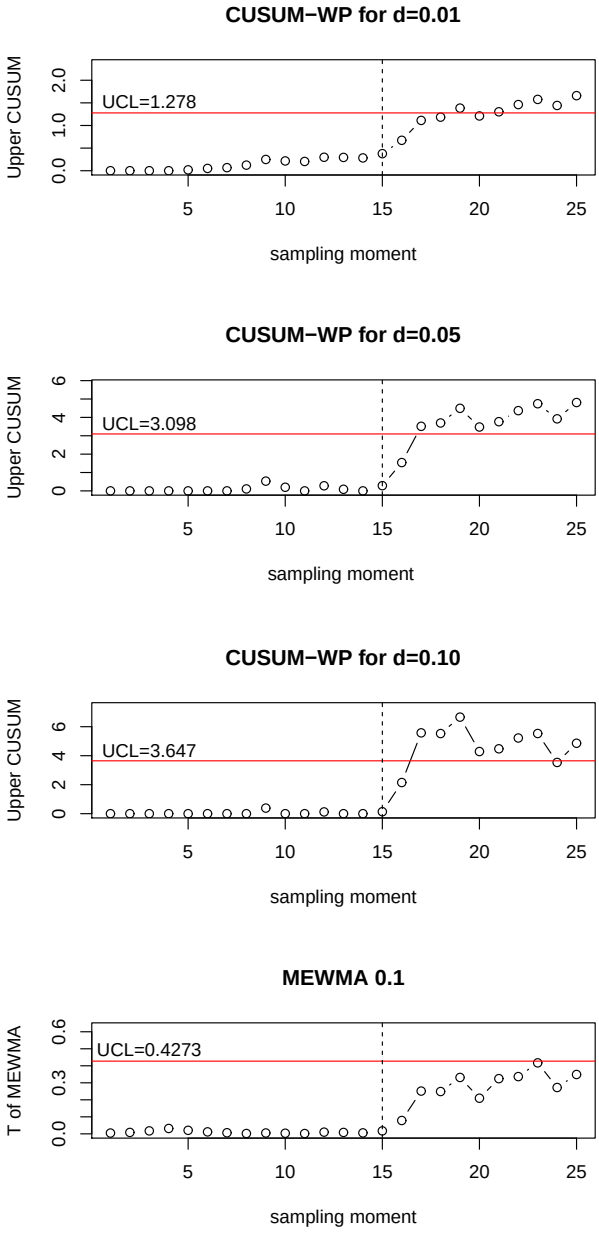

FIGURE 4.2. Control charts for the out–of–control process in the pharmaceutical industry example

A preliminary graphical analysis for all observations suggested that the Weibull accelerated failure time model of the form (4.1) was reasonable ($p - value = 1.7e - 15$). The fit results in the model

$$\hat{t}_{ik} = \exp\left(1.798 - 0.613x_i + 0.667z_{ik}\right) \tag{4.15}$$

where x_i, $i = 1, \cdots, 6$, is the log-transformation of the active principle concentration in percentages. For further discussion, it will be assumed that fit (4.15) represents the in-control model.

To check the stability of the process, the upper WRM-CUSUM charts for nominal $d_2 = 0.01$, 0.05 and 0.10 decreases in the slope and the MEWMA chart with $\lambda = 0.1$ were designed. All the designs result in a nominal $ARL_0 = 200$. The respective upper control limits are $h_{0.01} = 1.278$, $h_{0.05} = 3.098$ and $h_{0.10} = 3.647$ for the WRM–CUSUM charts and $h = 0.4273$ for the MEWMA chart. It can be seen in both Figures 4.1 and 4.2, the first 15 points in each chart, the ones before the vertical dashed line, are in-control, as they actually were.

For illustrating purposes, 10 additional data sets with the same dimension, covariate pattern and censoring times were artificially generated. In Figure 4.1, the last 10 points correspond to 10 additional batches generated from the in-control model (4.15). There is no evidence of out-of-control situations. In Figure 4.2, the additional batches were generated from a model whose slope shifts from $\beta_{20} = -0.613$ to $\beta_{21} = -0.644$. This is, the slope exhibits a 5% decrease approximately. The rest of the parameters remain at their previous values. Corresponding points to these batches are the last drawn after the in-control ones in each chart of Figure 4.2.

As it was expected, the WRM–CUSUM charts designed for nominal $d_2 = 0.05$ and $d_2 = 0.10$ detects the simulated decrease in β_2 earlier than any of the other charts (at the 2-nd batch after it actually occurs). The WRM–CUSUM for $d_2 = 0.01$ lasts a little more at the $4-$th batch. This is maybe due to the fact that the WRM–CUSUM 0.05 and 0.10 charts were specially designed to detect such decreases. The MEWMA chart does not react at all.

4.7 Monitoring WRM with time-varying dimension

In some applications such as healthcare surveillance, it is practically impossible to guarantee fixed values of the covariate matrix at every monitoring moment. It is necessary to develop methodologies for monitoring WRM with time-varying dimension and/or with random effects of the explanatory variables. This need arises when, for instance, observations in Table 4.1 are such that:

- The amount of individuals m_i subjected to the same experimental level $\mathbf{x}_i$, $i = 1, \cdots, n$, depends on the monitoring moment; this is, when we have $m_i^{(j)}$, $j = 1, 2, \cdots$. These could be survival times measured at different moments in different groups of advanced cancer patients having approximately the same prior to diagnosis status.

- The covariates $X_1, \cdots, X_p$ are exactly the same at every $j-$th moment but their values (and may be the amount of individuals having the same covariate value at the $j-$th moment) depend on the monitoring moment. This is, at the $j-$th monitoring moment, $j = 1, 2, \cdots$, we have $\mathbf{x}_i^{(j)} = (X_1^{(j)}, \cdots, X_p^{(j)})'$. These could be survival times measured at different moments in different groups of advanced cancer patients having a prior to diagnosis status of their own.

In SPC, control charts for monitoring quality characteristics with time-varying sample size have been developed in recent years. Dong et al. [16], Ryan and Woodall [52] and

Mei et al. [35] propose EWMA-based and CUSUM-based methodologies for monitoring processes with subgroups of observations having different sizes at every monitoring moment under the assumption of time-varying sample size can be characterized by a deterministic function or a random distribution.

Unfortunately, as it is pointed out in Zhou et al. [77], the afore-mentioned methodologies are very sensitive to the specification of sample sizes. However, in practice, there is no way to know which will be the size of future samples prior the monitoring. Making wrong assumptions of the mechanism generating sample sizes could lead to unexpected performance of the control schemes. To overcome this problem, Shen et al. [59] propose the use of probability limits based on on-line realization of sample sizes. Shen et al. [59] discuss in detail two computational procedures for determining the time-varying UCL of an EWMA-type statistic. The EWMA chart with probability limits was found to be an effective tool for monitoring Poisson count data. Shen et al. [59] also suggest the use of time-varying probability limits in any effective control chart.

As the numerical assessment of the upper CUSUM statistic given in (4.9) strongly depends on the total number of censored observations per sample, it is clear that also depends on the amount of individuals or items at each monitoring moment. Thus, the monitoring of WRM with type I right-censored observations and time-varying dimension N_j, $j = 1, 2, \cdots$ can be carried out by applying Shen's procedures to the upper CUSUM statistic (4.9). When the covariates are random variables, the monitoring is also possible by conditioning on the $\mathbf{x}_i^{(j)}$ values at every monitoring moment j.

According to Shen et al. [59], at the $j-$th monitoring moment, the UCL for the upper CUSUM D_j^+ has to be set to satisfy

$$\begin{aligned} P(D_1^+ > h_1(\alpha)|N_1) &= \alpha \\ P(D_j^+ > h_j(\alpha)|D_j^+ > h_l(\alpha), 1 \leq l < j, N_j) &= \alpha, \quad j > 1 \end{aligned} \tag{4.16}$$

where α is the desired false alarm rate. It is clear, from (4.16), that the UCL is determined right after the data-set dimension N_j is observed at time j. Consequently, future data-set dimensions do not have to be known.

Operatively, the UCL is evaluated as the $(1-\alpha)\times 100\%$ percentile of the upper CUSUM statistic D_j^+ at the $j-$th monitoring moment. A simulation-based procedure is summarized below:

1. At a given $j-$th monitoring moment, $j = 1, 2, \cdots$, if there is no out-of-control signal at moment $j-1$, M values of D_j^+ are calculated from randomly generated data sets with the structure in Table 4.1 for a given dimension N_j. The quantity M is a sufficiently large integer.

2. The $(1-\alpha)\times 100\%$ empirical quantile of the M values of D_j^+ is an approximation of the control limit $h_j(1-\alpha)$, where α is the desired false alarm rate.

3. Find the value of D_j^+ based on the observed data set and compare it with $h_j(1-\alpha)$. If $D_j^+ < h_j(1-\alpha)$, continue to the next monitoring moment. Otherwise, stop the monitoring.

4. If it is decided to continue, retain the first $M \times (1-\alpha)$ values of D_j^+, eliminate the ones in the upper tail and go to step 1.

As it was stated at the beginning of this section, there were identified two main scenarios at least, in which CUSUM charts with probability limits can be used for monitoring WRM with censored observations and time-varying dimension. Although much work is still to be done, preliminary results suggest that the WRM-CUSUM charts exhibit a similar performance to that reported in Tables 4.3–4.5 and in Tables B.1–B.3 when the total observations m_i^j in each fixed experimental level $i = 1, \cdots, n$ over time are uniformly distributed. Analogue conclusions were obtained when experimental levels change over time but the monitoring of the covariate values is not concerned.

4.8 Conclusions

In this chapter some different control mechanisms were presented for monitoring the slope of the linear specification of the WRM scale parameter in phase II processes. A LRT-ratio based CUSUM procedure is proposed to detect sustained decreases in the slope of the linear specification of the WRM scale parameter.

The performance of the WRM-CUSUM chart strongly depends on the known value of the shape parameter of the basic model, the data-set dimension, the theoretical censoring rate, the desired decrease to be detected and the fixed covariate pattern. The WRM-CUSUM procedure was found to exhibit a satisfactory performance in detecting decreases in the slope of the linear specification of the WRM scale parameter. The increase of the censoring rate makes the control schemes work less effectively.

The performance of the proposed WRM-CUSUM charts was compared with that of the MEWMA method for monitoring generalized linear profiles. It was found out that the WRM-CUSUM charts outperform the MEWMA method in most of the studied cases. Moreover, the use of the WRM-CUSUM chart is less restrictive than that of the MEWMA chart because its performance does not depend on unknown quantities.

Although the proposed methodologies detect decreases in the slope of the linear specification of the WRM scale parameter, they can be easily redefined for successfully detecting decreases in the intercept or combinations of changes (increases or decreases) in all the parameters of the linear specification of the WRM scale parameter as well. The results for monitoring decreases in the intercept of the WRM with $p = 2$ are presented in Appendix B.2.

Detecting increases in the mean response value is also possible but has to be faced carefully because they could lead to unwanted higher censoring rates. However, in highly reliable processes, the increase of the mean time response is expected, so it would be needed to develop control methodologies for monitoring degradation models, for example.

APPENDIX A

Monitoring WRM with uncensored observations

A.1 Data for the electrical insulating fluid example

Table A.1 contains the time to breakdown, in minutes, at each of seven levels of the voltage stress, in kilovolts. The results of this life test experiment were discussed in Nelson [38] and taken form Lawless [27, pag.3]

Voltage stress, kV						
26	**28**	**30**	**32**	**34**	**36**	**38**
5.79	68.85	17.05	0.40	0.96	1.97	0.47
1579.52	426.07	22.66	82.85	4.15	0.59	0.73
2323.70	110.29	21.02	9.88	0.19	2.58	1.40
	108.29	175.88	89.29	0.78	1.69	0.74
	1067.60	139.07	215.10	8.01	2.71	0.39
		144.12	2.75	31.75	25.50	1.13
		20.46	0.79	7.35	0.35	0.99
		43.40	15.93	6.50	0.99	2.38
		194.90	3.91	8.27	3.99	
		47.30	0.27	33.91	3.67	
		7.74	0.69	32.52	2.07	
			100.58	3.16	0.96	
			27.80	4.85	5.35	
			13.95	2.78	2.90	
			53.24	4.67	13.77	
				1.31		
				12.06		
				36.71		
				72.89		

TABLE A.1. Times to breakdown (in minutes) at each of seven voltage levels for the insulating fluid example.

A.2 Control charts for detecting increases in the mean response of the WRM

Tables A.2–A.7 show the approximated performance of the corrected LRT-based and MEWMA charts for detecting increases in the mean response due to changes in the WRM parameter vector for different data-set dimensions N and shifting patterns. Tables A.2 and A.3 present the results for $N = 30$; Tables A.4 and A.5, for $N = 50$ and Tables A.6 and A.7, for $N = 100$. Planned shifting patterns leading to increases in the mean response involve decreases in the scale parameter σ along with increases in both the intercept β_1 and the slope β_2 of the WRM.

The reported results were obtained by simulating random data sets with the structure in Table 2.1 from the model $y_{ik} = (3 + \Delta_1) + (2 + \Delta_2)\log(10i) + z_{ik}e^{0.4055+\Delta_3}$, where the drops Δ_f, $f = 1, 2$ or 3, depend on the contamination constants C_f, $f = 1, 2$ or 3, that are chosen as it was indicated in Section 3.5.2.

Shifting pattern			LRT-Chart		LRT-EChart		LRT-CChart		MEWMA	
C_1	C_2	$E(Y_1)$	ARL	SD	ARL	SD	ARL	SD	ARL	SD
0.00	0.0	6.75	200.14	(199.16)	199.97	(198.87)	200.41	(198.76)	199.92	(198.14)
0.00	0.1	6.95	113.12	(112.62)	80.90	(75.21)	94.64	(90.64)	28.29	(18.88)
	0.2	7.03	38.89	(38.39)	21.89	(15.36)	23.80	(20.14)	10.00	(8.42)
	0.3	7.11	12.86	(12.35)	8.80	(4.95)	8.56	(7.47)	6.05	(5.96)
	0.4	7.19	5.28	(4.75)	4.82	(2.39)	4.60	(2.48)	4.40	(2.98)
	0.5	7.27	2.71	(2.16)	3.12	(1.42)	3.16	(1.26)	3.50	(1.81)
	0.6	7.35	1.74	(1.13)	2.24	(0.97)	2.48	(1.08)	2.95	(1.63)
	0.7	7.43	1.31	(0.64)	1.72	(0.73)	2.14	(0.57)	2.54	(1.54)
	0.8	7.51	1.13	(0.38)	1.39	(0.56)	1.94	(0.37)	2.23	(1.44)
	0.9	7.60	1.04	(0.22)	1.20	(0.42)	1.75	(0.19)	2.07	(1.28)
	1.0	7.68	1.00	(0.10)	1.02	(0.38)	1.51	(0.10)	2.03	(0.56)
0.02	0.1	6.97	104.93	(104.43)	49.91	(42.15)	72.34	(68.76)	21.04	(12.71)
	0.2	7.06	31.89	(31.38)	17.79	(11.86)	18.80	(15.00)	8.83	(3.41)
	0.3	7.14	10.69	(10.17)	7.68	(4.06)	7.38	(4.49)	5.60	(1.67)
	0.4	7.22	4.54	(4.01)	4.38	(2.13)	4.22	(1.93)	4.21	(1.06)
	0.5	7.30	2.43	(1.87)	2.89	(1.32)	2.99	(1.05)	3.39	(0.75)
	0.6	7.38	1.62	(1.01)	2.12	(0.91)	2.40	(0.65)	2.86	(0.61)
	0.7	7.46	1.27	(0.58)	1.65	(0.68)	2.10	(0.44)	2.47	(0.54)
	0.8	7.54	1.11	(0.34)	1.36	(0.52)	1.90	(0.39)	2.19	(0.39)
	0.9	7.62	1.04	(0.19)	1.17	(0.39)	1.72	(0.46)	2.04	(0.23)
	1.0	7.70	1.00	(0.07)	1.01	(0.34)	1.39	(0.39)	2.00	(0.32)
0.04	0.1	7.00	80.00	(79.50)	48.69	(40.94)	55.40	(51.25)	16.67	(8.99)
	0.2	7.08	25.14	(24.64)	14.58	(9.27)	14.95	(11.51)	7.91	(2.87)
	0.3	7.16	8.96	(8.44)	6.77	(3.55)	6.42	(3.66)	5.26	(1.51)
	0.4	7.24	3.95	(3.42)	3.99	(1.91)	3.90	(1.71)	4.00	(0.98)
	0.5	7.33	2.22	(1.65)	2.71	(1.21)	2.84	(0.95)	3.26	(0.71)
	0.6	7.41	1.52	(0.89)	2.01	(0.86)	2.31	(0.59)	2.78	(0.59)
	0.7	7.49	1.22	(0.52)	1.58	(0.65)	2.06	(0.42)	2.40	(0.51)
	0.8	7.57	1.09	(0.30)	1.32	(0.50)	1.87	(0.40)	2.15	(0.36)
	0.9	7.65	1.03	(0.17)	1.15	(0.36)	1.67	(0.48)	2.03	(0.21)
	1.0	7.73	1.00	(0.05)	1.00	(0.31)	1.19	(0.36)	1.98	(0.29)

TABLE A.2. Performance of the proposed schemes for data-set dimension $N = 30$ of the simple WRM $y_{ik} = 3 + 2\log(10i) + 1.5z_{ik}$ with $C_3 = 1$ (no changes in $\sigma = 1.5$) and increases in both β_1 and β_2.

Shifting pattern			LRT-Chart		LRT-EChart		LRT-CChart		MEWMA	
C_1	C_2	$E(Y_1)$	ARL	SD	ARL	SD	ARL	SD	ARL	SD
0.00	0.1	7.06	90.17	(89.67)	48.49	(40.31)	54.44	(50.87)	17.22	(9.26)
	0.2	7.14	42.30	(41.79)	21.31	(14.59)	22.10	(17.99)	9.80	(3.77)
	0.3	7.22	16.57	(16.06)	9.62	(5.28)	8.89	(5.66)	6.34	(1.89)
	0.4	7.30	6.58	(6.06)	5.25	(2.49)	4.86	(2.29)	4.63	(1.13)
	0.5	7.39	3.11	(3.57)	3.36	(1.46)	3.28	(1.17)	3.66	(0.78)
	0.6	7.47	1.87	(1.28)	2.38	(0.99)	2.55	(0.73)	3.07	(0.59)
	0.7	7.55	1.34	(0.68)	1.81	(0.72)	2.18	(0.46)	2.64	(0.54)
	0.8	7.63	1.13	(0.38)	1.44	(0.56)	1.98	(0.33)	2.29	(0.46)
	0.9	7.72	1.04	(0.21)	1.22	(0.43)	1.81	(0.40)	2.08	(0.28)
	1.0	7.80	1.00	(0.08)	1.10	(0.55)	1.68	(0.42)	2.05	(0.48)
0.02	0.1	7.08	79.55	(79.05)	41.91	(33.79)	46.45	(42.21)	15.57	(12.06)
	0.2	7.17	37.20	(36.70)	17.90	(11.64)	18.06	(14.22)	8.93	(7.94)
	0.3	7.25	14.11	(13.60)	8.38	(4.43)	7.71	(4.59)	5.89	(3.23)
	0.4	7.33	5.58	(5.06)	4.77	(2.21)	4.41	(1.98)	4.38	(1.66)
	0.5	7.41	2.79	(2.23)	3.12	(1.33)	3.10	(1.08)	3.53	(1.03)
	0.6	7.50	1.72	(1.12)	2.24	(0.92)	2.45	(0.66)	2.98	(0.73)
	0.7	7.58	1.28	(0.61)	1.73	(0.69)	2.13	(0.41)	2.56	(0.57)
	0.8	7.66	1.10	(0.34)	1.40	(0.54)	1.96	(0.33)	2.23	(0.54)
	0.9	7.74	1.03	(0.19)	1.19	(0.39)	1.79	(0.42)	2.06	(0.43)
	1.0	7.83	1.00	(0.06)	1.08	(0.51)	1.66	(0.40)	2.02	(0.46)
0.04	0.1	7.71	74.91	(74.40)	36.36	(28.52)	39.95	(36.13)	13.84	(12.16)
	0.2	7.19	31.47	(30.96)	15.20	(9.45)	15.10	(11.47)	8.13	(6.56)
	0.3	7.28	11.73	(11.22)	7.43	(3.78)	6.78	(3.86)	5.54	(2.76)
	0.4	7.36	4.84	(4.31)	4.37	(1.99)	4.08	(1.72)	4.19	(1.50)
	0.5	7.44	2.49	(1.93)	2.91	(1.23)	2.95	(0.97)	3.40	(0.96)
	0.6	7.52	1.60	(0.98)	2.12	(0.86)	2.37	(0.60)	2.89	(0.68)
	0.7	7.61	1.24	(0.54)	1.65	(0.65)	2.09	(0.38)	2.49	(0.56)
	0.8	7.69	1.08	(0.30)	1.34	(0.51)	1.92	(0.34)	2.19	(0.52)
	0.9	7.77	1.01	(0.14)	1.16	(0.37)	1.75	(0.44)	2.04	(0.39)
	1.0	7.85	1.00	(0.04)	1.05	(0.49)	1.59	(0.38)	2.00	(0.44)

TABLE A.3. Performance of the proposed schemes for data-set dimension $N = 30$ of the simple WRM $y_{ik} = 3 + 2\log(10i) + 1.5z_{ik}$ with $C_3 = 0.9$ (10% decrease in $\sigma = 1.5$) and increases in both β_1 and β_2.

Shifting pattern			LRT-Chart		LRT-EChart		LRT-CChart		MEWMA	
C_1	C_2	$E(Y_1)$	ARL	SD	ARL	SD	ARL	SD	ARL	SD
0.00	0.0	6.75	199.69	(198.96)	199.76	(198.87)	200.13	(199.16)	200.90	(199.22)
0.00	0.1	6.93	153.35	(152.83)	80.44	(71.53)	91.72	(88.72)	22.34	(15.15)
	0.2	6.99	37.74	(37.23)	21.76	(15.37)	23.80	(19.56)	8.47	(3.48)
	0.3	7.05	14.39	(13.88)	8.82	(4.95)	8.49	(5.69)	5.49	(1.69)
	0.4	7.12	5.36	(4.84)	4.83	(2.37)	4.57	(2.12)	4.03	(1.08)
	0.5	7.18	2.67	(2.11)	3.16	(1.44)	3.14	(1.17)	3.24	(0.75)
	0.6	7.24	1.71	(1.10)	2.28	(0.99)	2.47	(0.69)	2.72	(0.61)
	0.7	7.31	1.31	(0.63)	1.73	(0.72)	2.14	(0.45)	2.35	(0.50)
	0.8	7.37	1.12	(0.36)	1.41	(0.55)	1.96	(0.37)	2.13	(0.36)
	0.9	7.43	1.06	(0.24)	1.22	(0.43)	1.78	(0.42)	2.02	(0.24)
	1.0	7.50	1.01	(0.11)	1.09	(0.28)	1.56	(0.49)	1.93	(0.27)
0.02	0.1	6.95	142.86	(142.36)	62.20	(54.21)	71.08	(66.69)	17.41	(10.01)
	0.2	7.01	30.30	(29.80)	17.24	(11.19)	17.83	(13.73)	7.96	(3.16)
	0.3	7.08	10.93	(10.42)	7.46	(4.19)	7.41	(4.51)	5.12	(1.54)
	0.4	7.14	4.34	(3.81)	4.35	(2.07)	4.21	(1.93)	3.84	(0.96)
	0.5	7.20	2.45	(1.89)	2.89	(1.28)	2.96	(1.03)	3.13	(0.73)
	0.6	7.26	1.58	(0.96)	2.19	(0.94)	2.39	(0.63)	2.68	(0.58)
	0.7	7.33	1.28	(0.60)	1.67	(0.68)	2.10	(0.42)	2.30	(0.48)
	0.8	7.39	1.10	(0.34)	1.37	(0.52)	1.92	(0.37)	2.10	(0.31)
	0.9	7.45	1.04	(0.19)	1.17	(0.38)	1.75	(0.45)	2.00	(0.22)
	1.0	7.52	1.01	(0.11)	1.08	(0.27)	1.54	(0.50)	1.90	(0.31)
0.04	0.1	6.97	60.61	(60.10)	44.87	(38.51)	54.54	(48.37)	14.33	(7.75)
	0.2	7.03	25.32	(24.81)	14.53	(8.80)	14.33	(10.50)	7.16	(2.62)
	0.3	7.10	8.33	(7.82)	6.71	(3.51)	3.46	(3.73)	4.78	(1.33)
	0.4	7.16	4.07	(3.54)	4.04	(1.86)	3.89	(1.61)	3.66	(0.92)
	0.5	7.22	2.27	(1.69)	2.71	(2.21)	2.83	(0.91)	3.00	(0.67)
	0.6	7.29	1.54	(0.92)	1.99	(0.83)	2.32	(0.58)	2.56	(0.58)
	0.7	7.35	1.23	(0.53)	1.59	(0.64)	2.06	(0.41)	2.25	(0.44)
	0.8	7.41	1.07	(0.29)	1.33	(0.51)	1.88	(0.39)	2.07	(0.28)
	0.9	7.48	1.03	(0.17)	1.16	(0.38)	1.72	(0.46)	1.97	(0.23)
	1.0	7.54	1.00	(0.07)	1.06	(0.23)	1.48	(0.50)	1.88	(0.33)

TABLE A.4. Performance of the proposed schemes for data-set dimension $N = 50$ of the simple WRM $y_{ik} = 3 + 2\log(10i) + 1.5z_{ik}$ with $C_3 = 1$ (no changes in $\sigma = 1.5$) and increases in both β_1 and β_2.

Shifting pattern			LRT-Chart		LRT-EChart		LRT-CChart		MEWMA	
C_1	C_2	$E(Y_1)$	ARL	SD	ARL	SD	ARL	SD	ARL	SD
0.00	0.1	7.04	68.97	(68.46)	31.49	(23.83)	33.53	(29.70)	10.95	(5.11)
	0.2	7.10	34.48	(33.98)	17.44	(11.25)	17.44	(14.25)	7.98	(2.97)
	0.3	7.17	18.02	(17.51)	8.83	(4.60)	8.21	(4.92)	5.53	(1.58)
	0.4	7.23	6.43	(5.91)	5.14	(2.39)	4.70	(2.20)	4.20	(1.02)
	0.5	7.29	3.18	(2.64)	3.40	(1.41)	3.26	(1.16)	3.38	(0.73)
	0.6	7.36	1.90	(1.30)	2.41	(0.95)	2.56	(0.73)	2.87	(0.60)
	0.7	7.42	1.31	(0.64)	1.87	(0.73)	2.19	(0.45)	2.44	(0.53)
	0.8	7.49	1.13	(0.39)	1.47	(0.56)	2.01	(0.32)	2.17	(0.38)
	0.9	7.55	1.04	(0.22)	1.24	(0.44)	1.87	(0.36)	2.03	(0.20)
	1.0	7.61	1.01	(0.11)	1.10	(0.30)	1.68	(0.47)	1.97	(0.18)
0.02	0.1	7.06	71.43	(70.93)	28.59	(21.60)	30.49	(16.47)	10.57	(4.73)
	0.2	7.12	29.85	(29.35)	15.19	(9.72)	15.46	(11.95)	7.29	(2.52)
	0.3	7.19	12.35	(11.84)	8.07	(4.24)	7.18	(4.22)	5.21	(1.45)
	0.4	7.25	5.48	(4.95)	4.68	(2.15)	4.30	(1.88)	4.03	(0.97)
	0.5	7.31	2.71	(2.16)	3.16	(1.29)	3.07	(1.04)	3.26	(0.69)
	0.6	7.38	1.68	(1.07)	2.29	(0.92)	2.47	(0.66)	2.77	(0.58)
	0.7	7.44	1.28	(0.60)	1.77	(0.68)	2.15	(0.41)	2.38	(0.50)
	0.8	7.51	1.11	(0.36)	1.43	(0.56)	1.97	(0.30)	2.13	(0.34)
	0.9	7.57	1.03	(0.18)	1.21	(0.41)	1.82	(0.39)	2.02	(0.20)
	1.0	7.64	1.01	(0.11)	1.09	(0.29)	1.63	(0.48)	1.97	(0.20)
0.04	0.1	7.08	46.51	(46.01)	25.46	(17.95)	26.97	(23.27)	9.89	(4.28)
	0.2	7.14	28.57	(28.07)	13.38	(7.94)	12.74	(9.29)	6.95	(2.32)
	0.3	7.21	11.63	(11.12)	7.07	(3.51)	6.56	(3.64)	4.93	(1.34)
	0.4	7.27	5.23	(4.71)	4.32	(1.94)	3.98	(1.62)	3.87	(0.89)
	0.5	7.34	2.44	(1.88)	2.91	(1.19)	2.92	(0.92)	3.14	(0.66)
	0.6	7.40	1.59	(0.97)	2.14	(0.86)	2.38	(0.59)	2.71	(0.56)
	0.7	7.47	1.25	(0.56)	1.70	(0.67)	2.09	(0.35)	2.31	(0.47)
	0.8	7.53	1.08	(0.30)	1.37	(0.52)	1.95	(0.32)	2.09	(0.30)
	0.9	7.59	1.03	(0.18)	1.16	(0.37)	1.80	(0.41)	2.01	(0.17)
	1.0	7.66	1.01	(0.09)	1.06	(0.24)	1.58	(0.50)	1.95	(0.23)

TABLE A.5. Performance of the proposed schemes for data-set dimension $N = 50$ of the simple WRM $y_{ik} = 3 + 2\log(10i) + 1.5z_{ik}$ with $C_3 = 0.9$ (10% decrease in $\sigma = 1.5$) and increases in both β_1 and β_2.

Shifting pattern			LRT-Chart		LRT-EChart		LRT-CChart		MEWMA	
C_1	C_2	$E(Y_1)$	ARL	SD	ARL	SD	ARL	SD	ARL	SD
0.00	0.0	6.75	200.02	(199.69)	199.89	(198.78)	200.23	(199.36)	200.42	(199.01)
0.00	0.1	6.91	125.00	(124.50)	83.55	(73.07)	96.13	(92.17)	23.14	(15.41)
	0.2	6.95	40.82	(40.31)	21.99	(14.87)	23.49	(19.86)	8.87	(3.57)
	0.3	7.00	13.51	(13.00)	9.08	(5.19)	8.27	(5.20)	5.52	(1.79)
	0.4	7.04	5.76	(5.24)	4.88	(2.42)	4.59	(2.06)	4.08	(1.06)
	0.5	7.09	2.98	(2.43)	3.18	(1.40)	3.17	(1.14)	3.28	(0.75)
	0.6	7.13	1.74	(1.14)	2.29	(0.96)	2.50	(0.70)	2.75	(0.60)
	0.7	7.18	1.31	(0.64)	1.77	(0.72)	2.14	(0.42)	2.35	(0.50)
	0.8	7.22	1.13	(0.38)	1.45	(0.56)	1.97	(0.35)	2.13	(0.35)
	0.9	7.27	1.04	(0.21)	1.23	(0.43)	1.84	(0.39)	2.01	(0.22)
	1.0	7.31	1.01	(0.10)	1.10	(0.30)	1.63	(0.48)	1.93	(0.26)
0.02	0.1	6.93	111.11	(110.61)	60.83	(50.62)	71.83	(68.88)	18.27	(10.91)
	0.2	6.97	37.04	(36.53)	17.80	(11.62)	18.19	(14.92)	7.91	(2.99)
	0.3	7.01	9.90	(9.39)	7.79	(4.09)	7.27	(4.49)	5.15	(1.53)
	0.4	7.06	4.74	(4.21)	4.41	(2.14)	4.23	(1.92)	3.92	(0.99)
	0.5	7.10	2.56	(1.99)	2.97	(1.24)	3.03	(1.09)	3.14	(0.72)
	0.6	7.15	1.65	(1.04)	2.18	(0.88)	2.41	(0.65)	2.66	(0.59)
	0.7	7.19	1.28	(0.60)	1.70	(0.67)	2.11	(0.41)	2.32	(0.49)
	0.8	7.24	1.10	(0.33)	1.39	(0.53)	1.96	(0.34)	2.09	(0.32)
	0.9	7.28	1.01	(0.21)	1.18	(0.39)	1.79	(0.42)	2.00	(0.20)
	1.0	7.33	1.01	(0.09)	1.09	(0.28)	1.62	(0.49)	1.93	(0.28)
0.04	0.1	6.94	71.43	(70.93)	46.03	(39.12)	53.09	(48.19)	14.43	(7.63)
	0.2	6.98	20.41	(19.90)	14.28	(8.88)	14.56	(11.48)	7.26	(2.61)
	0.3	7.03	9.48	(8.96)	6.85	(3.58)	6.39	(3.59)	4.89	(1.44)
	0.4	7.07	4.11	(3.58)	4.00	(1.86)	3.88	(1.62)	3.73	(0.93)
	0.5	7.12	2.22	(1.64)	2.79	(1.20)	2.86	(0.96)	3.04	(0.67)
	0.6	7.16	1.58	(0.95)	2.07	(0.85)	2.34	(0.59)	2.59	(0.58)
	0.7	7.21	1.24	(0.54)	1.62	(0.64)	2.05	(0.36)	2.26	(0.46)
	0.8	7.25	1.09	(0.32)	1.36	(0.52)	1.93	(0.34)	2.07	(0.28)
	0.9	7.30	1.02	(0.15)	1.18	(0.39)	1.77	(0.42)	1.97	(0.20)
	1.0	7.34	1.01	(0.10)	1.07	(0.25)	1.58	(0.49)	1.88	(0.33)

TABLE A.6. Performance of the proposed schemes for data-set dimension $N = 100$ of the simple WRM $y_{ik} = 3 + 2\log(10i) + 1.5z_{ik}$ with $C_3 = 1$ (no changes in $\sigma = 1.5$) and increases in both β_1 and β_2.

Shifting pattern			LRT-Chart		LRT-EChart		LRT-CChart		MEWMA	
C_1	C_2	$E(Y_1)$	ARL	SD	ARL	SD	ARL	SD	ARL	SD
0.00	0.1	7.02	29.85	(29.35)	25.44	(19.22)	25.32	(18.77)	23.04	(15.17)
	0.2	7.06	24.69	(24.19)	11.42	(6.55)	10.85	(7.23)	9.11	(3.80)
	0.3	7.11	12.74	(12.23)	7.59	(3.95)	6.68	(3.81)	5.57	(1.80)
	0.4	7.16	6.31	(5.79)	4.87	(2.18)	4.44	(1.92)	4.03	(1.05)
	0.5	7.20	3.12	(2.57)	3.32	(1.37)	3.20	(1.11)	3.26	(0.79)
	0.6	7.25	1.94	(1.34)	2.46	(0.97)	2.53	(0.69)	2.74	(0.62)
	0.7	7.29	1.38	(0.73)	1.88	(0.71)	2.20	(0.44)	2.36	(0.50)
	0.8	7.34	1.14	(0.40)	1.52	(0.58)	2.02	(0.29)	2.14	(0.36)
	0.9	7.38	1.06	(0.25)	1.27	(0.46)	1.90	(0.32)	2.01	(0.21)
	1.0	7.43	1.01	(0.12)	1.12	(0.33)	1.75	(0.44)	1.94	(0.27)
0.02	0.1	7.03	29.85	(29.35)	18.46	(10.87)	18.61	(11.11)	16.94	(10.71)
	0.2	7.08	19.80	(19.30)	10.62	(5.91)	9.87	(6.77)	8.12	(3.11)
	0.3	7.13	10.36	(9.85)	6.71	(3.39)	6.00	(3.16)	5.16	(1.51)
	0.4	7.17	5.33	(4.81)	4.41	(1.90)	4.09	(1.68)	3.90	(0.99)
	0.5	7.22	2.85	(2.30)	3.11	(1.27)	3.06	(1.01)	3.12	(0.73)
	0.6	7.26	1.78	(1.17)	2.33	(0.91)	2.46	(0.67)	2.65	(0.57)
	0.7	7.31	1.33	(0.66)	1.81	(0.69)	2.17	(0.42)	2.31	(0.47)
	0.8	7.35	1.11	(0.36)	1.49	(0.57)	2.00	(0.27)	2.10	(0.32)
	0.9	7.40	1.04	(0.22)	1.27	(0.45)	1.88	(0.34)	2.00	(0.22)
	1.0	7.44	1.01	(0.09)	1.09	(0.29)	1.71	(0.45)	1.92	(0.28)
0.04	0.1	7.05	23.90	(23.39)	14.53	(9.12)	14.32	(10.57)	14.19	(7.53)
	0.2	7.10	17.54	(17.04)	9.80	(5.14)	9.05	(5.53)	7.20	(2.26)
	0.3	7.14	10.17	(10.06)	6.17	(2.98)	5.52	(2.76)	4.86	(1.39)
	0.4	7.19	4.54	(4.01)	4.09	(1.78)	3.80	(1.46)	3.73	(0.92)
	0.5	7.23	2.55	(1.99)	2.88	(1.15)	2.90	(0.94)	3.03	(0.67)
	0.6	7.28	1.65	(1.04)	2.18	(0.86)	2.40	(0.61)	2.60	(0.58)
	0.7	7.32	1.25	(0.56)	1.72	(0.66)	2.12	(0.38)	2.27	(0.46)
	0.8	7.37	1.09	(0.31)	1.42	(0.56)	1.97	(0.28)	2.07	(0.29)
	0.9	7.41	1.03	(0.16)	1.22	(0.42)	1.86	(0.36)	1.97	(0.23)
	1.0	7.46	1.00	(0.08)	1.08	(0.27)	1.68	(0.47)	1.89	(0.31)

TABLE A.7. Performance of the proposed schemes for data-set dimension $N = 100$ of the simple WRM $y_{ik} = 3 + 2\log(10i) + 1.5z_{ik}$ with $C_3 = 0.9$ (10% decrease in $\sigma = 1.5$) and increases in both β_1 and β_2.

A.3 Data sets for the food industry example

Since 1997 a biscuit company has annually conducted accelerated tests to determine the shelf life of cookies in different storage conditions. Seven specimens of 4 g weight are subjected to five different high-temperature levels at a fixed 75% relative humidity level. Temperature levels range from 36 to $44°C$ with a $2°C$ increase between levels. A climatic device is used to control temperature levels. Temperature levels are shown in the second column of the table below.

The response variable is the elapsed time, in days, until a specimen achieves a 40% moisture gain. There are $N = 35$ uncensored observations in each annual batch. The complete data set consists of 14 annual batches collected in the period $1997 - 2010$ and 3 additional batches of the same dimension collected in 2011 that are known to be out-of-control because of a lack of calibration of the climatic device. Data are shown in the table below.

	X	97	98	99	00	01	02	03	04	05	06	07	08	09	10	11	11	11
[1,]	36	15	104	6	121	29	111	79	27	26	85	37	109	48	11	55	24	58
[2,]	38	99	5	2	42	78	20	76	47	14	23	37	67	37	6	95	43	73
[3,]	40	25	45	118	12	68	67	55	110	75	78	20	56	48	28	9	43	2
[4,]	42	19	62	29	24	16	15	15	42	45	43	75	18	23	1	16	37	74
[5,]	44	15	18	29	88	86	77	24	9	95	11	56	3	38	26	25	10	65
[6,]	36	22	166	109	105	42	7	176	39	43	62	56	83	183	18	109	22	61
[7,]	38	38	10	11	36	114	27	27	62	89	85	155	34	126	31	35	36	25
[8,]	40	94	22	58	116	130	190	39	7	126	7	54	99	72	38	2	22	97
[9,]	42	41	53	38	26	13	43	11	32	73	24	25	135	37	56	23	58	68
[10,]	44	16	7	25	20	62	50	16	39	33	46	64	57	11	23	22	17	28
[11,]	36	51	105	8	18	36	111	3	118	34	150	60	53	74	84	100	64	83
[12,]	38	45	20	44	30	10	98	63	59	62	33	57	42	40	96	38	60	3
[13,]	40	2	65	10	76	81	22	126	91	62	73	23	88	25	49	8	57	32
[14,]	42	49	108	57	95	28	36	105	19	23	16	6	31	27	7	37	4	41
[15,]	44	7	39	56	33	54	38	70	56	25	23	92	18	30	28	113	8	53
[16,]	36	129	45	182	89	138	102	136	48	128	117	24	8	66	80	56	42	8
[17,]	38	36	47	71	28	52	39	174	182	61	65	88	37	9	74	9	57	45
[18,]	40	97	2	33	58	127	36	137	40	9	60	22	15	26	47	6	58	29
[19,]	42	56	27	5	48	38	65	6	14	15	101	29	32	69	25	14	3	11
[20,]	44	39	45	4	22	44	27	60	14	26	17	34	13	50	25	8	16	12
[21,]	36	41	114	81	102	182	157	172	64	109	143	90	53	9	32	44	34	42
[22,]	38	31	69	53	26	23	14	74	13	183	97	110	170	27	63	32	76	9
[23,]	40	45	10	46	46	36	10	34	52	19	4	48	2	20	123	4	82	27
[24,]	42	27	34	36	31	9	24	84	16	20	18	38	93	67	25	32	28	72
[25,]	44	43	64	38	5	89	20	50	23	13	22	11	19	19	83	7	26	6
[26,]	36	114	32	35	93	31	64	46	4	2	48	92	25	43	139	3	2	111
[27,]	38	57	84	31	11	174	38	6	28	10	15	20	112	69	65	13	1	27
[28,]	40	60	91	73	57	59	11	64	59	57	39	5	79	15	20	187	31	26
[29,]	42	52	24	14	3	1	28	35	53	52	61	29	43	8	44	28	12	26
[30,]	44	53	54	55	7	24	29	49	23	58	119	24	31	56	12	4	44	31
[31,]	36	102	66	49	28	93	20	19	36	183	185	143	146	38	83	57	85	21
[32,]	38	22	81	52	46	178	111	83	21	69	95	115	17	3	15	10	5	16
[33,]	40	33	10	22	9	35	79	42	22	28	14	1	24	117	19	19	16	52
[34,]	42	56	18	29	37	73	82	59	59	29	82	18	44	13	11	1	66	72
[35,]	44	27	14	24	3	17	8	66	27	55	85	13	49	14	39	49	45	28

APPENDIX B

Monitoring WRM with right-censored observations

B.1 CUSUM control charts for a nominal decrease $d_2 = 0.03$ in the slope β_2 of the WRM with $p = 2$

Tables B.1,B.2 and B.3 show the approximated performance of the WRM-CUSUM charts for detecting a larger nominal decrease in the slope β_2 of the linear specification for the WRM scale parameter. The reported results were obtained by simulating random data sets with the structure in Table 4.1 from the model $t_{ik} = \exp\left[3 + 2(1 - d_2)\log 10i + \gamma^{-1} z_{ik}\right]$, where $0 < d_2 < 1$. Thus, the interest is focused on detecting a $(1 - d_2) \times 100\%$ decrease in β_2 with a CUSUM chart designed for a nominal 3% decrease.

d_2	$p_c = 30\%$			$p_c = 50\%$			$p_c = 70\%$		
	$N = 30$	$N = 50$	$N = 100$	$N = 30$	$N = 50$	$N = 100$	$N = 30$	$N = 50$	$N = 100$
0.00	199.66	200.61	200.88	200.50	201.02	200.01	200.41	199.87	199.28
0.01	65.99	54.51	40.15	73.68	61.76	46.62	87.42	73.58	56.78
0.02	30.08	22.30	14.21	35.89	26.80	17.51	46.15	35.51	23.91
0.03	17.61	12.46	7.60	21.48	15.37	9.53	28.95	21.14	13.40
0.04	12.13	8.45	5.08	14.87	10.47	6.35	20.34	14.55	8.98
0.05	9.18	6.37	3.82	11.24	7.87	4.75	15.43	10.93	6.70
0.06	7.38	5.11	3.08	8.98	6.29	3.80	12.34	8.71	5.33
0.07	6.19	4.29	2.61	7.49	5.22	3.18	10.25	7.20	4.42
0.08	5.33	3.71	2.28	6.40	4.47	2.75	8.73	6.15	3.77
0.09	4.70	3.28	2.06	5.62	3.92	2.43	7.58	5.34	3.30
0.10	4.21	2.95	1.89	4.99	3.50	2.19	6.69	4.72	2.93
0.20	2.22	1.84	1.00	2.46	1.93	1.04	3.04	2.22	1.42

TABLE B.1. Approximated performance of the WRM–CUSUM charts for the fixed shape parameter $\gamma = 0.5$ and different values of the data-set dimension N, censoring rate p_C and nominal 3% decrease in the slope of the linear specification of the scale parameter.

d_2	$p_c = 30\%$			$p_c = 50\%$			$p_c = 70\%$		
	$N = 30$	$N = 50$	$N = 100$	$N = 30$	$N = 50$	$N = 100$	$N = 30$	$N = 50$	$N = 100$
0.00	198.93	200.30	200.18	199.31	199.68	199.46	200.63	198.99	200.09
0.01	37.41	29.62	21.35	42.82	33.91	24.73	52.25	42.49	31.03
0.02	12.57	8.81	5.39	15.28	10.94	6.70	20.90	15.02	9.43
0.03	6.58	4.48	2.65	8.12	5.56	3.30	11.35	7.89	4.72
0.04	4.37	2.99	1.76	5.37	3.66	2.18	7.46	5.14	3.07
0.05	3.31	2.28	1.35	3.98	2.74	1.63	5.51	3.78	2.28
0.06	2.69	1.87	1.12	3.19	2.22	1.32	4.34	3.00	1.82
0.07	2.31	1.59	1.03	2.68	1.88	1.12	3.57	2.49	1.52
0.08	2.07	1.36	1.00	2.33	1.63	1.03	3.04	2.15	1.29
0.09	1.89	1.19	1.00	2.09	1.42	1.01	2.65	1.89	1.13
0.10	1.74	1.08	1.00	1.92	1.24	1.00	2.36	1.68	1.05
0.20	1.00	1.00	1.00	1.00	1.00	1.00	1.04	1.00	1.00

TABLE B.2. Approximated performance of the WRM–CUSUM charts for the fixed shape parameter $\gamma = 1.0$ and different values of the data-set dimension N, censoring rate p_C and nominal 3% decrease in the slope of the linear specification of the scale parameter.

d_2	$p_c = 30\%$			$p_c = 50\%$			$p_c = 70\%$		
	$N = 30$	$N = 50$	$N = 100$	$N = 30$	$N = 50$	$N = 100$	$N = 30$	$N = 50$	$N = 100$
0.00	200.34	199.61	199.95	198.74	199.92	200.41	199.32	200.09	200.94
0.01	25.81	20.38	14.36	29.43	22.76	18.08	37.09	29.65	21.06
0.02	7.24	4.96	2.92	9.67	6.05	3.78	11.92	8.49	5.09
0.03	3.57	2.41	1.44	4.28	2.90	1.77	6.05	4.13	2.44
0.04	2.37	1.59	1.07	2.84	1.92	1.22	3.91	2.66	1.59
0.05	1.82	1.23	1.01	2.14	1.44	1.03	2.87	1.97	1.22
0.06	1.48	1.06	1.00	1.73	1.17	1.00	2.26	1.56	1.06
0.07	1.24	1.01	1.00	1.44	1.04	1.00	1.89	1.29	1.01
0.08	1.09	1.00	1.00	1.23	1.01	1.00	1.61	1.11	1.00
0.09	1.02	1.00	1.00	1.09	1.00	1.00	1.38	1.03	1.00
0.10	1.00	1.00	1.00	1.03	1.00	1.00	1.20	1.01	1.00
0.20	1.00	1.00	1.00	1.00	1.00	1.00	1.00	1.00	1.00

TABLE B.3. Approximated performance of the WRM–CUSUM charts for the fixed shape parameter $\gamma = 1.5$ and different values of the data-set dimension N, censoring rate p_C and nominal 3% decrease in the slope of the linear specification of the scale parameter.

B.2 Control charts for detecting decreases in the intercept β_1 of the WRM

The WRM-CUSUM chart can also be used for detecting decreases the intercept β_1 of the linear specification for the WRM scale parameter. Decreases in the intercept lead to decreases in the mean response and to the deterioration of the process consequently.

Let $\ell_j(\beta_1)$ be the likelihood ratio statistic defined for the intercept β_1 of the WRM given a data set of times with type I right-censored observations (t_i, δ_i), $i = 1, \ldots, n$ at the $j-$th monitoring moment. Then,

$$\ell_j(\beta_1) = \ell_j(\beta_{11}) - \ell_j(\beta_{10}), \quad j = 1, 2, \ldots \tag{B.1}$$

where $\ell_j(\beta_{21})$ and $\ell_(\beta_{20})$ are the log-likelihood function for model (4.1) defined for the out-of-control and the in-control states, respectively.

A CUSUM statistic for detecting decreases in β_1 based on the scores (B.1) has the form

$$D_j^- = \min\left(0; D_{j-1}^- - k_j + \sum_{i=1}^{n}\left[\frac{t_i}{\exp\left(\mathbf{x}_i'\boldsymbol{\beta}\right)}\right]^{\gamma}\right), \quad j = 1, 2, ... \tag{B.2}$$

where $D_0^- = 0$ and $k_j = -ra(1-e^a)$ is the reference value with $a = d_1\beta_1\gamma$. The chart signals when $D_j^- < h^-$, for any j, indicating a possible decrease in β_1.

Tables B.4,B.5 and B.6 show the approximated performance of the WRM-CUSUM charts for detecting decreases in the intercept β_1 of the linear specification for the WRM scale parameter. The reported results were obtained by simulating random data sets with the structure in Table 4.1 from the model $t_{ik} = \exp\left[3(1-d_1) + 2\log 10i + \gamma^{-1}z_{ik}\right]$, where $0 < d_1 < 1$. Thus, the interest is focused on detecting a $(1-d_1)\times 100\%$ decrease in the intercept β_1 with CUSUM charts designed for a nominal 5% decrease.

d_1	$p_c = 30\%$			$p_c = 50\%$			$p_c = 70\%$		
	$n = 30$	$n = 50$	$n = 100$	$n = 30$	$n = 50$	$n = 100$	$n = 30$	$n = 50$	$n = 100$
0.00	200.71	200.30	200.59	199.58	199.54	200.16	199.39	200.82	198.91
0.01	120.25	107.21	90.94	127.38	115.06	98.43	138.74	126.91	110.95
0.02	77.46	63.97	47.74	86.38	72.50	54.86	100.31	85.66	67.47
0.03	53.69	41.88	28.79	61.48	48.77	34.34	75.33	61.24	44.62
0.04	39.43	29.56	19.44	46.50	35.31	23.64	58.85	46.15	31.89
0.05	30.58	22.36	14.23	36.48	27.10	17.56	47.30	36.08	24.22
0.06	24.73	17.71	11.16	29.64	21.73	13.80	39.02	29.35	19.22
0.07	20.49	14.70	9.08	24.87	18.03	11.34	33.13	24.54	15.87
0.08	17.57	12.48	7.69	21.30	15.33	9.59	28.58	20.95	13.40
0.09	15.26	10.85	6.65	18.60	13.35	8.28	25.02	18.27	11.61
0.10	13.56	9.57	5.86	16.50	11.77	7.28	22.16	16.17	10.23
0.15	8.61	6.08	3.74	10.39	7.39	4.56	14.00	10.09	6.34
0.20	6.36	4.49	2.79	7.58	5.38	3.35	10.13	7.27	4.58

TABLE B.4. Approximated performance of the WRM-CUSUM charts for the fixed shape parameter $\gamma = 0.5$ and different values of the data-set dimension N, censoring rate p_C and nominal 5% decrease in the intercept of the linear specification of the scale parameter.

d_1	$p_c = 30\%$			$p_c = 50\%$			$p_c = 70\%$		
	$n = 30$	$n = 50$	$n = 100$	$n = 30$	$n = 50$	$n = 100$	$n = 30$	$n = 50$	$n = 100$
0.00	200.99	200.61	200.60	201.01	200.55	199.30	200.51	200.11	198.79
0.01	86.84	75.89	61.85	94.31	82.97	68.01	106.02	93.84	78.60
0.02	44.20	34.50	24.33	50.73	40.29	28.57	62.20	50.44	36.48
0.03	25.83	19.00	12.06	31.03	23.15	14.88	40.17	30.52	20.45
0.04	17.15	12.15	7.42	20.82	14.97	9.29	28.20	20.52	13.03
0.05	12.51	8.68	5.20	15.35	10.76	6.51	21.04	15.11	9.33
0.06	9.72	6.69	3.99	11.94	8.33	4.99	16.50	11.68	7.15
0.07	7.91	5.46	3.24	9.75	6.74	4.05	13.45	9.49	5.76
0.08	6.69	4.58	2.75	8.19	5.67	3.40	11.34	7.96	4.80
0.09	5.79	3.98	2.39	7.06	4.89	2.94	9.78	6.82	4.13
0.10	5.10	3.52	2.14	6.21	4.29	2.60	8.56	5.99	3.62
0.15	3.28	2.32	1.39	3.88	2.72	1.71	5.20	3.66	2.28
0.20	2.49	1.87	1.04	2.86	2.08	1.21	3.73	2.64	1.71

TABLE B.5. Approximated performance of the WRM-CUSUM charts for the fixed shape parameter $\gamma = 1.0$ and different values of the data-set dimension N, censoring rate p_C and nominal 5% decrease in the intercept of the linear specification of the scale parameter.

d_1	$p_c = 30\%$			$p_c = 50\%$			$p_c = 70\%$		
	$n = 30$	$n = 50$	$n = 100$	$n = 30$	$n = 50$	$n = 100$	$n = 30$	$n = 50$	$n = 100$
0.00	200.81	199.54	199.87	200.08	198.97	200.33	200.51	199.77	200.50
0.01	69.99	60.35	48.70	76.53	66.18	53.10	87.43	75.94	62.00
0.02	29.78	22.83	15.70	34.68	26.94	18.41	43.83	34.33	23.91
0.03	15.62	11.21	6.93	18397	13.69	8.56	25.34	18.72	11.89
0.04	9.80	6.75	4.03	12.02	8.43	5.07	16.60	11.82	7.22
0.05	6.93	4.73	2.80	8.57	5.87	3.48	11.94	8.31	5.00
0.06	5.32	3.63	2.14	6.57	4.48	2.65	9.17	6.33	3.78
0.07	4.31	2.94	1.74	5.30	3.62	2.15	7.37	5.09	3.04
0.08	3.65	2.51	1.48	4.45	3.03	1.82	6.16	4.25	2.54
0.09	3.18	2.19	1.30	3.83	2.63	1.57	5.26	3.63	2.20
0.10	2.82	1.96	1.16	3.37	2.34	1.39	4.59	3.18	1.93
0.15	1.96	1.25	1.00	2.18	1.51	1.01	2.80	2.00	1.19
0.20	1.52	1.01	1.00	1.72	1.08	1.00	2.07	1.44	1.01

TABLE B.6. Approximated performance of the WRM-CUSUM charts for the fixed shape parameter $\gamma = 1.5$ and different values of the data-set dimension N, censoring rate p_C and nominal 5% decrease in the intercept of the linear specification of the scale parameter.

Tables B.7,B.8 and B.9 also show the approximated performance of the WRM-CUSUM charts for detecting decreases in the intercept β_1 of the linear specification for the WRM scale parameter. The interest is focused on detecting a $(1 - d_1) \times 100\%$ decrease in the intercept β_1, but this time with CUSUM charts designed for a larger nominal 10% decrease. As it was expected, the latter charts take a little longer to detect planned decreases $d_1 < 0.1$ than the WRM-CUSUM designed for detecting a lower 5% nominal decrease. These charts also detect planned decreases $d_1 \geq 0.1$ slightly faster than the WRM-CUSUM for the lower nominal decrease.

d_1	$p_c = 30\%$			$p_c = 50\%$			$p_c = 70\%$		
	$n = 30$	$n = 50$	$n = 100$	$n = 30$	$n = 50$	$n = 100$	$n = 30$	$n = 50$	$n = 100$
0.00	199.66	200.61	200.88	200.50	201.02	200.01	200.41	199.87	199.28
0.01	128.71	120.37	108.01	136.03	125.12	114.44	143.62	135.22	122.20
0.02	86.88	76.07	61.52	94.64	82.32	68.09	106.44	94.77	78.21
0.03	60.72	50.09	37.32	68.33	56.30	42.96	80.65	67.75	52.25
0.04	44.03	34.55	24.21	50.86	40.14	28.50	62.52	50.14	36.66
0.05	33.11	24.88	16.63	39.03	29.79	20.07	49.36	38.63	26.70
0.06	25.83	18.94	12.07	30.99	22.96	14.87	40.23	30.54	20.20
0.07	20.71	14.94	9.28	25.17	18.18	11.55	33.26	24.69	15.99
0.08	17.18	12.12	7.40	20.87	14.98	9.24	28.11	20.59	13.05
0.09	14.49	10.16	6.12	17.67	12.54	7.67	24.12	17.42	10.86
0.10	12.47	8.72	5.20	15.34	10.73	6.54	20.95	15.10	9.33
0.15	7.26	4.99	2.98	8.91	6.14	3.70	12.39	8.67	5.25
0.20	5.16	3.52	2.14	6.23	4.30	2.60	8.58	5.97	3.63

TABLE B.7. Approximated performance of the WRM-CUSUM charts for the fixed shape parameter $\gamma = 0.5$ and different values of the data-set dimension N, censoring rate p_C and nominal 10% decrease in the intercept of the linear specification of the scale parameter.

d_1	$p_c = 30\%$			$p_c = 50\%$			$p_c = 70\%$		
	$n = 30$	$n = 50$	$n = 100$	$n = 30$	$n = 50$	$n = 100$	$n = 30$	$n = 50$	$n = 100$
0.00	198.93	200.30	200.18	199.31	199.68	199.46	200.63	198.99	200.09
0.01	105.67	97.93	88.42	110.58	102.80	93.12	119.03	110.48	99.18
0.02	58.87	50.80	41.16	64.39	55.83	45.39	74.13	64.44	52.59
0.03	34.96	27.93	20.73	39.65	32.00	23.81	48.32	39.36	29.36
0.04	22.02	16.72	11.42	25.89	19.71	13.53	33.10	25.50	17.67
0.05	14.95	10.80	6.89	17.76	13.07	8.40	23.64	17.51	11.46
0.06	10.69	7.53	4.63	13.01	9.28	5.74	17.65	12.69	7.98
0.07	8.10	5.62	3.36	9.93	6.94	4.17	13.67	9.70	5.92
0.08	6.43	4.38	2.60	7.89	5.46	3.24	11.00	7.65	4.62
0.09	5.29	3.60	2.11	6.51	4.45	2.63	9.10	6.30	3.76
0.10	4.46	3.03	1.79	5.48	3.46	2.21	7.73	5.31	3.14
0.15	2.57	1.74	1.11	3.08	2.11	1.28	4.25	2.91	1.75
0.20	1.88	1.24	1.00	2.19	1.49	1.03	2.91	2.02	1.23

TABLE B.8. Approximated performance of the WRM-CUSUM charts for the fixed shape parameter $\gamma = 1.0$ and different values of the data-set dimension N, censoring rate p_C and nominal 10% decrease in the intercept of the linear specification of the scale parameter.

d_1	$p_c = 30\%$			$p_c = 50\%$			$p_c = 70\%$		
	$n = 30$	$n = 50$	$n = 100$	$n = 30$	$n = 50$	$n = 100$	$n = 30$	$n = 50$	$n = 100$
0.00	200.34	199.61	199.95	198.74	199.92	200.41	199.32	200.09	200.94
0.01	97.17	88.42	72.24	98.50	91.81	78.36	105.83	98.71	88.29
0.02	47.22	40.65	28.71	50.71	44.20	33.83	58.64	50.99	40.87
0.03	25.08	20.01	12.80	27.98	22.80	15.68	34.41	27.90	20.40
0.04	14.44	10.80	6.43	16.72	12.67	8.11	21.45	16.47	10.99
0.05	9.01	6.47	3.70	10.73	7.74	4.70	14.32	10.49	6.62
0.06	6.13	4.25	2.41	7.38	5.18	3.06	10.09	7.17	4.37
0.07	4.49	3.05	1.76	5.45	3.75	2.20	7.58	5.27	3.14
0.08	3.49	2.36	1.39	4.23	2.88	1.71	5.90	4.07	2.41
0.09	2.83	1.92	1.20	3.43	2.34	1.41	4.81	3.29	1.94
0.10	2.39	1.62	1.09	2.88	1.96	1.23	4.03	2.73	1.64
0.15	1.38	1.06	1.00	1.62	1.16	1.00	2.18	1.50	1.06
0.20	1.06	1.00	1.00	1.15	1.01	1.00	1.50	1.09	1.00

TABLE B.9. Approximated performance of the WRM-CUSUM charts for the fixed shape parameter $\gamma = 1.5$ and different values of the data-set dimension N, censoring rate p_C and nominal 10% decrease in the intercept of the linear specification of the scale parameter.

B.3 Data sets for the pharmaceutical industry example

There are presented the results of annually conducted accelerated experiments in the laboratory of a pharmaceutical company. The results were collected during the period 1999–2013. In each annual experiment, six specimens of ticks were tested at six different concentration levels of a poisonous solution ranging from 2% to 12% with a 2% increase between levels. Concentration levels are shown in the second column of the table. The experiment is planned to terminate testing after a fixed time in hours, that depends on the concentration level, had elapsed. The censoring times for each of the levels were set to be $C_1 = 75.2$, $C_2 = 49.1$, $C_3 = 38.3$, $C_4 = 32.1$, $C_5 = 28.0$ and $C_6 = 25.1$. The elapsed time, in hours, until death is reported in the respective column of the presented table. The plus symbol indicates a censored observation that has to be replaced by the corresponding value C_i, $i = 1, \cdots, 6$. The complete data set is given below.

	X	1999	2000	2001	2002	2003	2004	2005	2006	2007	2008	2009	2010	2011	2012	2013
[1,]	0.02	52.6	20.2	52.1	20.1	25.3	+	57.7	42.1	59.3	41.9	24.7	53.8	+	32.2	+
[2,]	0.04	+	26.3	6.3	16.2	27.8	41.9	+	18.3	31.1	27.4	17.2	33.4	37.6	+	+
[3,]	0.06	34.0	21.6	+	17.2	19.5	16.2	+	9.9	+	+	+	22.7	24.2	21.3	8.6
[4,]	0.08	+	+	13.9	8.1	15.3	5.5	19.7	6.6	12.7	+	5.8	12.7	26.8	22.1	+
[5,]	0.10	18.1	22.3	2.8	0.6	12.4	+	+	+	7.9	18.0	+	10.7	25.3	+	9.0
[6,]	0.12	24.6	20.5	13.1	4.9	7.2	8.5	23.7	+	+	+	+	+	19.2	9.5	+
[7,]	0.02	13.0	54.6	9.9	67.1	+	56.5	30.5	+	71.7	+	51.3	48.1	52.4	+	71.0
[8,]	0.04	14.5	+	35.7	28.5	36.5	11.9	46.8	+	21.4	34.2	+	9.4	11.0	12.6	26.1
[9,]	0.06	11.9	16.6	29.8	30.9	30.3	34.2	5.0	27.1	34.7	+	29.9	32.6	27.2	+	28.7
[10,]	0.08	23.2	24.8	9.1	14.2	22.7	17.4	+	+	18.6	10.6	23.7	14.1	+	11.7	4.6
[11,]	0.10	17.9	11.8	9.6	+	+	13.0	16.1	24.8	19.9	+	12.7	19.1	19.9	+	20.5
[12,]	0.12	6.8	+	+	22.1	4.6	+	21.8	21.6	22.7	13.2	12.5	11.0	8.7	3.6	19.6
[13,]	0.02	35.8	36.3	23.8	16.0	20.0	37.7	27.3	+	52.1	71.0	45.1	+	+	42.2	43.5
[14,]	0.04	+	48.5	+	+	46.6	+	43.8	+	+	16.7	27.1	+	+	41.2	+
[15,]	0.06	18.8	10.7	7.6	+	+	12.5	18.1	18.9	30.4	13.0	+	20.4	16.0	12.9	+
[16,]	0.08	28.4	+	15.7	12.0	+	14.8	+	9.0	17.6	8.9	17.9	21.5	24.1	20.1	13.8
[17,]	0.10	17.6	15.4	13.8	19.5	+	20.6	+	25.7	22.7	22.0	15.8	+	+	27.9	15.8
[18,]	0.12	4.3	0.9	+	6.3	13.6	+	4.2	+	23.5	6.6	+	7.5	13.6	15.4	+
[19,]	0.02	69.6	+	45.8	40.2	+	41.1	+	62.5	63.1	+	72.6	63.2	18.2	73.0	61.1
[20,]	0.04	35.2	18.2	15.2	+	2.3	29.9	26.4	24.6	27.7	37.3	26.2	+	+	+	25.9
[21,]	0.06	11.1	25.9	+	+	5.3	21.9	+	33.1	+	19.7	1.3	30.6	+	32.0	32.4
[22,]	0.08	29.2	14.5	15.8	14.6	+	26.9	16.4	17.9	26.3	18.8	20.0	23.7	12.3	+	24.2
[23,]	0.10	11.5	18.6	15.1	14.8	15.3	+	+	15.0	15.8	19.8	5.9	21.4	11.2	+	+
[24,]	0.12	8.3	12.2	9.5	9.6	+	14.2	6.2	16.3	18.6	9.6	23.4	+	+	4.2	19.9
[25,]	0.02	+	+	39.8	30.1	8.3	29.8	+	13.9	+	33.0	+	+	19.8	73.6	+
[26,]	0.04	32.0	16.5	+	4.1	+	+	23.9	+	+	40.3	40.3	+	46.2	38.1	19.7
[27,]	0.06	+	36.9	24.2	31.3	36.5	+	+	21.7	15.4	21.3	29.2	35.9	8.1	12.8	21.0
[28,]	0.08	30.2	26.5	+	+	21.4	24.7	7.1	9.3	+	+	32.1	5.4	13.3	29.2	30.3
[29,]	0.10	+	10.5	7.0	+	12.7	25.0	9.0	4.1	16.7	16.4	12.0	+	+	13.0	7.5
[30,]	0.12	+	+	6.8	+	9.0	13.8	+	4.7	17.0	12.5	3.1	12.4	18.1	+	+
[31,]	0.02	22.4	41.9	+	+	+	+	28.1	9.4	28.2	26.3	+	23.4	58.4	49.6	35.4
[32,]	0.04	21.9	39.8	48.5	23.0	7.5	7.9	22.5	46.5	+	40.4	48.9	44.0	2.0	17.3	24.8
[33,]	0.06	8.5	13.1	+	+	24.8	+	9.9	+	+	11.7	7.6	19.4	13.6	8.4	+
[34,]	0.08	28.5	+	29.0	12.3	+	29.2	8.2	+	23.4	+	5.4	+	+	30.9	+
[35,]	0.10	24.1	+	23.7	19.3	16.6	+	15.2	+	+	15.2	+	+	19.3	23.9	15.5
[36,]	0.12	9.2	19.0	+	6.8	+	14.3	3.2	16.4	+	+	+	+	21.2	20.9	13.9

Conclusions and recommendations

We have presented three different ways of monitoring Weibull regression models with common shape parameter and censored and uncensored observations in phase II processes. It was shown that existing control schemes can be also used for monitoring the parameter vector of regression models with severely skewed response variable. However, existing control procedures have to be modified or generalized so the monitoring of one or more of the parameters in the WRM parameter vector can be carried out.

In the case of monitoring WRM with uncensored observations, the design of the existing control charts is based on the asymptotic normality of the MLE of the WRM parameter vector. Nevertheless, it is almost impossible to guarantee the existence of large enough data sets in on-line monitoring. Existing control charts have to be adapted so they can work with finite data-set dimensions. We proposed to implement Bartlett's adjustments to LRT statistic in chart designing in order to improve control scheme performance when non-large enough data sets are available over time. The resulting control charts have proved to work fairly acceptable for data-set dimensions greater than 30 uncensored observations.

We have also extended Dickinson's LRT-based CUSUM procedure for monitoring the characteristic life of right-censored Weibull lifetimes to the more general case of monitoring type I right-censored lifetimes that depend on a set of explanatory variables. The methodology can be used for virtually any data-set dimension because it does not depend on distributional assumptions beyond those required to the response variable. However, chart performance strongly depends on multiple known factors that must be taken into account for designing purposes. Conducted simulations suggest that this CUSUM chart outperforms the MEWMA chart in most of the studied cases.

Current and further work

Our current research work is mainly focused on completing the monitoring of WRM with type I right-censored observations, time-varying dimension and/or random explanatory variables. The fact is that not all the scenarios of interest have been exhaustively and deeply explored. Especially, it is needed to

- Investigate other mechanisms for generating the number of observations in each experimental level over time rather than the uniform distribution. However, it is expected that the generating mechanism, deterministic or random, does not seriously affect the performance of the WRM-CUSUM with probability limits.
- Evaluate the effect of the distribution of the explanatory variables on charting procedures when the monitoring of the coveriates is not concerned.
- Investigate drops from the in-control state due to drops in the values of the explanatory variables. This is, the monitoring of the random predictors is also concerned.

For further work, it could be useful to implement the conditional expected value (CEV) method for monitoring WRM with censored observations. It was established that higher censoring rates make the control schemes work less effectively. The use of the CEV method could improve the performance of control charts when a censoring mechanism is operating. The CEV method proposes to replace censored observations by its conditional expected value based on the Weibull or the extreme value distributions. The method has been proved to overcome the difficulty of having too many censored observations in the available samples. Existing proposals of CEV-based control charts work fairly acceptable for monitoring lifetimes without covariates.

Some other related topics are also of great relevance when the main goal of the monitoring aims to the WRM with uncensored observations. For instance, in Chapters 2 and 3, it was established that the control limits of the resulting corrected schemes appear to be robust to the data-set dimension, if $N > 30$ approximately. Thus, we have thought, as it was presented in Section 4.7, that the proposed methodologies can also be adapted for monitoring WRM with uncensored observations and time-varying dimension by conditioning on the values of the experimental levels.

Bibliography

[1] C. Acosta-Mejía and J. Pignatiello, *Monitoring process dispersion without subgrouping*, Journal of Quality Technology **32** (2000), no. 2, 89–101.

[2] S. B. Akhundjanov and F. Pascual, *Moving range EWMA control charts for monitoring the Weibull shape parameter*, Journal of Statistical Computation and Simulation **85** (2015), no. 9, 1864–1882.

[3] F.B. Alt and N.D. Smith, *Multivariate process control*, Handbook of Statistics, vol. 7, P.R. Krishnaiah & C.R. Rao, eds, North Holland, Amsterdam, 1988, pp. 333–351.

[4] A. Amiri, M. Eyvazian, C. Zou, and R. Noorossana, *A parameter reduction method for monitoring multiple linear regression profiles*, International Journal of Advanced Manufacturing Technology **58** (2012), 621–629.

[5] A. Amiri, W. A. Jensen, and R. B. Kazemzadeh, *A case study on monitoring polynomial profiles in automotive industry*, Quality and Reliability Engineering International **26** (2009), 509–520.

[6] A. Amiri, M. Koosha, A. Azhdari, and G. Wang, *Phase I monitoring of generalized linear model-based regression profiles*, Journal of Statistical Computation and Simulation **85** (2015), no. 14, 2839–2859.

[7] O. E. Barndorff-Nielsen, *Inference on full or partial parameters based on the standardized signed log-llikelihood ratio*, Biometricka **73** (1986), 307–322.

[8] O. E. Barndorff-Nielsen and D. R. Cox, *Bartlett's adjustments to the likelihood ratio statistic and the distribution of the maximum likelihood estimator*, Journal of the Royal Statistical Society **B 46** (1984), 483–495.

[9] C. W. Champ and W.H. Woodall, *Exact results for Shewhart control charts with supplementary runs rules*, Technometrics **29** (1987), no. 4, 393–399.

[10] Y. Chan, B. Han, and F. Pascual, *Monitoring the Weibull shape parameter with type II censored data*, Quality and Reliability Engineering International **31** (2014), no. 5, 741–760.

[11] A.F.B. Costa, *X chart with variable sample size and variable sampling intervals*, Journal of Quality Technology **29** (1997), 197–204.

[12] S. V. Crowder, *A simple method for studying run-length distributions of exponentially weighted moving average charts*, Technometrics **29** (1987), no. 4, 401–407.

[13] T. DiCiccio, *Approximate inference for the generalized gamma distribution*, Technometrics **29** (1987), 33–40.

[14] ———, *Likelihood inference for linear regression models*, Biometrika **75** (1988), 29–34.

[15] R. M. Dickinson, R. D. A. Olteanu, A. G. Ryan, W. Woodall, and G. G. Viniing, *CUSUM charts for monitoring the characteristic life of censored Weibull lifetimes*, Journal of Quality Technology **46** (2014), no. 4, 340–358.

[16] Y. Dong, A. S. Hedayat, and B. K. Sinha, *Surveillance strategies for detecting changes in incidence rates based on exponentially weighted moving average methods*, Journal of the American Statistical Association **103** (2008), 843–853.

[17] A. J. Duncan, *Quality control and industrial statistics*, 5th ed., IRWIN, 1986.

[18] D. Fraser, *Inference and linear models*, McGraw-Hill, N.Y., 1979.

[19] B. Guo and B. X. Wang, *Control charts for monitoring the Weibull shape parameter based on type II censored samples*, Quality and Reliability Engineering International **30** (2014), 13–24.

[20] F. Haghighi and P. Castagliola, *Conditional control chart for monitoring the Weibull shape parameter under progressively type II censored data*, Quality and Reliability Engineering International **31** (2015), no. 6, 1013–1022.

[21] F. Haghighi, F. Pascual, and P. Castagliola, *Conditional control charts for Weibull quantiles under type II censoring*, Quality and Reliability Engineering International **31** (2015), no. 8, 1649–1664.

[22] D. Hinkley, *Likelihood inference about location and scale parameters*, Biometrika **65** (1978), 253–261.

[23] N. L. Johnson, *Cumulative sum control charts and the Weibull distribution*, Technometrics **8** (1966), 481–491.

[24] L. Kang and S. L. Albin, *On-line monitoring when the process yields a linear profile*, Journal of Quality Technology **32** (2000), no. 4, 418–426.

[25] R. B. Kazemzadeh, R. Noorossana, and A. Amiri, *Phase I monitoring of polynomial profiles*, Communications in Statistics: Theory and Methods **37** (2008), no. 10, 1671–1686.

[26] M. Khedmati and S. T. A. Niaki, *Phase II monitoring of general linear profiles in the presence of between profile autocorrelation*, Quality and Reliability Engineering International **32** (2016), no. 2, 443–452.

[27] J. Lawless, *Statistical models and methods for lifetime data*, 2nd ed., John Wiley and Sons, Inc., New York, NY, USA., 1982.

[28] J. F. Lawless, *Confidence interval estimation for the Weibull and extreme value distributions*, Technometrics **20** (1978), 355–364.

[29] C.A. Lowry and D.C. Montgomery, *A review of multivariate control charts*, IIE Transactions **27** (1995), 800–810.

[30] C.A. Lowry, W.H. Woodall, C.W. Champ, and S.E. Rigdon, *A multivariate exponentially weighted moving average control chart*, Technometrics **34** (1992), 46–53.

[31] M. A. Mahmoud, P. A. Parker, and W. H. Woodall, *A change point method for linear profile data*, Quality and Reliability Engineering International **23** (2007), no. 2, 247–268.

[32] M. A. Mahmoud and W. H. Woodall, *Phase I analysis of linear profiles with calibration applications*, Technometrics **46** (2004), 277–391.

[33] T. Martinussen and T. H. Sheike, *Dynamic regression models for survival data*, New York, NY, USA, 2006.

[34] W.Q. Meeker and L.A. Escobar, *Statistical methods for reliability data*, John Wiley and Sons., New York, NY, USA., 1998.

[35] Y. Mei, S. W. Han, and K-L. Tsui, *Early detecting of a change in Poisson rate after accounting for population size effects*, Statistica Sinica **21** (2011), 597–624.

[36] D. Montgomery, *Introduction to statistical quality control*, 5th ed., John Wiley and Sons, Inc., New York, 2009.

[37] A.L. Moreno and J. A. Vargas, *Carta de control R con intervalos de muestreo variable*, Revista Colombiana de Estadística **23** (2000), 15–25.

[38] W. Nelson, *Graphical analysis of accelerated life test data with the inverse power law model*, IEEE Transactions on Reliability **R-21** (1972), 945–965.

[39] R. Noorossana, A. Saghaei, and A. Amiri, *Statistical analysis of profile monitoring*, John Wiley and Sons, Inc., New Jersey, 2011.

[40] E. S. Page, *Continuous inspection scheme*, Biometrika **41** (1954), 100–115.

[41] C. A. Panza and J. A. Vargas, *Monitoring the shape parameter of a Weibull regression model in Phase II processes*, Quality and Reliability Engineering International **32** (2016), no. 1, 195–207.

[42] F. Pascual, *EWMA charts for the Weibull shape parameter*, Journal of Quality Technology **42** (2010), no. 4, 400–416.

[43] F. Pascual and S. Li, *Monitoring the Weibull shape parameter by control charts for the sample range of type II censored data*, Quality and Reliability Engineering International **28** (2011), 233–246.

[44] F. Pascual and D. Nguyen, *Moving range charts for monitoring the Weibull shape parameter with single observation samples*, Quality and Reliability Engineering International **27** (2011), 905–919.

[45] F. Pascual and H. Zhang, *Monitoring the Weibull shape parameter by control charts for the sample range*, Quality and Reliability Engineering International **27** (2011), 15–25.

[46] S. R. Paul and K. Thiagarajah, *Asymptotic variance-covariance of maximum likelihood estimators for the parameters of the extreme value regression model for censored data*, Windsor Mathematics Statistics Report 92-14, University of Windsor, Ontario, Canada, 1992.

[47] S.S. Prabhu, E.C. Runger, and J.B. Keats, *An adaptive sample size X chart*, Intenational Journal of Production Research **31** (1993), 2895–2909.

[48] D. Qi, Z. Wang, X. Zi, and Z. Li, *Phase II monitoring of general linear profiles using weighted likellihood ratio charts*, Computers & Industrial Engineering **94** (2016), 178–187.

[49] M. Reynolds, R. Amin, J. Arnold, and J. Nachlas, *X charts with variable sampling intervals*, Technometrics **30** (1988), 181–192.

[50] M. Reynolds and Z.G. Stoumbos, *Monitoring the process mean and variance using individual oobservation and variable sampling intervals*, Journal of Quality Technology **33** (2001), 181–205.

[51] S. W. Roberts, *Control chart tests based on geometric moving averages*, Technometrics **1** (1959), 239–250.

[52] A. G. Ryan and W. H. Woodall, *Control charts for Poisson count data with varying sample sizes*, Journal of Quality Technology **42** (2010), 260–272.

[53] T. Ryan, *Statistical methods for quality improvement*, 2nd ed., John Wiley and Sons, Inc., 2000.

[54] A. Saghaei, M. Mehrjoo, and A. Amiri, *A CUSUM method for monitoring simple linear profiles*, International Journal of Advanced Manufacturing Technology **45** (2009), 1252–1260.

[55] A. Shadman, H. Mahlooji, A. B. Yeh, and C. Zou, *A change point method for Phase II monitoring of generalized linear profiles*, On line in Communications in Statistics-Simulation and Computation, 2014.

[56] ———, *A change point method for monitoring generalized linear profiles in Phase I*, Quality and Reliability Engineering International **31** (2015), no. 8, 1367–1381.

[57] M. S. Shafae, R. M. Dickinson, W. Woodall, and J. A. Camelio, *CUSUM control charts for monitoring Weibull distributed time between events*, Quality and Reliability Engineering International **31** (2014), no. 5, 839–849.

[58] Y. Shang, F. Tsung, and C. Zou, *Profile monitoring with binary data and random predictors*, Journal of Quality Technology **43** (2011), no. 3, 196–208.

[59] X. Shen, C. Zou, W. Jiang, and F. Tsung, *Monitoring Poisson count data with probability control limits when sample sizes are time varying*, Naval Research Logistics NRL **60** (2013), no. 8, 625–636.

[60] W. A. Shewhart, *Economic control of quality of manufactured product*, D Van Nostrand Company, New York, 1931.

[61] M. E. Soleymanian, M. Khedmati, and H. Mahlooji, *Phase II monitoring of binary response profiles*, Scientia Iranica E. **20** (2013), no. 6, 2238–2246.

[62] D. Sprott, *Maximum likelihood in small samples: estimation in the presence of nuisance parameters*, Biometricka **67** (1980), 515–523.

[63] S.H. Steiner and R.J. MacKay, *Detecting changes in the mean from censored lifetime data*, Frontiers in Statistical Quality Control **6** (2001), 275–289.

[64] J.H. Sulllivan and W.H. Woodall, *Adapting control charts for the preliminary analysis of multivariate observations*, Communications in Statistics and Simulation **27** (1998), no. 4, 953–979.

[65] J. A. Vargas, *Robust estimation in multivariate control charts for individual observations*, Journal of Quality Technology **35** (2003), no. 4, 367–376.

[66] ———, *Control estadísitco de calidad*, Unibiblos. Universidad Nacional de Colombia, Bogotá, 2006.

[67] J. A. Vargas and T. P. Montaño, *CEV X control chart for Weibull distributions with censored data*, Revista Colombiana de Estadística **28** (2005), no. 2, 125–139.

[68] J. A. Vargas, S. Yáñez, and N. González, *Cartas de control multivariadas T^2 usando R y SAS*, 1st ed., Colección notas de clase. Universidad Nacional de Colombia, Bogotá, 2011.

[69] Western Electric Corporation, Indianapolis, IN., *Statistical Quality Control Handbook*.

[70] J. D. Williams, J. B. Birch, W. H. Woodall, and N. M. Fery, *Statistical monitoring of heteroscedastic dose-response profiles from high-throughput screening*, Journal of Agricultural Biological and Environmental Statistic **12** (2007), 216–235.

[71] W. Woodall, *Current research in profile monitoring*, Revista Producao **17** (2007), 420–425.

[72] W. H. Woodall, D. L. Sprintzer, D. C. Montgomery, and S. Gupta, *Using control charts to monitor processes and product quality profiles*, Journal of Quality Technology **36** (2004), 309–320.

[73] W.H. Woodall and D.C. Montgomery, *Some current directions in the theory and application of statistical process monitoring*, Journal of Quality Technology **46** (2014), no. 1, 78–94.

[74] A. Yeh, L. Huwang, and Y Li, *Profile monitoring for a binary response*, IEE Transactions **41** (2009), 931–941.

[75] L. Zhan and G. Chen, *EWMA charts for monitoring the mean of censored Weibull lifetimes*, Journal of Quality Technology **36** (2004), 321–328.

[76] J. Zhang, Z. Li, and Z. Wang, *Control chart based on likelihood ratio for monitoring linear profiles*, Computational Statistics and Data Analysis **53** (2009), 1440–1448.

[77] Q. Zhou, C. Zou, Z. Wang, and W. Jiang, *Likelihood-based EWMA charts for monitoring Poisson count data with time varying sample sizes*, Journal of the American Statistical Association **107** (2012), 1049–1062.

[78] C. Zou, F. Tsung, and Z Wang, *Monitoring general linear profiles using multivariate exponentially weighted moving average schemes*, Technometrics **49** (2007), 395–408.